



National Library
of Canada

Bibliothèque nationale
du Canada

Canadian Theses Service

Service des thèses canadiennes

Ottawa, Canada
K1A 0N4

NOTICE

The quality of this microform is heavily dependent upon the quality of the original thesis submitted for microfilming. Every effort has been made to ensure the highest quality of reproduction possible.

If pages are missing, contact the university which granted the degree.

Some pages may have indistinct print especially if the original pages were typed with a poor typewriter ribbon or if the university sent us an inferior photocopy.

Reproduction in full or in part of this microform is governed by the Canadian Copyright Act, R.S.C. 1970, c. C-30, and subsequent amendments.

AVIS

La qualité de cette microforme dépend grandement de la qualité de la thèse soumise au microfilmage. Nous avons tout fait pour assurer une qualité supérieure de reproduction.

S'il manque des pages, veuillez communiquer avec l'université qui a conféré le grade.

La qualité d'impression de certaines pages peut laisser à désirer, surtout si les pages originales ont été dactylographiées à l'aide d'un ruban usé ou si l'université nous a fait parvenir une photocopie de qualité inférieure.

La reproduction, même partielle, de cette microforme est soumise à la Loi canadienne sur le droit d'auteur, SRC 1970, c. C-30, et ses amendements subséquents.



National Library
of Canada

Bibliothèque nationale
du Canada

Canadian Theses Service Service des thèses canadiennes

Ottawa, Canada
K1A 0N4

The author has granted an irrevocable non-exclusive licence allowing the National Library of Canada to reproduce, loan, distribute or sell copies of his/her thesis by any means and in any form or format, making this thesis available to interested persons.

The author retains ownership of the copyright in his/her thesis. Neither the thesis nor substantial extracts from it may be printed or otherwise reproduced without his/her permission.

L'auteur a accordé une licence irrévocable et non exclusive permettant à la Bibliothèque nationale du Canada de reproduire, prêter, distribuer ou vendre des copies de sa thèse de quelque manière et sous quelque forme que ce soit pour mettre des exemplaires de cette thèse à la disposition des personnes intéressées.

L'auteur conserve la propriété du droit d'auteur qui protège sa thèse. Ni la thèse ni des extraits substantiels de celle-ci ne doivent être imprimés ou autrement reproduits sans son autorisation.

ISBN 0-315-56119-X

Canada

IMPROVED VERSION OF BTA DEEP-HOLE DRILLING TOOLS
WITH STAGGERED DISPOSABLE CARBIDE INSERTS

Seyed.J. Torabi

A Thesis
in
The Department
of
Mechanical Engineering

Presented in Partial Fulfillment of the Requirements
for the Degree of Master of Engineering at
Concordia University
Montreal , Quebec , Canada

February 1990

© Seyed.J.Torabi, 1990

ABSTRACT

Improved Version of BTA Deep-Hole Drilling Tools
with Staggered Disposable Carbide Inserts

Seyed J. Torabi
Concordia University, 1990

The present investigation examines the effects of equal pad load on the performance of BTA (Boring and Trepanning Association) tools with staggered cutters. For this purpose a BTA deep drilling tool with unsymmetrically located inserts with respect to the rotational axis is designed such that a predetermined equal force is exerted on guide pads. This force in turn exerts a sufficient pressure on the machined bore-wall to provide the head with a stable guidance. To achieve the above requirement a multi-parameter penalty function optimization method is used. Moreover, to analyze the stability of the tool the Monte Carlo simulation technique and the Pfleghar method are utilized and the results are compared with those of BTA multi-edge with disposable inserts and BTA single-edge solid boring tools.

The designed tool prototype was manufactured and tested under different cutting conditions and compared to the performance of the two mentioned commercially available tools. The results show that the designed tool drills holes of less run-out. In general it produces holes with smaller

size error compared to BTA multi-edge tool. In the case of hole roundness error and surface finish it is slightly inferior to both BTA tools presently available on the market.

ACKNOWLEDGEMENTS

The author wishes to express his gratitude and appreciation to his thesis supervisor, Dr. V. Latinovic for his continuous guidance and support throughout the research.

The financial support of the National Research Council Grant No D78 is also acknowledged.

Thanks are also forwarded to Mr. J. Seeger and the machine shop technicians of Concordia University for their assistance.

TABLE OF CONTENT

	PAGE
LIST OF FIGURES	viii
LIST OF TABLES	xi
NOMENCLATURE	xii
 I CHAPTER I	
INTRODUCTION	1
1.1 Historical Background	2
1.2 Deep Hole Drilling Tools	5
1.2.1 Gundrilling	5
1.2.2 BTA Drilling	6
1.2.3 Ejector Drilling	11
1.3 Cutting Force System	12
1.4 Literature Survey	15
1.4.1 Cutting Force Measurement and Analysis	15
1.4.2 Friction Coefficient	18
1.4.3 Hole Quality and Surface Integrity	18
1.4.4 Tool Design	22
1.4.5 Vibrations	24
1.4.6 Tool Wear	26
1.5 Objectives of Present Investigation	28
 II CHAPTER II	
2 Tool Force System Formulation	30
2.1 Design Concept	33
2.2 Optimum Tool Design	38
2.3 Optimization Method	40
2.4 Optimum Tool Configuration	45

III CHAPTER III

3	Tool Stability Analysis	48
3.1	Monte Carlo Simulation	51
3.2	Pfleggar Method	60

IV CHAPTER IV

4	Experimental Set-up	64
4.1	Tool Tests	64
4.2	Machine Tool	71

V CHAPTER V

5	Tool Model Tests	76
5.1	Hole Run-out	77
5.2	Hole Size Error	88
5.3	Hole Roundness Error	91
5.4	Hole Surface Finish	108

VI CHAPTER VI

6.1	Summary	117
6.2	Conclusion	119
6.3	Recommendation for Future Work	120

REFERENCES	121
------------	---	---	---	---	---	---	-----

APPENDIX	128
----------	---	---	---	---	---	---	-----

LIST OF FIGURES

FIGURES		PAGE
1	The Principle of BTA Machining	3
2	Gundrill	7
3	Typical BTA Tools	9
4	BTA Tool with Distributed Cutters	10
5	Ejector Drill	13
6	Cutting Force System	14
7	Rolved View of Cutters	35
8	Flow Chart of the Interior Penalty Function Method	43
9	Tool Force System	50
10	Tool Force System	52
11	Tool Force System	53
12	PDF of The Designed Tool Force System	55
13	PDF of The BTA Multi-Edge Tool Force System	56
14	PDF of The BTA Solid Boring Tools Force System	57
15	Results Obtained from Tools Force System Simulation	59
16	Tool Force System	61
17	Designed Tool's Prototype	65
18	The Blocked Chip Mouth	67
19	BTA Multi-edge Tool with Disposable Inserts	68
20	Coolant Pressure Distribution on BTA Solid Boring Tools Chip Mouth	70
21	Experimental Set up for Tools' Testing	72
22	Possible Configurations of Hole Run-Out	79

FIGURE		PAGE
23	Hole Run-out Components	80
24	Run-Out of the Hole Drilled by the Prototype .	82
25	Run-Out of the Hole Drilled by the BTA Multi-Edge Tool	83
26	Run-out of the Hole Drilled by the BTA Solid Boring Tool	84
27	Hole Axis Deviation Angle	85
28	Hole Axis Deviation Angle	86
29	Hole Axis Deviation Angle	87
30	Hole Size Error	89
31	Hole Size Error	92
32	Size Error of the Hole Drilled by the Prototype	93
33	Size Error of the Hole Drilled by the Prototype	94
34	Size Error of the Hole Drilled by the BTA Multi-Edge Tool	95
35	Size Error of the Hole Drilled by the BTA Multi-Edge Tool	96
36	Size Error of the Hole Drilled by the BTA solid Boring Tool	97
37	Size Error of the Hole Drilled by the BTA Solid Boring Tool	98
38	Hole Roundness Error	100
39	Hole Roundness Error and Surface Finish .	101
40	Roundness Error of the Hole Drilled by the Prototype	102
41	Roundness Error of the Hole Drilled by	

FIGURE		PAGE
	the Prototype	103
42	Roundness Error of the Hole Drilled by the BTA Multi-Edge Tool	104
43	Roundness Error of the Hole Drilled by the BTA Multi-Edge Tool	105
44	Roundness Error of the Hole Drilled by the BTA Solid Boring Tool	106
45	Roundness Error of the Hole Drilled by the BTA Solid Boring Tool	107
46	Hole Surface Finish	109
47	Surface Finish of the Hole Drilled by the Prototype	111
48	Surface Finish of the Hole Drilled by the Prototype	112
49	Surface Finish of the Hole Drilled by the BTA Multi-Edge Tool	113
50	Surface Finish of the Hole Drilled by the BTA Multi-Edge Tool	114
51	Surface Finish of the Hole Drilled by the BTA Solid Boring Tool	115
52	Surface Finish of the Hole Drilled by the BTA Solid Boring Tool	116
A1	Detail Drawing of Designed Tool	131
A2	The Prototype's Inserts and Pad	132

LIST OF TABLES

TABLE		PAGE
A1	Properties of AISI-P20 Steel	130
A2	Properties of AISI-C12L14 and AISI-C1045 Steels	130

NOMENCLATURE

A	undeformed chip cross-sectional area
b	width of cut
c	constant, multiplier of penalty parameter
c_p, c_q	cutting force for $b = 1$ mm and $s = 1$ mm in the direction p and q
d	diameter of cutting head
e	magnitude of error
F_N	pad normal force
$F_{p,q}$	cutting force components in the directions p and q
$F_{F,R,T}$	cutting force components in the feed, radial and tangential directions
$F_{X,Y}$	cutting force components in the X and Y directions
$F'_{X,Y}$	pads force components in the X and Y directions
$F(X^*)$	optimum value of objective function resulted from current move
i,j,k	subscripts
k_p	unit cutting force
M_C	cutting moment
M_T	total drilling moment
M_h	holding moment
M_t	tilting moment
N	number of measured points in least square method
R	resultant cutting force

R'	pads resultant force
$R_{X,Y}$	resultant cutting force components in the X and Y directions
r_i	radius of chip mouth
r	magnitude of hole run-out
r_{dir}	directional component of hole run-out
r_{dis}	distributed component of hole run-out
s	depth of cut
S	degree of stability
V	number of observations on each section of drilled hole
W	number of equally spaced sections along each drilled specimen
$x_{1,2}$	exponents to the width of cut
$y_{1,2}$	exponents to the depth of cut
z	normalized distance of equally spaced sections on each drilled specimen
α	hole run-out deviation angle
β	multiplier of pattern search direction
δ	relative dimensional error
ϵ_1, ϵ_2	constants in optimization problem
γ	penalty parameter
ψ	pad position angle
κ	approach angle
λ	pad resultant force position angle
μ	pad friction coefficient
ν	sum of square error in the least square method

θ	position angle of measured point on each section of drilled specimen
ρ	pattern search direction
σ	penalty function
φ	cutter position angle
ξ	chip mouth factor
ζ	constant in optimization problem

CHAPTER I

INTRODUCTION

Producing internal cylindrical features in metal workpieces may be the most difficult of all metal removal processes. Drilling tools are one among many types of hole making tools used in industry and the production of holes constitutes a very wide and important area in manufacturing technology.

The machining of holes with large length to diameter ratios requiring high standards of size, parallelism, straightness and fine surface finish has always presented problems. Conventional drilling tools such as twist drills are found inadequate for precision drilling since hole quality begins to deteriorate when hole length to diameter ratio exceeds approximately three. This is mainly due to the fact that the cutting lips of twist drills and other similar drilling tools are far away from the clamping area as well as uncertainty of state of resultant cutting force.

Invention of BTA (Boring and Trepanning Association) technique overcomes those disadvantages of conventional drills by using tools in which cutting forces generated at the cutting edges are balanced by reaction forces at supporting pads. The pads are situated on tool periphery in such a way that the resultant cutting force always acts within their included angle. Thus, these tools are self

guided and are capable of producing precision bores with depth of up to 100 times the diameter in a single pass. Despite their original task they are now adopted to shorter workpieces to benefit from a shorter machining time and high accuracy. In mass production, a very close tolerance and a reasonably good surface finish can be maintained.

The machining process utilizes high pressure cooling oil to remove chips, transfer heat, dampen vibration and lubricate the cutting edges and pads [1]. The principle of the BTA deep hole machining is shown in Fig. 1.

1.1 Historical Background

Present day's deep hole drilling process had its origin in the firearms industry of the eighteenth century. During the period between 1500-1750 the town of Suhl in Germany was known as a center of deep hole drilling. This technique employed a water mill as the machine tool and spade drill bits as the cutting tool. Two barrels could be drilled at the time by two parallel boring spindles. The feed and the thrust were provided by the operator actuating a lever which supplied a certain force amplification, thus enabling him to provide an infinitely variable feed [2]. In 1713 a vertical gun drilling machine was built by Maritz. A cutter head had been mounted on the end of a boring bar which was rotated by animal power and a downward feed motion was given to the gun barrel. The first boring machine in which the workpiece was rotated and feed motion

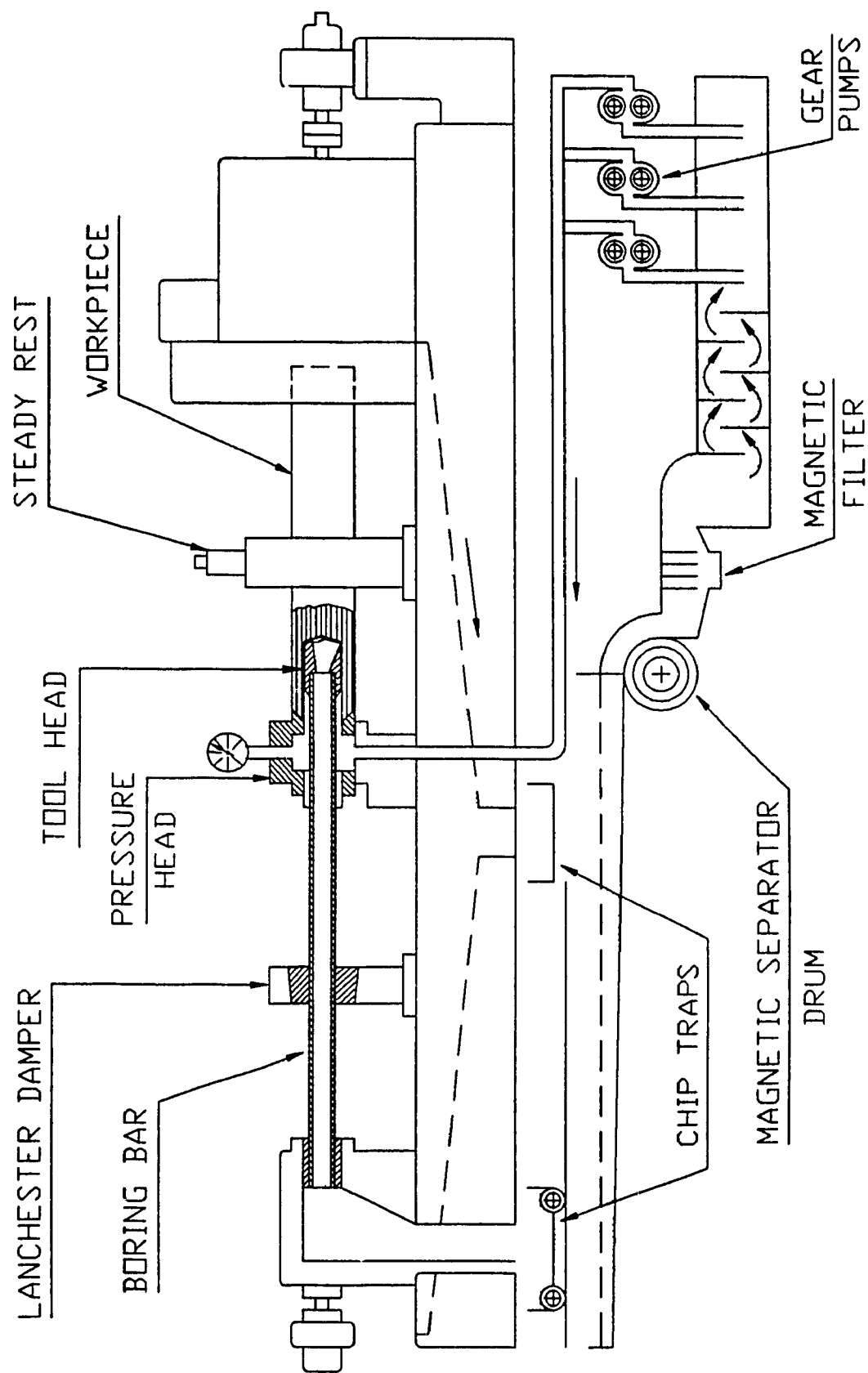


FIG. 1 THE PRINCIPLE OF BTA MACHINING

was given to the drilling tool appears to have been used about 1758 by J. Verbruggen in Germany. The machine had a massive construction and is regarded as the first example of engineering application. But the best and the most comprehensive record of information on gun drilling methods during the eighteen century is given in G. Monge's book, "L'Art de fabriquer les canons". He wrote his book at the instigation of the committee of public safety of the French Revolution [3].

An article published in 1886 by Landis [4] describing gun barrel manufacture shows that by this time a variety of self supporting tools was available. These tools were employed to drill holes of a considerable depth using a pressurized cutting oil system. The self supporting tools that he illustrated were remarkably similar in design to present day tools. He even showed a tool with replaceable pads and an indexable cutting edge. This very detailed and comprehensive article shows that the advantages of self guided tools had been recognized and were employed to improve the efficiency of gun manufacture. It remains a fact however, that the foundation of modern deep hole drilling process had been laid down by the first half of 20th century where, it was only after a visit of a machine tool commission to Germany at the end of 2nd world war, the present day deep hole drilling process was found to be used in that country. This method which is known today as BTA system is also called Beisner method to honour the founder

of this technique. It was in 1950s when gundrills were introduced extending the deep hole drilling process to small bores [5].

1.2 Deep Hole Drilling Tools

The term " deep hole drilling " is used to mean those processes in which cutting forces generated at a single or multi-edge tool are balanced not by another cutting edge but by pads located at tool periphery near cutting edges. These pads bear against the wall of the drilled hole and counteract the resultant cutting force. Thus, deep hole drilling tool is considered as end cutting tool which is guided by its pads in a hole it just generated. To start a hole in a workpiece, a guiding bushing is placed in the front of the workpiece to support the pads initially, or if such a bushing is not available, an initial hole must be premachined in the workpiece.

There are three main types of processes and tools which fall under the general name of deep hole drilling depending on the coolant induction and chip removal method. They are gun-drilling, Beisner or BTA drilling and ejector drilling. Each of the three main drilling methods may be solid boring, counter-boring and trepanning. These are briefly described in following sections.

1.2.1 Gundrilling

A gundrill has approximately two thirds of a circular

cross section solid, and one third V-grooved. The configuration of a general-purpose gundrill is shown in Fig.2. It basically consists of a V-grooved shank to which a cutting head is connected. The cutting head or tip is detachable or brazed to the drill shank. The function of drill shank is to provide the means for adequate support of the drilling head, to give sufficient torsional stiffness, to allow a continuous feed and also to provide the means for flooding the cutting zone with cutting fluid pumped through it. The shank has a kidney shaped cross section forming a V-groove which serves as the passage for swarf from the cutting head to the disposal point. The tool tip which cuts through the workpiece consists of the outer and inner cutting edges. The cutting edges intersection which is called the tool point, is generally located $1/3$ to $1/5$ of the drill diameter from the drill outer point. The tool nose angle measured at the tool point can vary widely depending on the location of the tool point and angles of the inner and outer cutting edges to yield optimum chip formation for disposal according to the workpiece material and finished hole specifications. The tool head may be made of solid carbide for diameters as small as 5 mm or less, or have carbide tips brazed on steel body for larger diameters.

1.2.2 BTA Drilling

BTA tool differs from the gundrill by tool design,

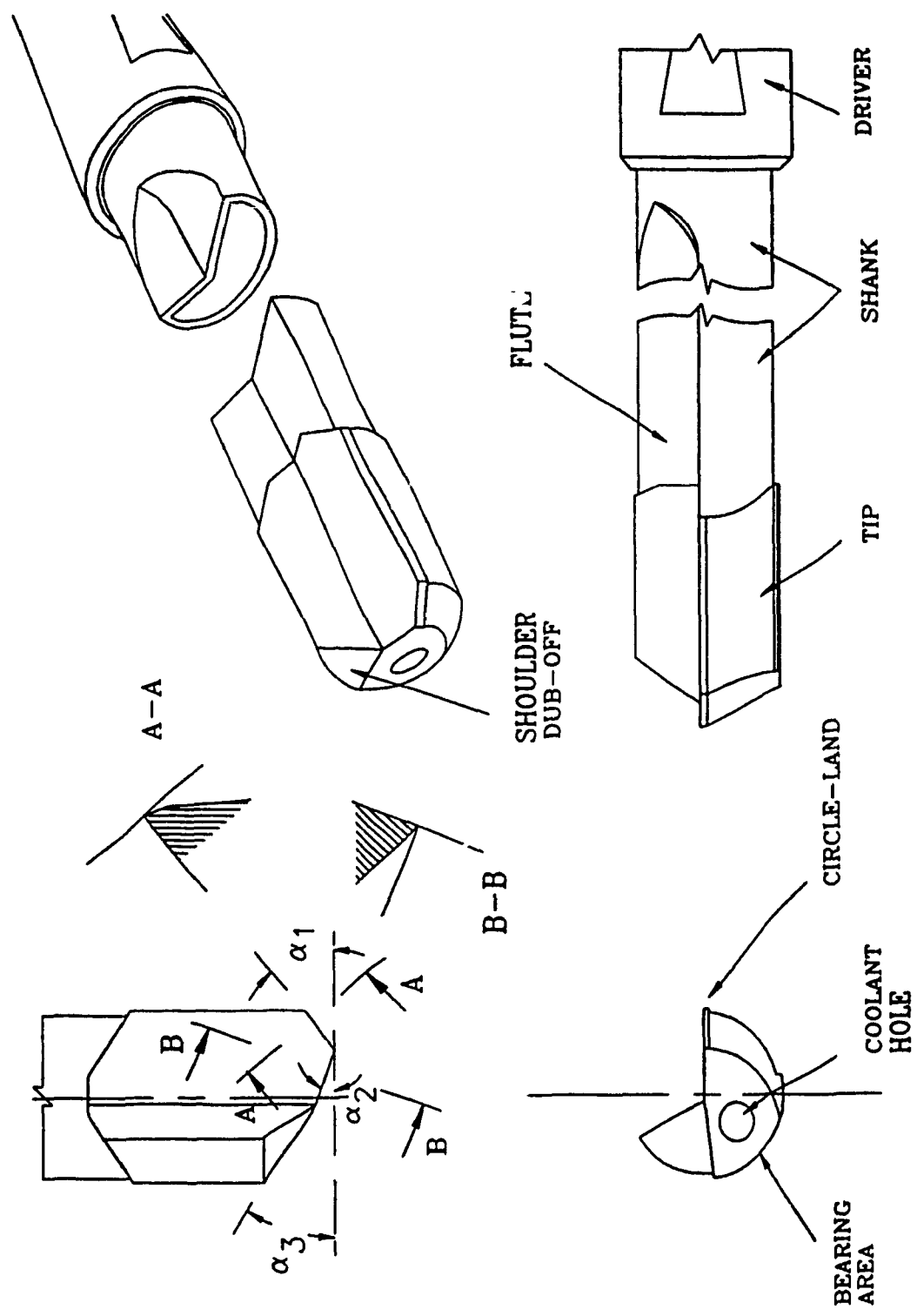


FIG. 2 GUNDRILL

fluid induction, and chip formation and removal. In gundrilling process, the kidney shaped section of the shank is a limiting factor to torque resistance. The BTA process overcomes this problem by using a tubular boring bar. The higher stiffness of the tubular boring bar in comparison to the shank of gundrill, allows higher penetration rates. Fig.3 shows the three typical BTA tools which have one cutting edge and two guide pads in common.

The BTA solid boring tool cuts into solid metal and its cutting edge is designed so that almost a pure end cutting process is taking place. To obtain narrower chips, the cutting edge is usually divided into up to three steps depending upon hole diameter and chip forming characteristics of workpiece material. The inner edge is reversed so that an edge rather than a point is at the axis of rotation. The inner edge has a 30° or less negative rake angle, usually introduced to strengthen the cutting edge thus, to resist a relatively higher cutting force in that region. The outer and middle edges are separated by steps having slightly different approach angles causing the chips to converge and break. Chip breaker groove is also introduced along the outer and middle cutting edges to form C-shape chips which must be small enough to exit freely through the chip mouth. Another version of the standard solid boring head is shown in Fig.4. In this tool the cutting edge is distributed over several overlapping carbide inserts located on either side of the center. The

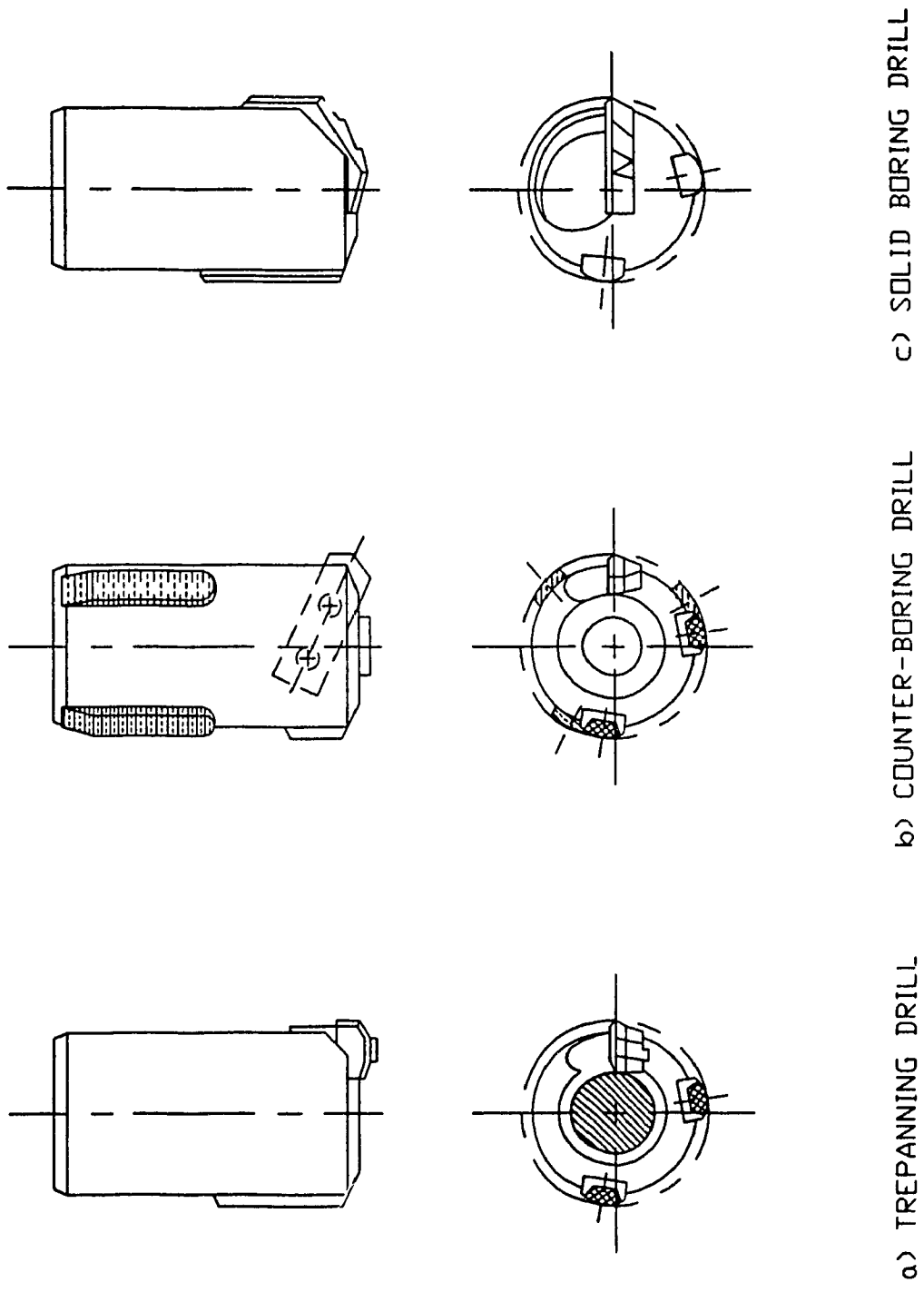


FIG. 3 TYPICAL BTA TOOLS

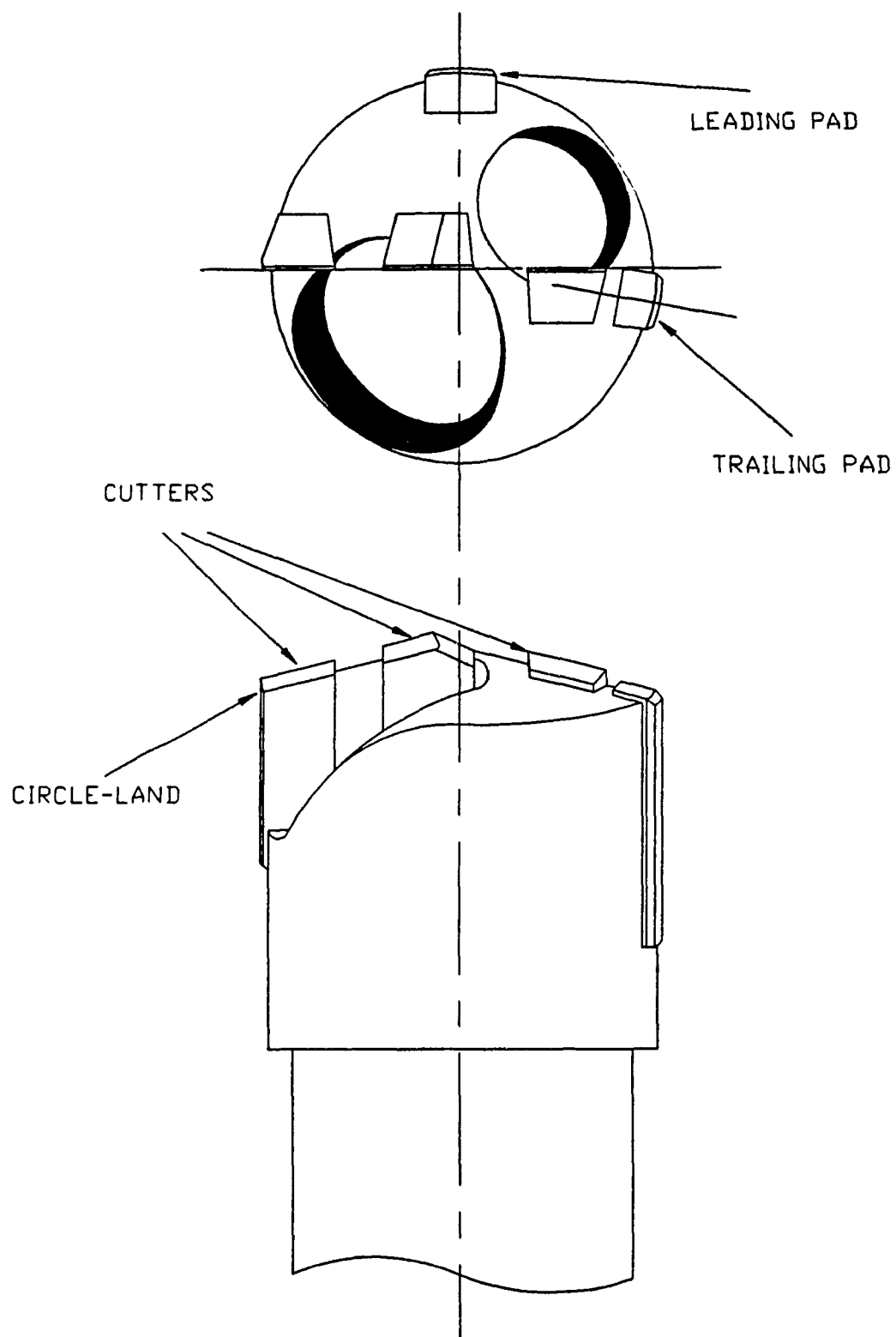


FIG. 4 BTA TOOL WITH DISTRIBUTED CUTTERS

inserts are indexable or brazed to the boring head. This feature of tool simplifies chip breaking and regrinding because no complicated steps are required as with a single edge. Carbide grades can be varied to suit the particular cutting speed along the head radius. The central insert is not pointed but has a straight cutting edge at the center with zero rake angle which gives rise to a more favorable cutting process and a better chip shape near the center where the machining condition is less favorable.

Counter-boring head is a single edge end cutting tool which does not cut to center. It is used for finishing bores of predrilled holes, eliminating the errors in concentricity and run-out and producing stepped bores.

Trepanning tool is a single edge end cutting tool which cuts into the solid by removing an annular groove leaving a turned core in the center. It is used when a large diameter hole is required and it is not necessary to drill along the complete radius. Usually the cutting takes place only over some 55-65% of the diameter. The advantages of trepanning as opposed to solid drilling are reduction in power requirements due to removing a fraction of the hole volume, avoidance of zero cutting speed and, hence reducing total drilling cost.

1.2.3 Ejector Drilling

The ejector deep drilling method developed by Sandvik Coromant, overcomes some problems inherent with BTA deep

drilling system, the sealing being probably the most serious one. As a result, instead of a special deep hole drilling machine, a universal lathe may be used to drill holes of high standard. The process is shown in Fig.5. The ejector tool is designed for a double-walled boring bar where the coolant is introduced between inner and outer tube. Part of the coolant is diverted through the annular nozzles on tool head body into the inner tube. This sets up a partial vacuum in the chip passages of the ejector tool so that the portion of the cutting oil flowing through the drilled hole passes over the cutting edges, collects the chips and is sucked through the inner tube and carried away. The cutting edge from the periphery to the center is divided in such a way that the cutting action is distributed over the opposite sides of a diameter. Due to this distribution of cutting action, the forces exerted on pads and thus, the power consumption are reduced.

1.3 Cutting Force System

Deep hole drilling and boring operation may be considered as an orthogonal cutting process, because the cutters are located around center line of tool head in such a way that the cutting velocity vector at any point is perpendicular to the cutting edge [2]. The resultant cutting force R for orthogonal cutting shown in Fig.6(a) can be resolved into two main components, the tangential or power contributing component $F_p = F_T$ parallel to cutting

COOLANT PASSAGES
TO CUTTING EDGES

ANNULAR NOZZLE

CHIPS AND
COOLANT

CHIP PASSAGES

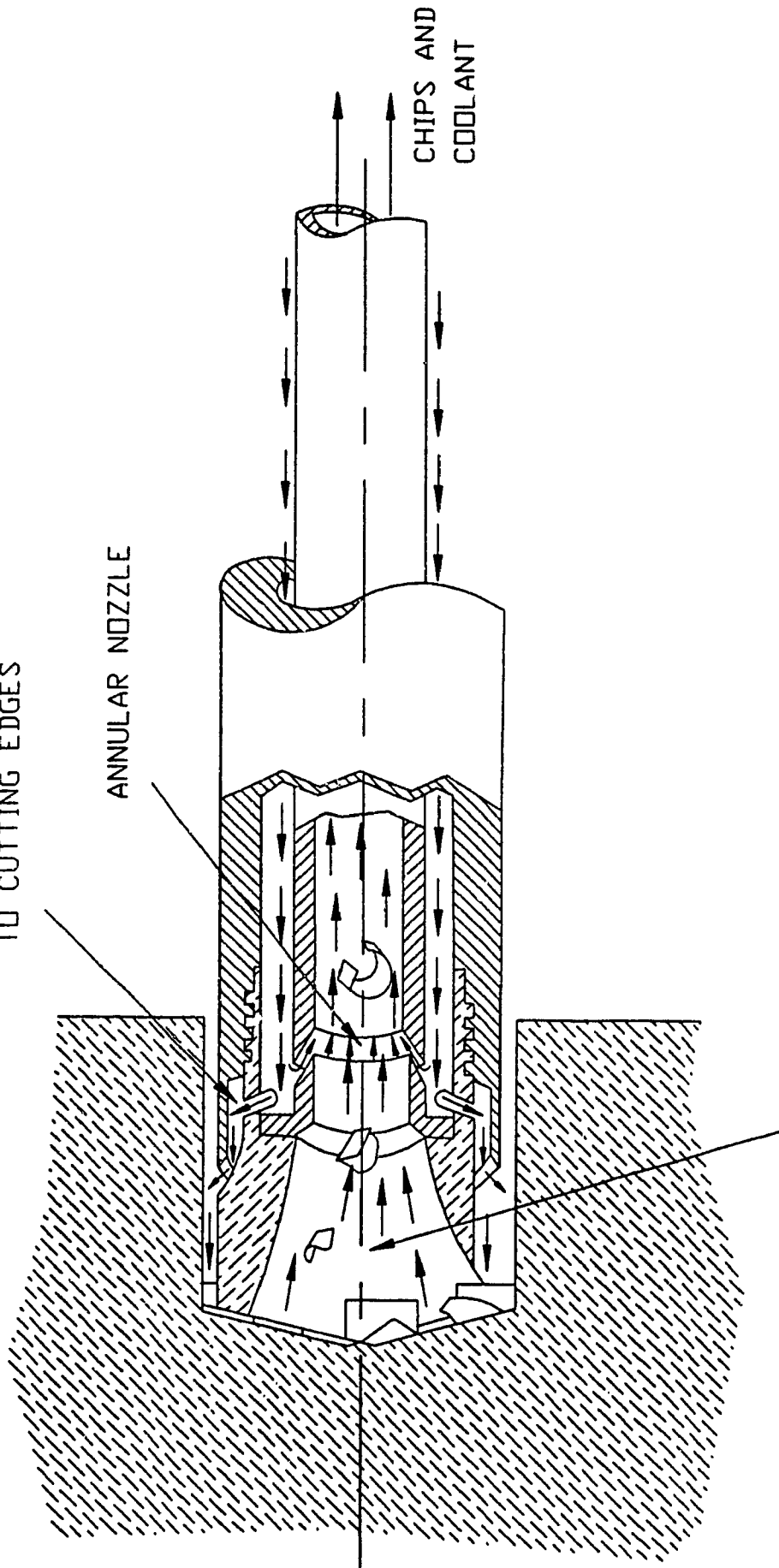


FIG. 5 EJECTOR DRILL

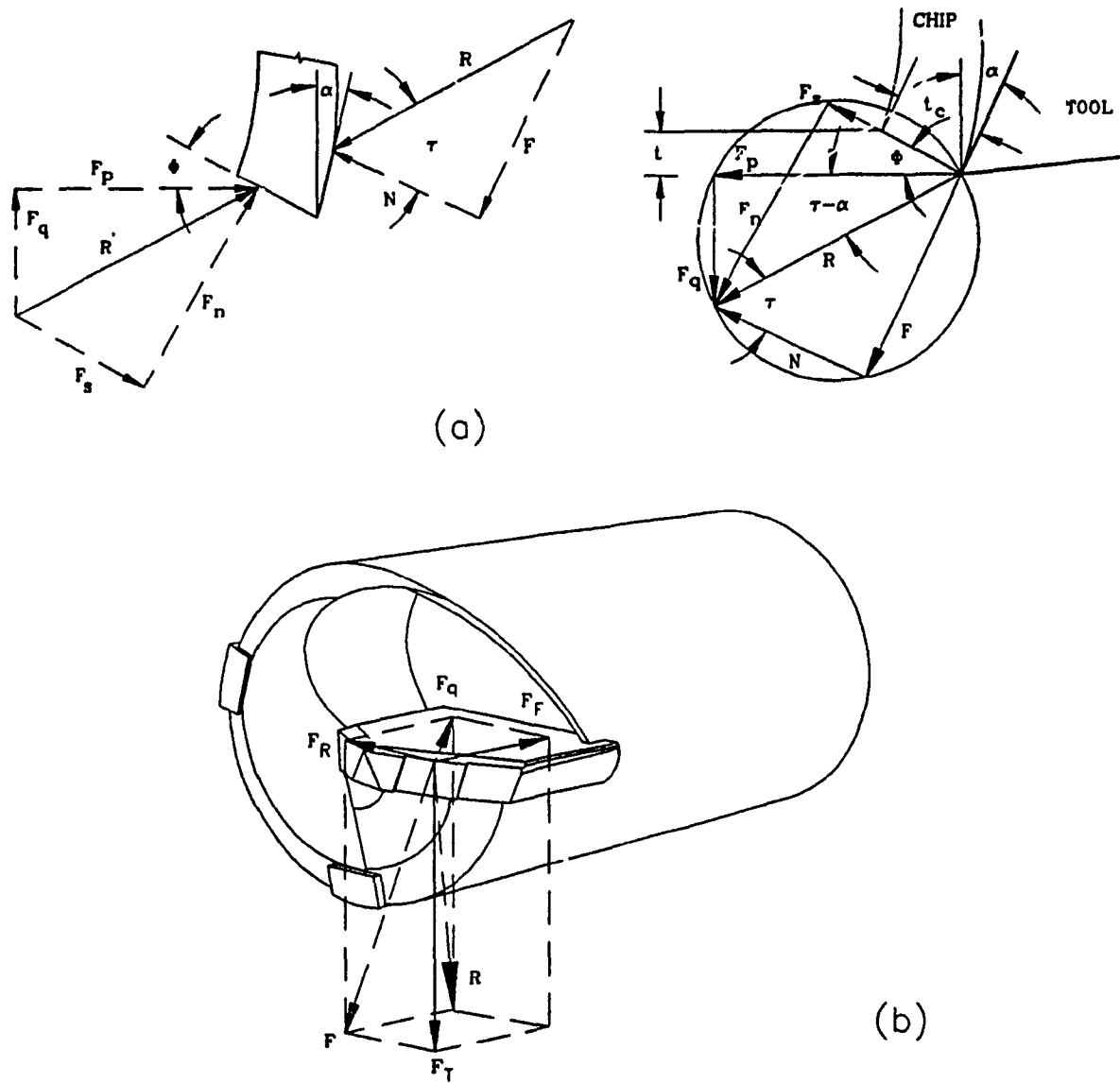


FIG. 6 CUTTING FORCE SYSTEM

velocity and F_q perpendicular to cut surface. In deep drilling tools the F_q is further resolved into two components, the radial component F_R and the feed component F_F due to the inclination of cutting edges relative to the radial direction as shown in Fig. 6(b).

1.4 Literature Survey

In the past few decades an extensive research work has been carried out to analyze the process and explore the solutions to problems concerning deep hole boring and drilling system. Any attempt to improve the performance of these tools and quality of holes needs a thorough understanding of the deep drilling process, the force system involved and tool dynamic behavior for different design concepts and under different cutting conditions. A literature survey therefore is carried out and some of the concepts introduced in research described are taken as the basis for the present work.

1.4.1 Cutting Force Measurement and Analysis

The first attempt to measure the cutting force system in deep drilling operation was that of Astanin [6]. He measured the torque and thrust force in gundrilling operation and showed the effect of speed and feed on force system. Later, Greuner [7,8] tried to measure cutting forces during drilling with BTA solid boring tools by using a dynamometer attached to the workpiece. He was able to

relate forces to the cutting edge form and to show that the maximum forces occurred just before the pads entered the hole. He also measured the magnitude and ratios of tangential, feed and radial forces but shortcoming of his method was that the cutting forces could only be measured when the pads were supported by the guiding bushing. At this stage of drilling he found the tangential, feed and radial forces to be in ratio of 2 : 2.2 : 1. Griffiths [9] used another approach to measure the cutting forces in drilling process and found the force components ratios to be 4 : 2 : 1. These cutting force measuring methods failed to determine the correct value of forces acting during most of the machining process i.e. when the drill penetrated deep into the workpiece. Measurement of cutting forces at any stage of drilling process was carried out for first time by Weber [10]. He built load cells under the cutting edges of a BTA solid boring head. By this method he found cutting force ratios being 5.3 : 4.2 : 1 at low speed and 3.6 : 3.9 : 1 at high feed.

Several other researchers examined the influence of cutting parameters on deep hole drilling force system. They measured the mean values of drilling torque and thrust force using different tools, workpiece materials and tool sizes. They derived the empirical equations for torque and thrust force based on measured values. Griffiths, [11] Chandrashekhar [12] and Latinovic and Osman [13] using BTA solid tool and Pflieger [14] using gundrill found that

cutting velocity has a negligible effect on torque and thrust force since they are only function of feed and tool diameter provided the range of change of velocity is not extensive. On the other hand, the thrust force equation found for BTA solid by Weber [10] and the equations derived for BTA Sandvik and ejector tools by Griffiths revealed a strong influence of cutting speed.

Statistical properties of torque and thrust force in BTA solid boring tools was studied by Chandrashekhar et al [15] and the results revealed that these are random in nature and their dynamics can be characterized as a weakly stationary, wide band random process with Gaussian distribution.

The contribution of friction, burnishing and cutting forces to machining power in BTA solid drilling process was measured by Weber [16], Griffiths and Greive [17] and Thai [18] for different tool sizes. Weber has shown that almost 35 % of the drilling energy is dissipated at the pads, 15 % of that is due to burnishing effect and the rest 20 % is due to friction. Griffiths found these proportions to be almost opposite, 24 % and 13 % respectively. Thai studied the circle land rubbing contribution to drilling torque and has shown that it expends more power than pads during drilling since its share of total torque was 20 % compared to 15 % for the pads.

1.4.2 Friction Coefficient

During deep hole drilling process the bore wall is rubbed and burnished by tool pads. This phenomenon may be compared to that occurring to chip back surface when it is passing over cutter rake face where first the chip material undergoes high strain rate of order of $(10^4 - 10^5)$ micro strain per second, then is rubbed before leaving the cutter [17,19]. Thus, classical definition of friction coefficient can not be applied for either case. But for convenience, the same linear relationship between pad normal and tangential forces is assumed by several authors and its range was found for different tools, using measured values. Greuner [7] found the coefficient of friction on BTA solid tool ranging from 0.2 to 0.29 for a carbide pad when drilling a steel workpiece. In the same way Weber [20] showed that it is ranged between 0.2 to 0.3 and that of Pflieggar for gundrill was from 0.22 to 0.28 [14]. The value calculated by Griffiths was in the range of 0.13 to 0.27. He drilled similar workpiece material and called it tangential friction coefficient. He also calculated the friction coefficient in feed direction and reported an average value of 0.031 [11].

1.4.3 Hole Quality and Surface Integrity

The term " surface integrity " refers to the nature of the manufactured surface and it includes surface texture as well as surface metallurgy. In deep drilling process,

the burnishing action at the front side of the pad is responsible for the surface integrity whereas the rubbing action of the pads is mainly responsible for the hole quality. Surface texture is principally concerned with surface roughness and topography whereas surface metallurgy is concerned with the nature of the surface and sub-surface layers produced in the machining operation. The nature of surface layer has a strong influence on mechanical properties of manufactured parts such as fatigue and stress corrosion. Surface integrity of holes produced by deep hole drilling tools was studied for first time by Drewes and Tiemann [11]. Further study of surface integrity was carried out by Greuner [7] who was particularly concerned with bell mouth region and Sakuma et al [21] whose study was concerned with the surface topography. The most comprehensive study of surface integrity was that of Griffiths [11]. He used a quick stop device to observe the cut surface and concluded that the reason for improved surface finish in deep drilling process compared to conventional drilling methods is burnishing of the bore surface by tool pads. The circle land generates the bore and the pads burnish the surface peaks by extruding the crest material into the valleys such that the peaks are flat topped corresponding to the surface finish of pads. Under high pressure at the front side of guide pads the hole surface is deformed so that two deformed regions are created, a fragmented layer adjacent to the surface with

high hardness compared to bulk hardness where neither the individual grains nor the structure can be resolved, and a deformed region beneath the fragmented region which is less heavily worked. The resulting work hardening extends below the surface, a distance almost eight times greater than the depth of observable grain deformation. He also found that a thin but very hard layer adjacent to the surface similar to white layers observed in other machining and deformation processes, is created. He concluded that this layer is formed due to a thermomechanical process consisted of a heavy cyclic deformation with strain rate of an order of 10^5 micro strain per second, temperature flashes and rapid cooling under high flow rate of coolant.

Parameters affecting the hole quality including surface finish, roundness error and run-out have been studied by several investigators. The hole surface which is observed as plateau-valley forms separated with feed grooves is affected by feed in different ways. Drilling with low feed does not produce enough pressure on hole wall by pads thus, creating poor finish due to insufficient burnishing action. On the other hand, high feed creates deeper feed grooves which deteriorate surface finish despite a better smoothing effect by pads. Consequently there is an optimum feed which gives the best surface finish [22].

Greater roughness of hole surface is created at low cutting speeds (45 m/min) due to tearing of work material

and also due to formation of built-up edge on some carbide grades. The quality of surface finish is improved remarkably with an increase in speed [22,23]. Pads configuration and position also affect the optimum surface finish of the hole. Bergman [24] has shown that the rounded edge pads produce better surface finish as compared to conventional chamfered pads. Frazao et al [25] developed a new BTA solid boring tool with 3 pads where the third pad was located near opposite to the leading pad. By using probabilistic approach and experiments they showed that holes with better surface finish can be produced.

The influence of different coolants on hole finish was studied by Nicolson [26] and Osman et al [27]. Nicolson compared the effect of pure oil and water mixed coolants and showed that the surface finish improved by using pure oil. Osman et al conducted an extensive experiments and developed a new highly compound oil which yields better surface finish of bore and improved tool life relative to conventional deep hole boring coolant oil Shell Garia H.

Rao et al [22] studied the effect of cutting parameters on roundness error and found that it increases at higher speeds due to vibratory displacement of the tool. The same effect was found when the feed was increased. Chandrashekhhar et al [28] derived an equation to predict the maximum possible out of roundness based on the stochastic description of the cutting tool tip motion and concluded that the main factors affecting roundness error

are the feed rate, hole length and damping ratio of spindle-workpiece assembly. Furthermore, the axial force for shallow holes and the radial and tangential forces for deeper holes are the major factors influencing roundness error.

The hole run-out phenomenon in deep drilling process was studied by Griffiths [29], Sakuma et al [30,31] and Rao et al [22]. Griffiths concluded that the directional component of run-out is only due to misalignment and clamping problem but the distributed component is random with normally distributed amplitude. Sakuma found that alignment error of both steady rest and starting bush affect the run-out and the hole deviation is increased with greater starting bush clearance. He also compared the hole run-out produced by a single edge and multi-edge solid boring tools and concluded that a smaller run-out occurs when drilling with multi-edge tools. Rao showed that run-out is increased at higher cutting speeds and concluded that the causes may be vibration, whip of rotating boring bar and the imbalance of forces.

1.4.4 Tool Design

Self guidance ability of deep hole drilling tools is provided by the pads rubbing against the bore wall, thus creating reaction forces to cutting forces. The magnitude and direction of reaction forces on pads is an indicator of the quality of the cutter guidance. For a uniform and

steady drilling process the pads must keep the tool in a stable position. Pflieger [32] developed a stability criterion for deep drilling tool design by considering the moments of the forces acting about each pad. He examined gun-drilling stability with respect to several pad positions and found that the greatest stability can be achieved when the pads are positioned at angles of 90° and 180° from the cutting edge in the direction opposite to the tool relative rotation. He compared the degree of stability of single edge and multi-edge BTA solid boring tool and found that single edge tools were more stable but they suffered from higher pad forces which resulted in higher wear. A different approach for design of multi-edge deep drilling tools has been used by Osman and Latinovic [33]. For this purpose they showed that the symmetrical multi-edge tools have inconsistent performance because the cutting forces are balanced and hence the resultant force becomes indeterminate. They developed a method to design unsymmetrical multi-edge cutting tools based on a given magnitude and direction of resultant cutting force and calculated limiting normal reaction force on the pad such that a hydrodynamic film of coolant be maintained between the pad and hole wall. The resultant cutting force approach was developed further by Latinovic et al [13,34] by extending the earlier model to take into account the cutting force fluctuation and unbalanced forces caused by unsymmetrical cutting head design. Stockert [35] also used

used the resultant cutting force approach for deep drilling tool design but for more specific cases which were concerned with optimum pads position and forces. He defined a criterion called "degree of goodness" for tools with staggered cutters based on relative value of pads normal forces and maximum angular fluctuation of resultant force direction, and concluded that low normal forces on pads result in a better tool design but the goodness for tools having more than two cutting edges can not be increased since this creates more instability in cutting process.

1.4.5 Vibrations

In deep hole drilling process the cutting torque and feed force are transmitted to cutting edges by means of a long, hollow boring bar. It is the weakest part of the system due to relatively low bending and torsional stiffness. The fluctuation of resultant force causes instability in drilling process which may result in self-excited or spiralling vibrations. In extreme cases these types of vibrations may cause a complete destruction of the tool. Stockert [35] and Cronjager et al [36] studied the spiralling vibration of BTA drilling tools and concluded that high amount of dynamic components of forces relative to the static value is the cause of a relatively low reserve of stability of the tool. At this condition the leading pad tilts and the trailing pad rises up for a short period of time, creating a polygonal form of hole. He

asserted that the main cause of spiraling in deep drilling hole is the cutting edge and guide pads arrangement, and it is independent of bending vibration of tool-boring bar system. On the other hand, Sakuma [37] found that the frequency of bending vibration of boring bar during drilling corresponds to the number of lobes of the polygonal form of hole produced by spiraling and concluded that the angular positions of guide pads is the main factor influencing the spiralling vibration.

Among different types of vibration the self-excited vibration is the most dangerous one since it occurs suddenly with large amplitudes. Streicher [38] measured variation of drilling torque relative to cutting speed in gun drilling and concluded that the main cause of this type of instability is descending torque / speed characteristic due to negative effect of speed on total damping of vibrating system. On the other hand, Weber [10] found ascending torque / speed characteristic in BTA drilling. Thai [18] studied the self-excited vibration in deep hole drilling process and concluded that under this type of machining operation a periodic discontinuity in cutting process occurred due to negative relative velocity of cutting edge caused by regenerative effect or coupling phenomenon. He found that the stability of boring tool is mainly function of the torsional and longitudinal stiffness as well as the cutting parameters. He recorded ascending characteristic for torque / speed with smaller positive

slope at higher speeds and feeds. He measured the contribution of cutting edges, circle-land and pads to total fluctuation of drilling torque and showed that the cutters have the strongest influence on tool instability with 67 % followed by circle-land with 24 % and pads with 9 % . He also claims that, contrary to Sakuma's [37] conclusion the polygonal bore is not produced by self-excited vibration.

1.4.6 Tool Wear

In deep hole drilling operation the cutting speed varies along the cutting edge such that near tool center speed is almost zero but increases to a maximum value at tool periphery. This phenomenon creates different working condition along the cutting edge which may cause different wear pattern. A similar condition also occurs along guide pads due to combined burnishing and friction effects and different reaction forces on each pad. The study of several researchers has shown that the wear always occurred at rake face and flank of the cutting edge, the circle land and at the very front end of each pad.

Lundgren [39] studied the wear on BTA tool cutting edge and found different cutting speed ranges where the wear mechanism and pattern changed relatively. Sakuma [23] observed the wear pattern along the cutting edge of BTA tool using different carbide grades and found that from the view point of tool life an optimum tool material exists

for different drill diameters. Nicolson [26] studied the wear of gundrill and found that the flank wear is reasonably constant along the intermediate and the most of the outer cutting edge. It accelerates towards the point where the outer edge and circle-land meet, but very little flank wear is evident in section near the tool center. Corney and Griffiths [40] studied the pads wear in BTA drilling. They showed that the wear on leading pad is much higher than that of trailing pad. But later, Griffiths [11] and Griffiths and Grieve [17] conducted an extensive study on BTA drilling tool wear and found that despite lower initial wear on trailing pad, it is increased faster than that of leading pad such that it is greater at the end of tool life. They found that the pads wear increase with increasing feed but contrary to generally accepted fact about tool wear increase with increasing speed, the opposite is the case for the pads of deep drilling tools. Griffiths [11] measured the ratio of tangential to radial forces for a new and a worn drill and found that its value decreases from 3.45 to 1.35. This shows that the value of radial force increases faster than that of the tangential force during cutting process, which at certain stage, makes the force acting on the trailing pad exceed the force on the leading pad. This has been attributed to the wear of circle-land and cutting edge corner. He also found that the influence of speed on pads wear is much higher than feed. Jurgen [41] showed that outer corner of cutting edge of BTA

tool undergoes higher wear compared to circle-land and flank wear. The circle-land had second highest wear. He measured the pads wear and concluded that the leading pad undergoes higher wear. Rao and Shunmugam [42] studied the influence of cutting parameters on cutting edge and guide pads wear of BTA tools. They found that the crater and flank wear are predominant on the intermediate cutting edge. The crater wear increases with increasing speed whereas that of flank and circle land is decreased. The guide pads wear is minimum at intermediate speeds. Furthermore, flank wear attains a minimum value at an intermediate feed whereas crater, circle land and pads wear increase with increasing feed.

1.5 Objectives of the Present Investigation

Both single-edge and multi-edge BTA solid boring tools with conventional design concept of deep hole drilling and boring tools have been studied by several investigators. Pad forces in these tools are uneven so that the ratio of pad forces is usually greater than 2.0. The design of deep hole drilling tools with equal pad forces was suggested to be advantageous by Cronjager et al [36] which used BTA solid for this purpose. Latinovic [13] designed a multi-edge BTA solid boring tool based on the same approach where no comparative study was conducted. In view of the above, a multi-edge BTA staggered tool is designed with equal mean pad forces and the performance of tool and hole

quality were compared to those of commercially available single-edge and multi-edge BTA solid boring tools.

In Chapter 2, the BTA tool force system is formulated and multi-parameter penalty function method is used to find the optimal tool configuration. Chapter 3 deals with the stability analysis of the designed and two existing tools using Monte Carlo simulation and Pflieghar's method. In Chapter 4 a brief description of experimental set up is given which is followed by Chapter 5 in which the experimental results found from the drilling tests of three tools are studied for performance evaluation and hole quality. Finally, summary and conclusions are drawn in Chapter 6 along with recommendations for future work.

CHAPTER II

2. Tool Force System Formulation

To completely specify the cutting process in deep hole drilling, the magnitude and direction of resultant cutting force are to be determined. For this purpose the steady state and variable components of foregoing values defining the state of resultant force have to be considered. The steady state component can be calculated using two approaches where the limits of variable components can be found either from the previous research work or from experiments.

The two approaches for calculation of the steady state components of cutting forces may be either analytical or empirical method. In first approach the cutting force equations are modeled based on the nature of deformation in cutting zone. There have been two schools of thought regarding the nature of the deformation zone, namely the thin shear plane model and thick deformation zone model. In second approach, the steady state cutting forces are found, using the mathematical relationship developed based on the experimental results.

Chandrashekhar [12] used first approach to evaluate cutting forces assuming the thin shear plane model in deformation zone due to high cutting velocity in deep hole drilling operation. He assumed an average value for chip compression factor in deep drilling process to derive a

general expression for cutting force system.

Latinovic [2] applied second approach in his work, using the method developed by Kronenberg [43] the so called elementary and extended cutting force laws. It is based on unit cutting force concept in metal cutting. In present work, the empirical approach is used for tool design.

The general expression for the unit cutting force is given as [43] :

$$K_p = \frac{F_T}{A} \quad (2.1)$$

where :

A represents the uncut chip cross sectional area.

F_T denotes the tangential or main cutting force. Kronenberg found that unit cutting force is decreased with increasing of uncut chip cross sectional area, but on log log grid they are linearly related.

$$K_p = C_p \cdot f(A) = C_p \cdot f(b, s) \quad (2.2)$$

where :

C_p represents the specific cutting force.

b denotes the width of cut.

s represents the feed per revolution.

The specific cutting force, C_p is the cutting force when depth of cut and feed are equal to unity. Kronenberg also showed that the unit cutting force is independent of width of cut, thus it can be rewritten as :

$$K_p = C_p \cdot s^{-n_1} \quad (2.3)$$

by using the expressions (2.1) and (2.3) the tangential cutting force can be written as follows,

$$F_T = C_p \cdot b \cdot s^{1-n_1} \quad (2.4)$$

or in general it can be written as,

$$F_T = C_p \cdot b^{x_1} \cdot s^{y_1} \quad (2.5)$$

The cutting force perpendicular to cut surface can also be written in the same way in terms of feed and depth of cut.

$$F_q = C_q \cdot b^{x_2} \cdot s^{y_2} \quad (2.6)$$

The feed and radial forces of deep hole drilling tools are determined from F_q by using the approach angle of each individual insert κ_i ,

$$F_R = F_q \cdot \sin \kappa_i \quad (2.7)$$

$$F_F = F_q \cdot \cos \kappa_i \quad (2.8)$$

C_p and C_q can be determined from the experimental results, but due to lack of such information in deep hole drilling process, the data established for turning operation is used since it is a common practice by researchers and

manufacturers of deep hole drilling machines and tools. This assumption can be reliable since it has been found that the tangential cutting force during deep drilling process is almost 10 % smaller than that of turning operation [11].

Latinovic [2] collected the values of the constants and exponents in the expressions given for the cutting forces for cutters with zero rake angle. The collected data showed that the values for x_1 and y_1 the exponents in the expression for tangential force are identical for different steel materials and are equal to 1.0 and 0.78 respectively. In the case of the expressions for feed and radial forces the average values for exponents x_2 and y_2 were found to be 1.0 and 0.65 respectively.

2.1 Design Concept

The concept of staggered multi-edge BTA solid tools with cutters located unsymmetrically on the drill head was first developed by Latinovic [2] and Stockert [34]. They also designed tools based on equal pads forces but no comparative study was conducted with commercially available tools and no quantitative information was given.

In the present work the design is based on an existing BTA multi-edge tool of a major tool manufacturer. It consists of inserts with their cartridges and three pads. The inserts were distributed such that the outer and central inserts are located on one side of tool axis

whereas the middle insert is located on the opposite side. This tool configuration causes the force acting on the leading pad to be four times greater than the force on the trailing pad. The new tool is designed for equal pad forces which will alter the tool configuration.

The resultant cutting force components from Fig.7 can be determined as:

$$F_{Xi} = F_{Tj} \cdot \sin \varphi_i - F_{Ri} \cdot \cos \varphi_i \quad (2.9)$$

$$F_{Yi} = - F_{Tj} \cdot \cos \varphi_i - F_{Ri} \cdot \sin \varphi_i \quad (2.10)$$

The resultant cutting force components have to balance the pad forces.

$$\begin{cases} \sum_{i=1}^3 F_{Xi} - \sum_{j=1}^2 F'_{Xj} = 0 \\ \sum_{i=1}^3 F_{Yi} - \sum_{j=1}^2 F'_{Yj} = 0 \end{cases} \quad (2.11)$$

where,

$$F'_{Xj} = F_{Nj} (\cos \psi_j - \mu_j \cdot \sin \psi_j) \quad (2.12)$$

$$F'_{Yj} = F_{Nj} (\sin \psi_j + \mu_j \cdot \cos \psi_j) \quad (2.13)$$

From the given equations it is clear that the magnitude and angular position of pads resultant force are basically function of :

- The tangential force of each cutter.
- The radial force of each cutter.
- The angular position of each cutter.
- The friction coefficients at the pads.

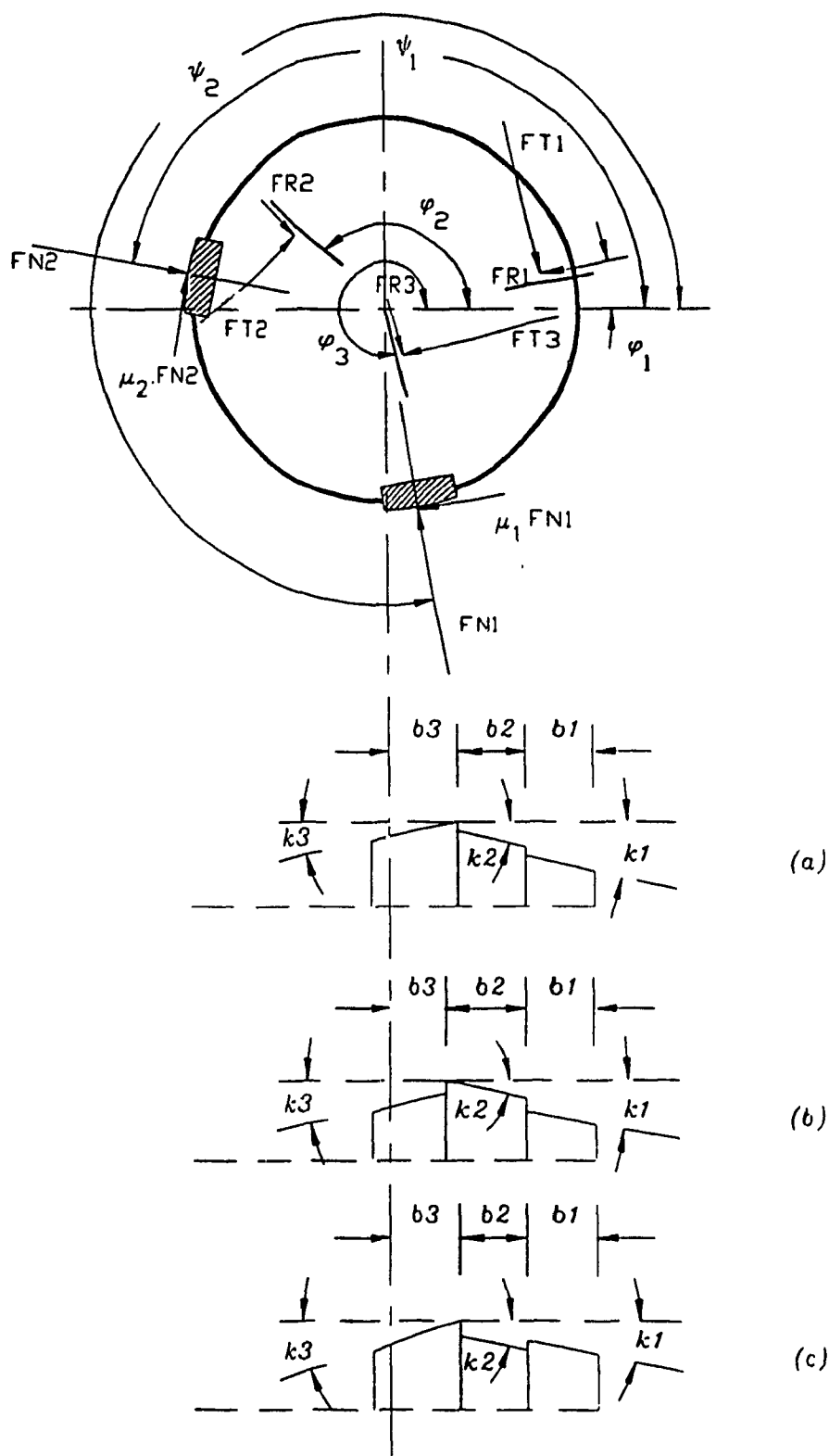


FIG. 7 REVOLVED VIEW OF CUTTERS

- The angular position of the pads.

The resultant cutting force will be transmitted to the supporting pads if the so-called encastre' effect of boring bar is neglected.

From equation (2.11) it is seen that for a given values of pad total forces, coefficients of friction at pads and tool diameter, the problem variables are the cutters width and angular locations of pads and cutters. The problem may have more than one solution but for feasible tool configuration several constraints have to be satisfied.

The value of pad total forces are calculated based on the magnitude of resultant cutting force of the BTA multi-edge tool for the same machining conditions. The average value of coefficient of friction for pads was found from the range of values given in several references and is equal to 0.25 when drilling steel workpiece. The diameter of tool is taken equal to that of the BTA multi-edge tool since the same inserts with the cartridges are used. This selection makes it possible to conduct comparative study of the two commercially available tools.

The arrangement of inserts on tool head can acquire three different configurations based on the revolved view of cutters as shown in Fig.7. In any of the three arrangements, the width of one of the cutters is fixed but those of the other two vary such that the required conditions for resultant force magnitude and direction

to be satisfied. Thus, by knowing the total width of cut equal to radius of the tool only one of the cutters width can be taken as problem variable. Therefore, the total number of variables in equation (2.11) is reduced to six.

The number of constraints necessary for feasible tool design are basically eight. To maintain tool stability and acceptable hole quality the pads have to be located on tool periphery such that the resultant cutting force be balanced at all stages of drilling process. For this purpose the tool needs to be supported at very beginning and end stages of drilling operation as well as steady state stage when drill penetrates in workpiece. To control the hole size, one of the pads should be placed near opposite to circle-land such that the force acting on the pad varies by the hole size and consequently controls it. Also for a stable drilling process the resultant reaction force direction should always bisect the included angle of pads. This one is limited by a minimum and a maximum value. The minimum value is usually taken 90° whereas the maximum value of 120° can be allowed, but conventional deep drilling tools are usually manufactured with maximum pads included angle of 98° .

Another set of constraints are applied to permit enough area for chip throats as well as insert cartridges. Each cutting edge requires chip throat's cross sectional diameter proportional to its width of cut. Latinovic [33] introduced an expression for chip mouth radius as a

function of cutting width and tool diameter given as :

$$r_i = \xi \cdot b_i - d + \sqrt{d^2 - \xi \cdot d \cdot b_i} \quad (2.15)$$

where,

ξ is a parameter which for the best fit of the chip mouth shape its value has been given to be in the range of 1.1-1.2.

d denotes the tool diameter.

b_i represents the cutting width of the i -th insert.

2.2 Optimum Tool Design.

The set of equations given in (2.11) can not be solved analytically due to excessive number of variables and associated inequality constraints for tool feasible design. For this purpose a nonlinear constrained optimization method is applied. The objective is to minimize the difference of resultant cutting force and pad force resultant in such a way that several constraints are satisfied. Therefore the objective function can be written as,

$$F(\varphi_i, \psi_j, b_i) = |R - R'| \quad (2.16)$$

The constraints can take several different forms due to different possible tool configurations. The inserts may form three different revolved view arrangements while the insert holders may be placed on tool head in different

positions relative to each other. All possible tool configurations were tried and only one of them was found to be feasible from the required tool design point of view for the existing inserts as well as their cartridges. In another words, the optimum solution was found only for one of the tool configurations (Fig.7-c).

The constraints for feasible optimum solution are given as follows,

$$\varphi_i, \psi_j, b_i \geq 0 \quad (2.17)$$

The pads included angle constraint,

$$\pi/2 \leq |\psi_1 - \psi_2| \leq 17/12 \pi \quad (2.18)$$

The constraints for tool guidance,

If $(\varphi_1 - \psi_2) < 0$, $(\varphi_3 - \psi_1) < 0$ then

$$(\varphi_1 - \psi_2) + 17/18 \pi \geq 0 \quad (2.19)$$

$$(\varphi_3 - \psi_2) - 1.4 \geq 0 \quad (2.20)$$

If $(\varphi_1 - \psi_2) < 0$, $(\varphi_3 - \psi_1) > 0$ then

$$(\varphi_1 - \psi_2) + 17/18 \pi \geq 0$$

$$(\psi_1 - \varphi_3) + 1.4 \geq 0 \quad (2.21)$$

If $(\varphi_1 - \psi_2) > 0$, $(\varphi_3 - \psi_1) < 0$ then

$$(\varphi_1 - \psi_2) - 19/18 \pi \geq 0 \quad (2.22)$$

$$(\varphi_3 - \psi_2) - 1.4 \geq 0$$

If $(\varphi_1 - \psi_2) > 0$, $(\varphi_3 - \psi_1) > 0$ then

$$(\varphi_1 - \psi_2) - \frac{19}{18} \pi \geq 0$$

$$(\psi_1 - \varphi_3) + 1.4 \geq 0$$

The constraints for angular positions of inserts,

$$|\varphi_2 - \varphi_1| - 1.2 \geq 0 \quad (2.23)$$

$$|\varphi_1 - \varphi_3| - 1.95 \geq 0 \quad (2.24)$$

And the constraints for width of cut is given as,

$$6.0 \leq b_2 \leq 7.86 \quad (2.25)$$

2.3 Optimization Method

To optimize the objective function subjected to inequality constraints, the interior penalty function method is applied. Penalty function method transforms the basic optimization problem into an alternative formulation such that numerical solutions are sought by solving a sequence of unconstrained minimization problem.

If the optimization problem is of the form :

$$\text{Find } X = \begin{Bmatrix} x_1 \\ x_2 \\ \vdots \\ \vdots \\ x_n \end{Bmatrix} \text{ which minimizes } F(X) \text{ subject to :} \quad (2.26)$$

$$g_j(X) \geq 0 \quad j = 1, 2, \dots, n$$

Then the problem can be converted into an unconstrained minimization problem by constructing a function of form :

$$\sigma_k = \sigma (X, \gamma_k) = F(X) + \gamma_k \sum_{j=1}^n G_j (g_j(X)) \quad (2.27)$$

where,

G_j represents a function of constraint g_j .

γ_k denotes a positive constant known as penalty parameter.

Second term on the right side of (2.27) is called penalty term. If the unconstrained minimization of the σ - function is repeated for a sequence of values of the penalty parameter γ_k ($k = 1, 2, \dots$) the solution may be brought to converge to that of the original problem stated in (2.26).

In interior penalty function method for inequality constrained problems two forms of G_j -function are generally used,

$$G_j = \frac{1}{g_j(X)} \quad (2.28)$$

$$G_j = \log (g_j(X)) \quad (2.29)$$

The penalty term is chosen such that its value will be small at points away from constraints boundary and will tend to infinity as they are approached. Therefore, the initial value of penalty parameter (γ_k) and its decreasing sequence have to be chosen such that the optimum value of penalty function can be achieved. It might appear that by

choosing a very small value for initial value of penalty parameter, an excessive number of evaluations of the penalty function can be avoided but from computational point of view it will be easier to reach the optimum of the function if penalty parameter is large. In practice a moderate value is usually chosen in order to achieve a quick convergence. Once the initial value of γ_k is chosen, the subsequent values are found such that,

$$\gamma_{k+1} = c \gamma_k$$

where $c < 1$. The flow chart of the interior penalty function method is given in Fig.8 .

An unconstrained optimization method called as Hooke and Jeeves method is used to minimize the penalty function. It is a direct search method and consists of two different types of searches, called as exploratory and pattern searches. The former is included to explore the local behavior of the objective function, where the later is used to take advantage of the pattern direction.

In exploratory search, one variable is changed at the time and it is sought to produce a sequence of improved approximations towards the minimum of the function. Starting from the initial base point X_1^k , the value of $n-1$ variables are fixed and the remaining variable is varied by prescribed step size of $\pm \Delta X$ in the corresponding direction. If the search is successful where,

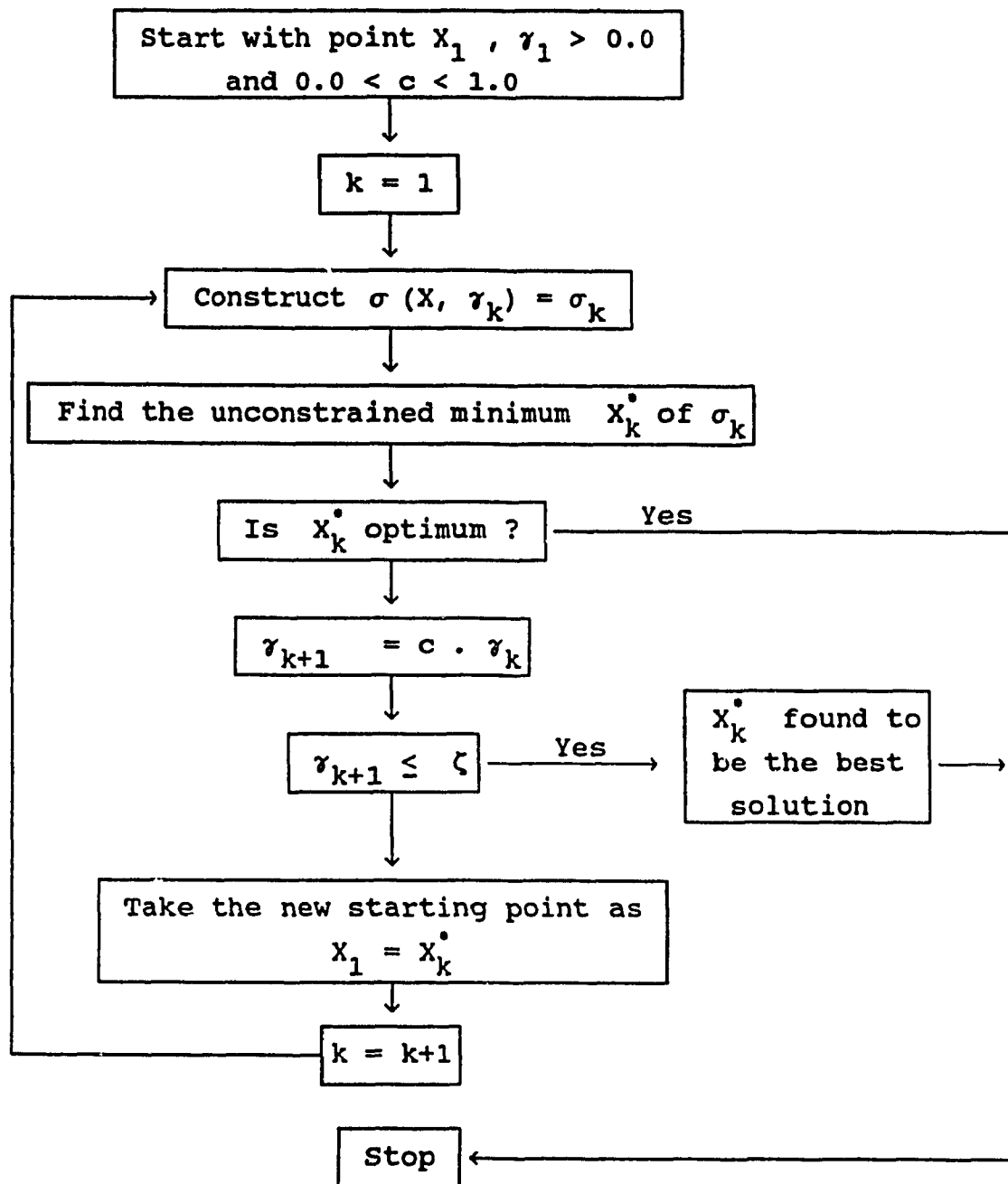


FIG. 8 FLOW CHART FOR THE INTERIOR PENALTY
FUNCTION METHOD

$$\sigma (X_2^k , \gamma_k) < \sigma (X_1^k , \gamma_k)$$

then X_2 is a new point from which the exploratory search for second variable is conducted. The same procedure is repeated for other variables until last point for first set of exploratory search is found. If the exploratory search for all variables fail then the step size is reduced and another set of exploratory search is tried from base point. If it fail again, the same procedure is repeated until the convergence criteria based on minimum step size is reached.

In the case of a successful exploratory search, a pattern search at the direction of a vector which joins the base point and the point found from last exploratory search is attempted. In general the pattern search direction can be given as,

$$\rho = X_{n+1}^k - X_1^k$$

where,

X_{n+1}^k represents the point obtained at the n-th univariate exploratory search.

The step size in pattern search can be taken as unity or optimum step size can be found by applying any one-dimensional optimization method to the function of the form,

$$\sigma (X_1^{k+1} , \gamma_k) = \sigma (X_{n+1}^k + \beta \cdot \rho , \gamma_k)$$

where

$\beta \cdot \rho$ denotes the step size in pattern search.

and if,

$$\sigma (X_1^{k+1}, \gamma_k) < \sigma (X_{n+1}^k, \gamma_k)$$

Then X_1^{k+1} is taken as a new base point which another set of exploratory search is conducted, otherwise X_{n+1}^k is assumed as a new base point of the new set of exploratory search. The process is terminated whenever one of the convergence criteria is satisfied. One of them is based on the step size in the exploratory move,

$$|(\Delta X_i)| \leq \epsilon_1$$

and the other one is based on the relative difference between the values of the objective function obtained at the end of any two consecutive unconstrained minimization,

$$|(F(X_m^*) - F(X_{m-1}^*)) / F(X_m^*)| \leq \epsilon_2$$

where, ϵ_1 and ϵ_2 are small numbers.

2.4 Optimum Tool Configuration

In design of new tool the overall feature of BTA multi-edge tool was maintained except the cutters angular and radial locations and the angular locations of pads. The material chosen for tool was the prehardened AISI-P20 tool steel similar to that of the BTA multi-edge tool. The physical properties of AISI-P20 steel are given in Appendix.

To derive the objective function of the optimization problem the forces involved in drilling process have to be known. For this purpose the experimental data obtained for a steel material with medium strength is used. It is DIN-C60 a steel similar to SAE-9255 with specific cutting forces of [2],

$$C_p = 1730 \quad \text{N/mm}^2, \quad C_q = 1130 \quad \text{N/mm}^2$$

The magnitude of equal pad forces for new tool was found such that the resultant forces of equal magnitude be created on new and BTA multi-edge tools when cutting DIN-C60 steel under the same condition. The exponents of force equations based on previous sections are,

$$X_1 = 1.0, \quad X_2 = 1.0, \quad Y_1 = 0.8, \quad Y_2 = 0.65$$

And the approach angle of cutters are given as,

$$\kappa_1 = 12^\circ, \quad \kappa_2 = 12^\circ, \quad \kappa_3 = -12^\circ$$

The optimum values of tool parameters with minimum value of original objective function are found to be as follows,

$$F(X) = F(\varphi_i, \psi_j, b_i) = 0.6914138794 \text{ E-5}$$

$$\varphi_1 = 0.0^\circ$$

$$\varphi_2 = 0.7582916260 \text{ E+02}^\circ$$

$$\varphi_3 = 0.2475585938 \text{ E+03}^\circ$$

$$\psi_1 = 0.2711932373 \text{ E+03}^\circ$$

$$\psi_2 = 0.1666308136 \text{ E+03}^\circ$$

$$b_2 = 0.6004549980 \text{ E+01}$$

The width of cut of other cutter therefore can be found based on Fig 7-c.

$$b_1 = 8.64 \text{ mm}$$

$$b_3 = 10.76 \text{ mm}$$

The detail drawing of the tool is given in Appendix.

CHAPTER III

3. Tool Stability Analysis

At present time it is a well established fact that the cutting forces in any machining process are dynamic in nature with random characteristics. It has been found that in deep hole drilling like in turning operation the cutting forces are stationary random process with Gaussian distribution [15]. Very few results on the variation of amplitude of cutting force components from mean value have been reported. Greuner [7] found that the fluctuation of tangential and radial forces was $\pm 8.0 \%$ and $\pm 21.5 \%$ respectively relative to their mean values. On the other hand, Cronjager [44] was using $\pm 10. \%$ variation in magnitude for both tangential and radial forces. Weber [10] found the fluctuation of tangential force in BTA drilling to be $\pm 10 \%$ with respect to its mean value. Stockert [35] reported a fluctuation for force ratio of F_R / F_T in the range of 0.1 - 0.2 for BTA tool of 50.mm diameter. Based on foregoing research works, the data given by Greuner seems to be more reliable than that of given by Cronjager. In the same way the pads friction forces or coefficients of friction are random in nature. No information is available on their statistical properties but for a conservative analysis they are assumed to be uniformly distributed. From the variation ranges reported for coefficient of friction, it seems that the range 0.2 - 0.3 is most reliable.

In order to analyze the tool for its stability, the state of pads resultant force regarding its magnitude, direction and position angle have to be studied.

Dynamic behavior of cutting forces and pads coefficients of friction during drilling operation causes the resultant of pads reaction forces and its position angle vary between a maximum and a minimum value. For stable drilling of a given work material with a given tool, the variation magnitude of the pads resultant force and its position angle have to be within certain limits. The minimum pads' resultant force should be such that a sufficient pad normal forces is applied on bore wall in order to achieve a proper self-guidance action during drilling process. In the case of pads resultant force position angle fluctuation, it has to be as small as possible and not to approach any of the two guide pads.

The parameters varying during drilling process are the coefficient of friction at the pads, tangential and radial forces. The magnitude of the pads resultant force on the plane perpendicular to tool axis is only function of tangential and radial forces whereas its position angle varies by change in coefficient of friction as well.

The state of pads resultant force when, the resultant cutting force components ratio varies but its magnitude and pads coefficient of friction are constant, is shown in Fig.9. It is seen that pads resultant force moves parallel to resultant cutting force direction on tool periphery such

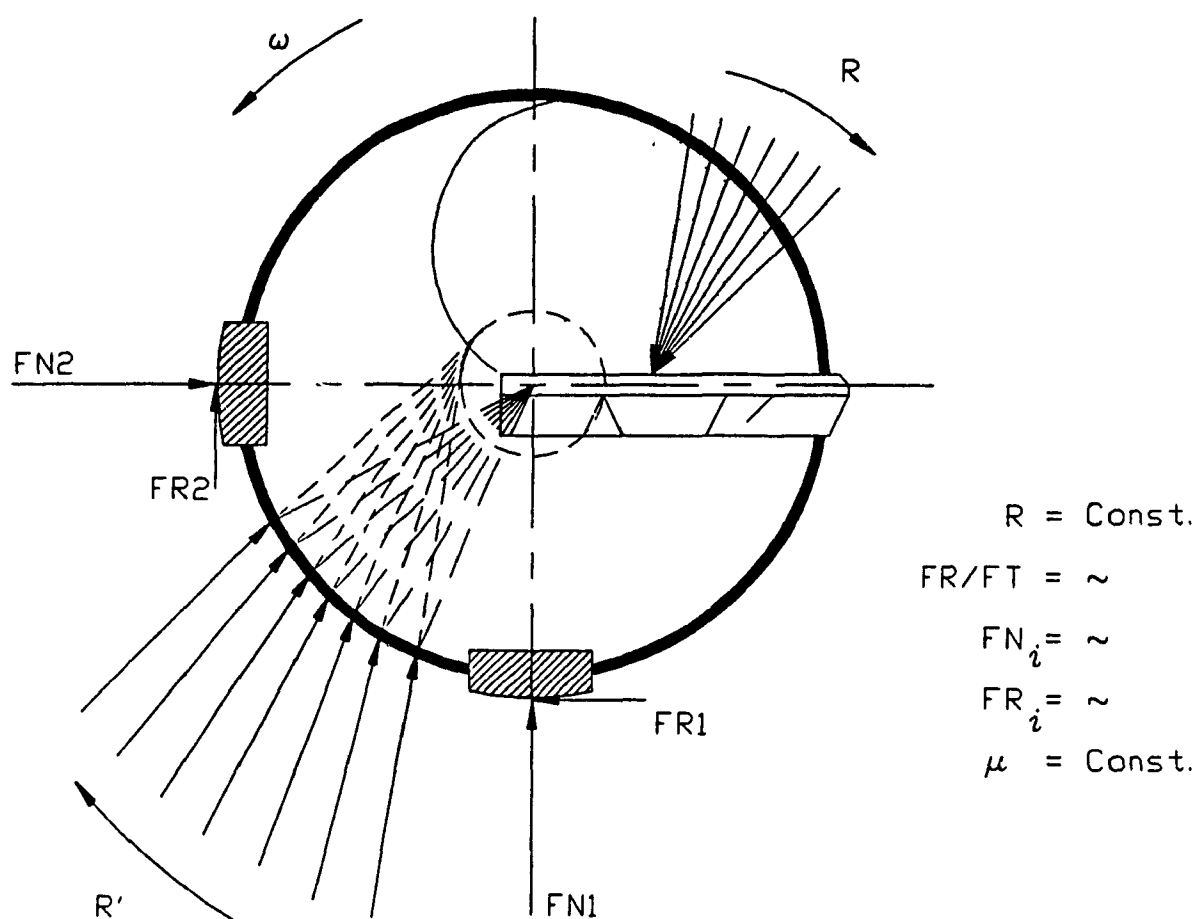


FIG. 9 TOOL FORCE SYSTEM

that it always remains tangent to a circle with constant diameter. Fig. 10 represents the condition when the magnitude of resultant cutting force and its components ratio are constant but the coefficient of friction of pads increase from initial value of zero. It is observed that the point of action of pads resultant force will move at the opposite direction of tool relative rotation such that its magnitude and direction remain unchanged i.e. the same as that of resultant cutting force. In practice, the pads resultant force magnitude, direction and point of action vary randomly around a mean value since all parameters influencing it behave in the same way (Fig.11).

In this study two different approaches are applied to assess the stability of drilling process, the Monte Carlo simulation and the method introduced by Pfleggar [32].

3.1 Monte Carlo simulation

By this method the generated sets of random numbers between -1.0 and 1.0 with given statistical distributions are multiplied by maximum dynamic components of forces and pads coefficient of friction. The magnitude and position angle of pads resultant force are found for the number of the generated random numbers using the calculated and steady state values. Further, the variation range of the magnitude and the position angle of pads resultant force can be obtained.

There is no information available about the

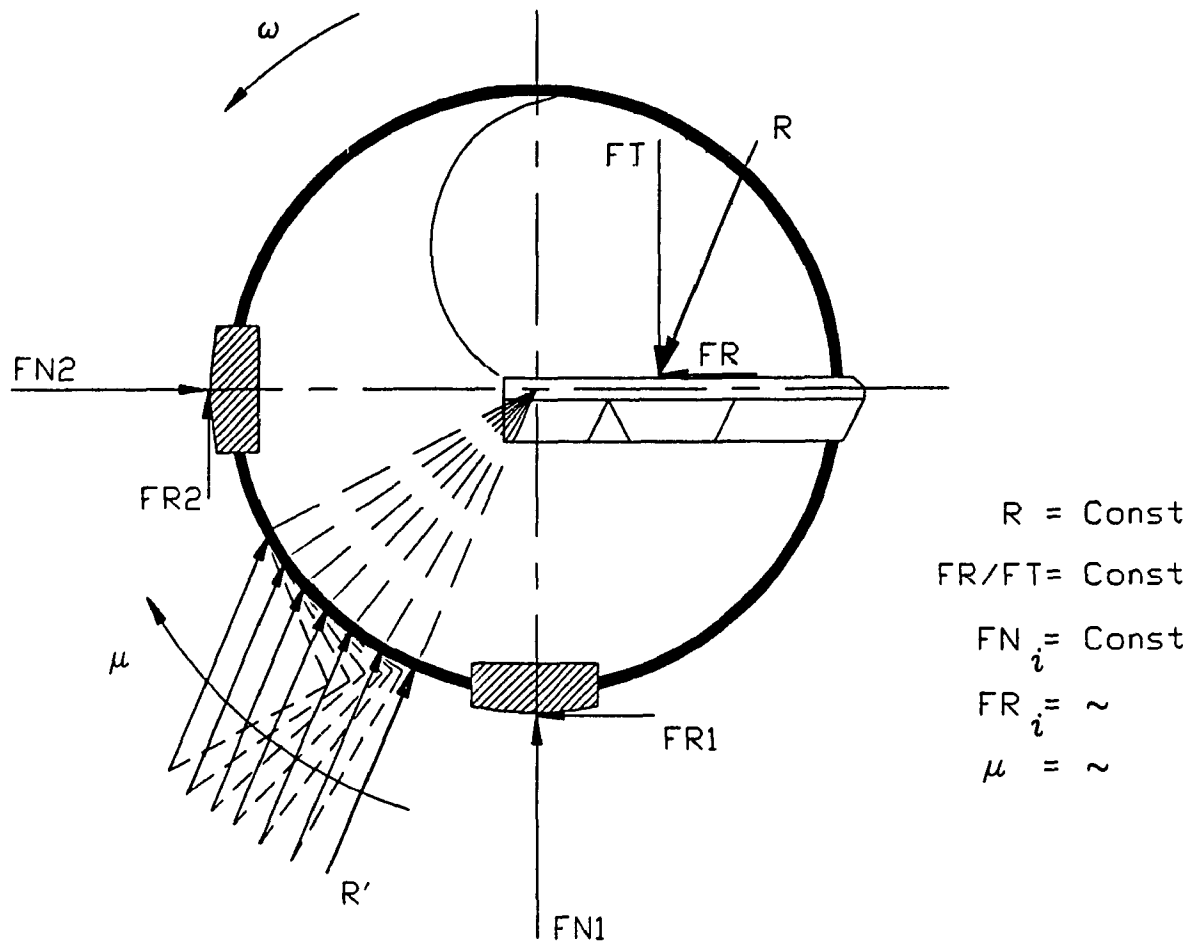


FIG. 10 TOOL FORCE SYSTEM

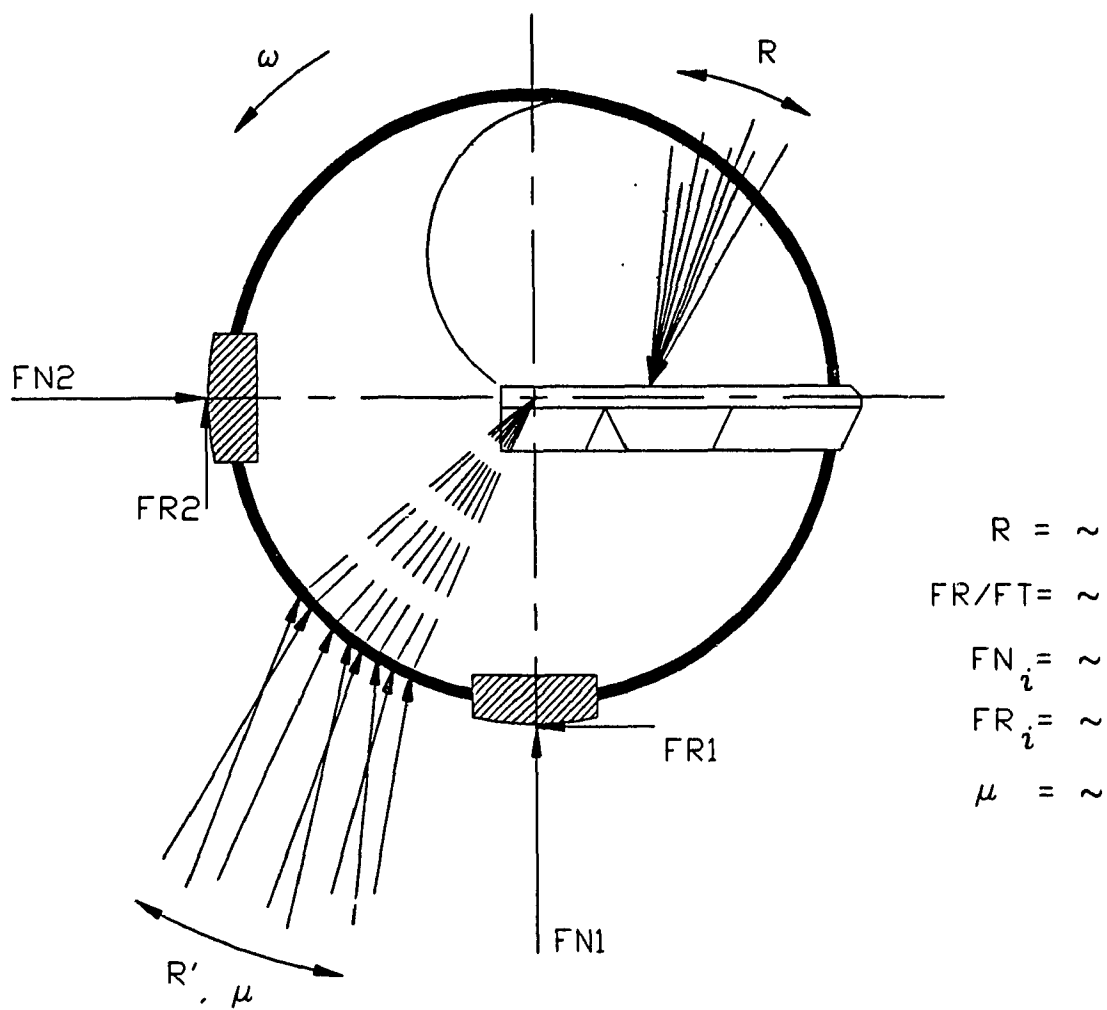


FIG. 11 TOOL FORCE SYSTEM

correlation between cutting forces of different cutters and between friction coefficient of pads, but they are expected to be correlated to a certain extent. Variation of tangential and radial forces seems to be strongly correlated since any axial fluctuation of boring bar or wave cutting affects all cutters simultaneously. Sudden change in magnitude of forces on any of cutters may occur due to inhomogeneity in the workpiece material. In the case of coefficients of friction at guide pads, they are expected to be less correlated. This is a conclusion of Thai's work [18]. He measured the dynamic components of pads normal forces and moments and found that for a small change in pad normal force, a large change in coefficient of friction occurred.

To be able to compare the behavior of designed tool with that of the two commercially available BTA tools, the simulation was conducted for all three tools. For this purpose the probability density function of pads resultant force magnitude and angular position along with pads normal forces for three drilling tools are determined for fully correlated cutting forces and uncorrelated pads coefficients of friction and are shown in Fig.12,13,14. The properties of PDF diagrams can be studied with respect to their distribution and standard deviation as well as the range of each parameter. The mean values of resultant cutting force components along with the mean values and standard deviations of pads resultant force magnitude and

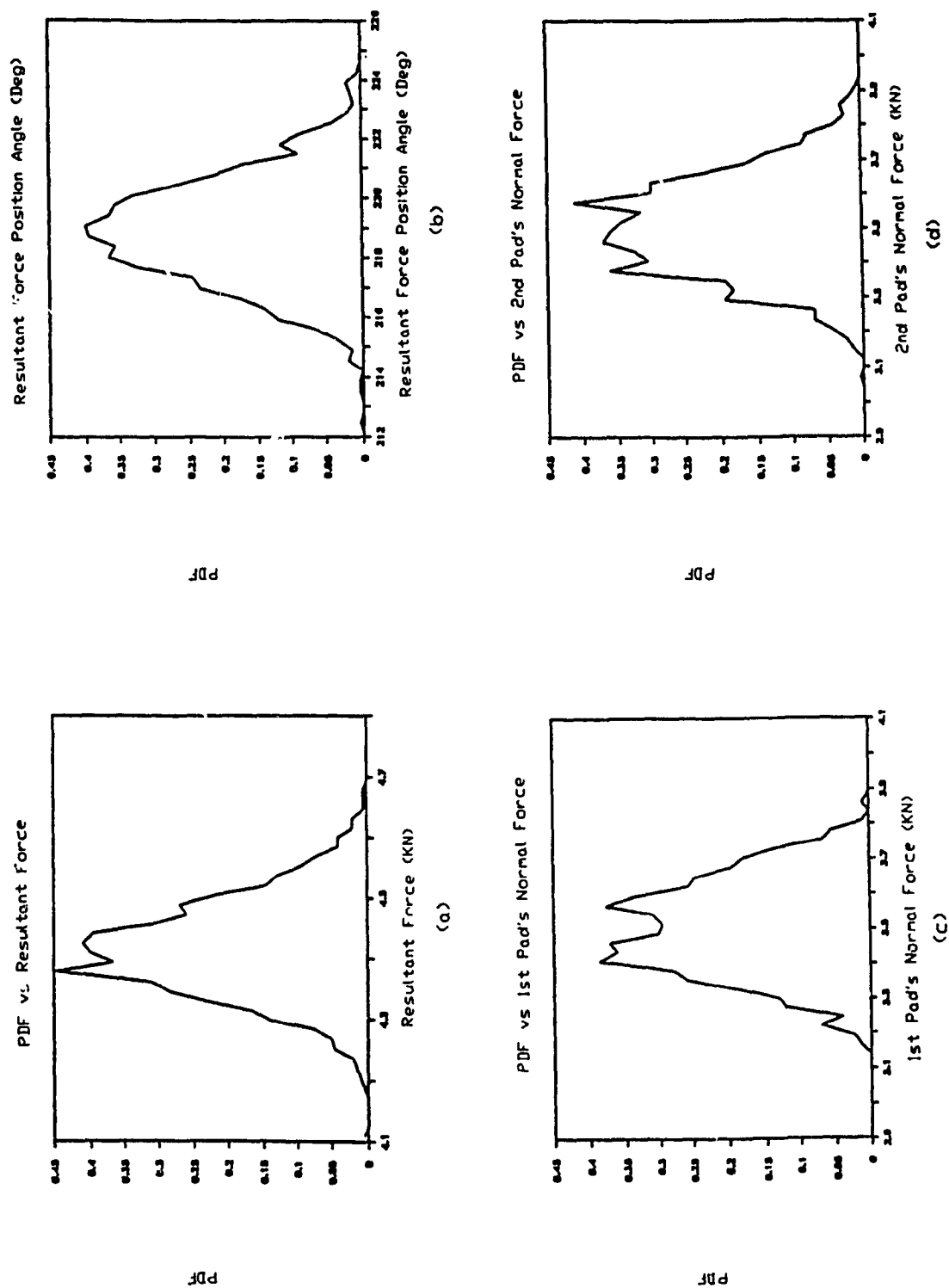


FIG. 12 PDF OF THE DESIGNED TOOL FORCE SYSTEM

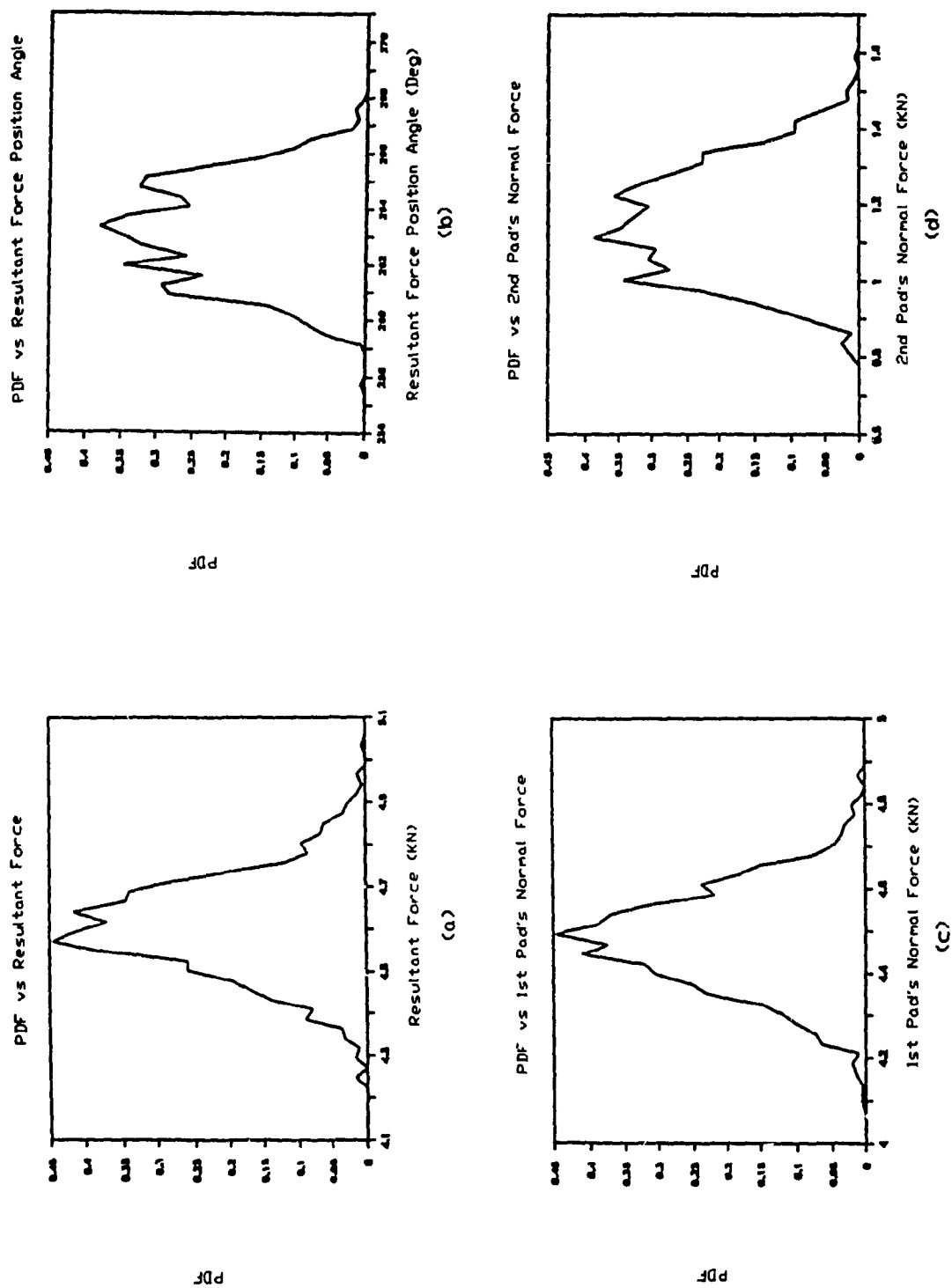


FIG. 13 PDF OF THE BTA MULTI-EDGE TOOL FORCE SYSTEM

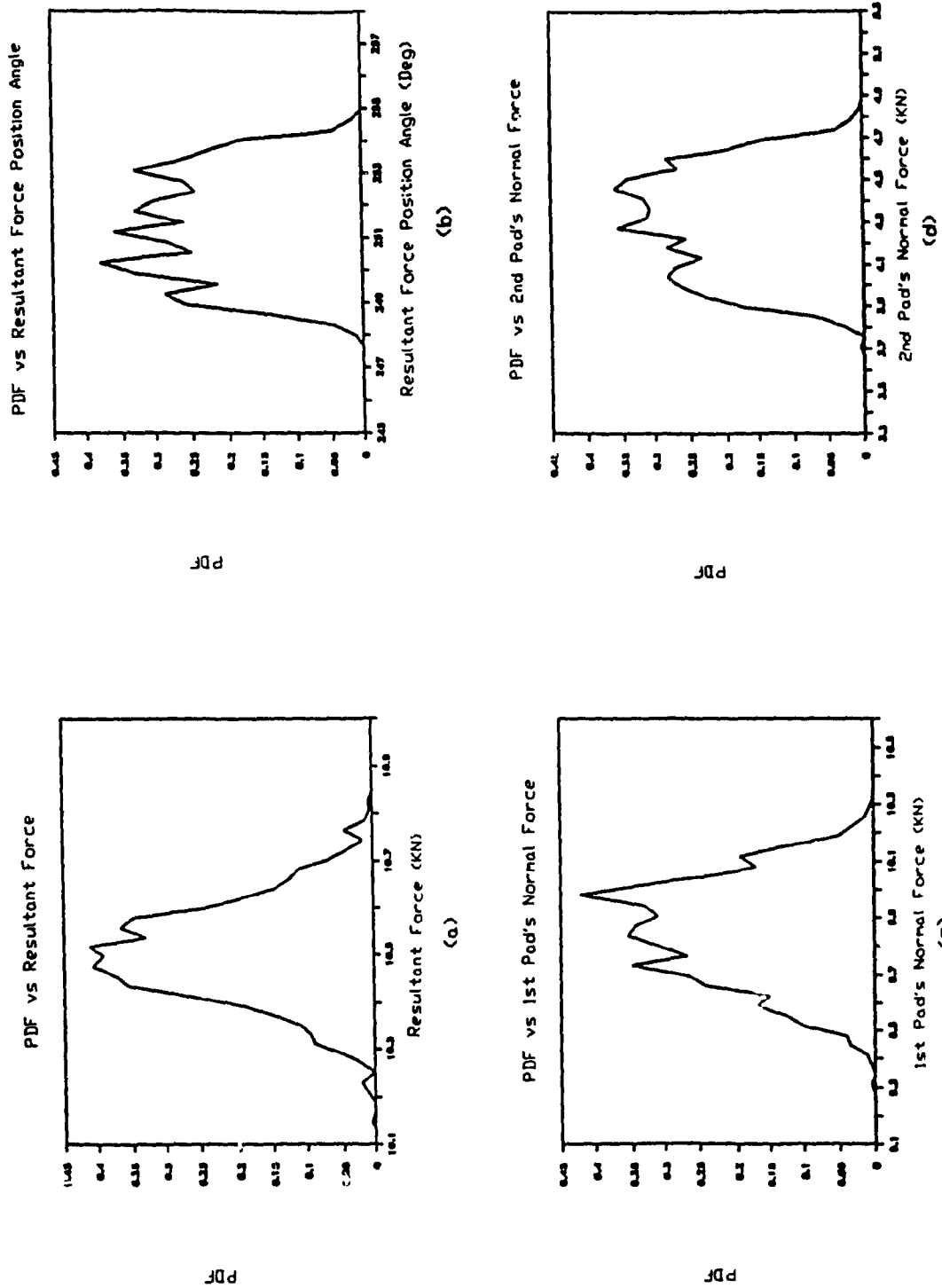


FIG. 14 PDF OF THE BTA SOLID BORING TOOL FORCE SYSTEM

position angle and pads normal forces of tools are given in Fig.15.

The pads resultant force mean position angle of BTA multi-edge tool when the pads friction coefficients are taken equal to 0.2, may approach 268° (Fig. 13-b). It is almost equal to first pads position angle. This characteristic of BTA multi-edge tool results in a force acting on the leading pad four times higher than that on the trailing pad (Fig. 13-c,d). On the other hand, the magnitude of reaction force of second pad may approach comparatively small values. This in turn gives a low reserve of stability to BTA multi-edge tool. In the case of designed tool, it is seen from Fig. 12-c,d that the pads mean forces are equal since it is the main criterion of its design. Their values are large enough to secure a stable drilling performance for the tool. This quality of designed tool may be enhanced when it is observed that the standard deviation of resultant force is smaller and the pads resultant force position angle probability density function (PDF) reveals a Gaussian distribution compared to that of BTA multi-edge tool which exhibits a distribution close to the uniform but with smaller range of variation (Fig. 12-b, Fig. 13-b). The BTA solid boring tool yields different characteristics. Its resultant cutting force and pad forces are much larger than that of the designed tool and the BTA multi-edge tool. Its leading pads mean reaction force is more than two times that of the trailing pad. Although its

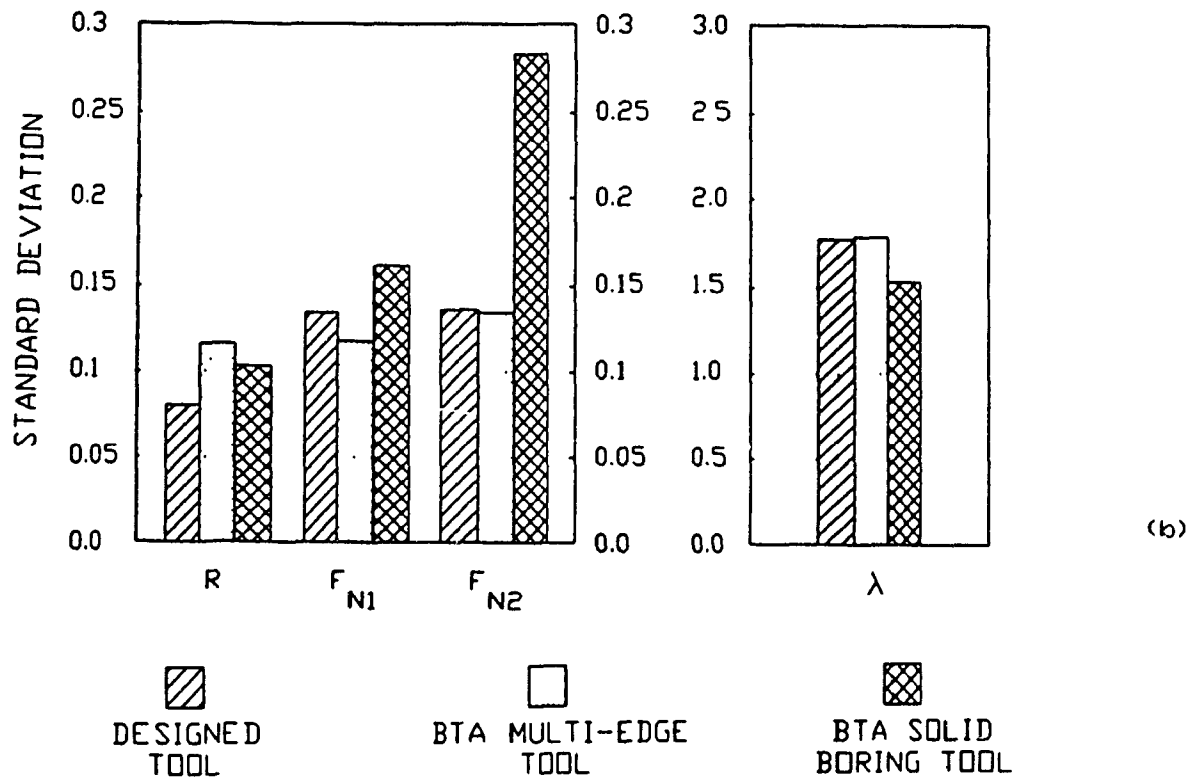
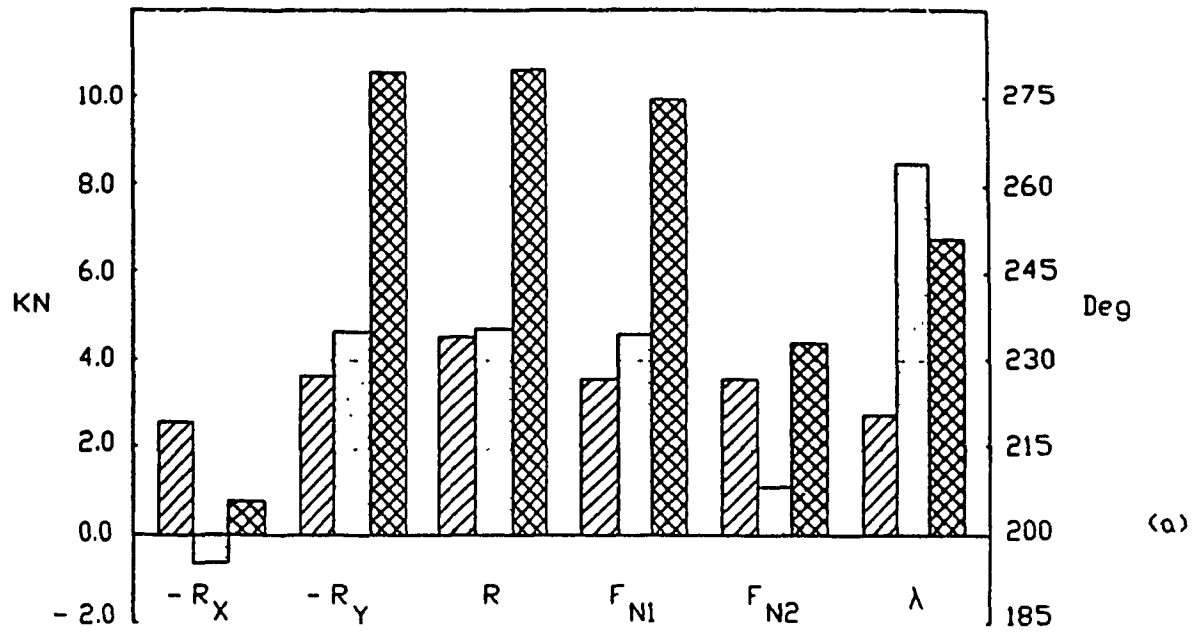


FIG. 15 RESULTS OBTAINED FROM TOOLS
FORCE SYSTEM SIMULATION

PDF exhibits almost a uniform distribution (Fig. 14-b), due to the comparatively small range of variation of pads resultant force position angle and large pad forces it still performs with large reserve of stability.

3.2 Pfleghar Method

Guide pads play a key role in deep hole drilling and boring processes. In addition to the forces on the cutting edges there are reaction forces on the guide pads. Their value and direction is an indicator of the quality of the tool guidance. Thus, for a stable drilling process, the guide pads have to be pushed consistently on bore wall. Based on that Pfleghar defined the degree of stability for deep drilling tools as the ratio of sums of opposite moments acting on each pad given such as,

$$S = \frac{\sum \text{Holding Moment}}{\sum \text{Tilting Moment}}$$

A high degree of stability indicates a stable support of the tool, i.e. a very low tendency for the cutter to tilt around one of its guide pads. Considering one pad to be the moment point, the holding moment is a moment which presses the other pad against the bore surface. On the other hand, the tilting moment tends to tilt the tool around the reference pad such that the other pad is lifted from the bore surface.

Considering Fig.16 which shows the force system on a

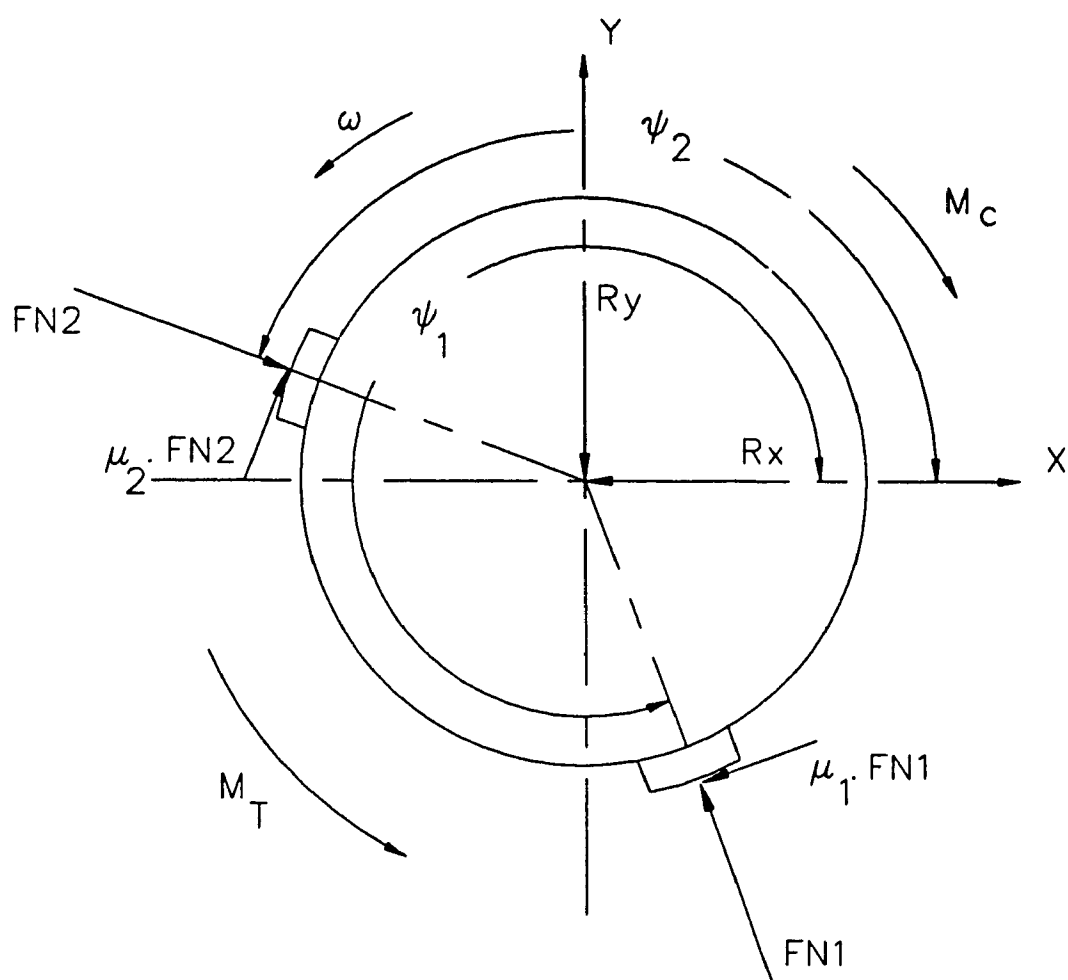


FIG. 16 TOOL FORCE SYSTEM

tool head, the resultant force is given by its components R_X and R_Y passing from tool center and cutting moment M_C . The total drilling moment M_T which the tool exerts in the direction of cutting moment is given as,

$$M_T = M_C + \mu_1 \cdot F_{N1} + \mu_2 \cdot F_{N2}$$

and by considering the general coordinate directions, the holding and tilting moments around the leading guide pad can be written as,

$$M_{h1} = M_T - d/2 (R_X \cdot \sin \psi_1 - R_Y \cdot \cos \psi_1)$$

$$M_{t1} = M_C$$

Then the degree of stability is given by,

$$S_1 = M_{h1} / M_{t1}$$

When tilting around the trailing guide pad is considered, the tilting torque is,

$$M_{h2} = M_C + d/2 (R_X \cdot \sin \psi_2 - R_Y \cdot \cos \psi_2)$$

$$M_{t2} = M_T$$

or,

$$S_2 = M_{h2} / M_{t2}$$

The smaller one of the S_1 and S_2 determines the overall degree of stability of the tool (S) which is responsible for tool failure or quality.

The following cases may occur corresponding the degree of stability.

Stable condition $S > 1.0$

Unstable condition $S \leq 1.0$

Pfleggar conducted experiments using gundrills with different configurations and showed that the tools with higher degree of stability perform better and produce bores of higher quality.

The degree of stability of three drilling tools were calculated using randomly distributed values for cutting forces and coefficients of friction in the same way used in Monte Carlo simulation. They are given as follows

Designed tool $S = 1.26$

BTA multi-edge tool $S = 1.16$

BTA solid boring tool $S = 1.6$

It was found that the degree of stability of the tools are almost insensitive to change in statistical correlation coefficients of the cutting forces and the friction coefficients .

Based on the results obtained from Monte Carlo simulation and Pfleggar's method it is expected that the designed tool is inferior with respect to BTA solid boring tool but better than the BTA multi-edge tool.

CHAPTER IV

4. Experimental Set-up

The designed tool was built at University Machine Shop and tested along with BTA multi-edge tool and BTA solid boring tool of the same diameter.

4.1 Tool Tests

Designed Tool

The tool was designed with three cutting edges and with a nominal diameter of 2.0 inches using BTA standard indexable carbide inserts and corresponding cartridges. All inserts have the cutting edge rake angle equal to 1.0° . Two BTA standard indexable coated carbide pads are also used as leading and trailing guide pads along with a third pad of hardened steel which precedes the circle-land. The third pad is mainly utilized to prevent the hole surface being scratched by the circle-land while the tool is withdrawn. The guide pads included angle is 104.5° and the third pad has been located 67° from the circle-land. The detail drawing of the inserts and pads are given in Appendix.

After building the prototype and setting up the machine, the tool was tested for its performance. The prototype is shown in Fig.17. At the first test the outer



FIG. 17 DESIGNED TOOL'S PROTOTYPE

insert crashed at the hole depth of about 10 mm. The workpiece material was cold rolled AISI-C12L14 steel and the drilling feed and speed were 50 mm/pm and 57 smpm respectively. Later, when the machining stopped after a few millimeters of drilling to observe the tool condition, it was found that the breakage of the insert is due to inadequate size of the outer cutter chip mouth. Fig. 18 shows the blocked chip mouth of the outer cutting edge. The problem was partially solved by opening up the chip mouth to maximum allowable size due to limitation imposed by tool configuration.

BTA Multi-Edge Tool

The BTA multi-edge with 2.0 inches diameter has three distributed cutting edges which are of indexable inserts identical to those used in the designed tool. The inserts are located at either sides of tool axis along a straight line. The guide pads are located at 98 deg from each other along with a third pad at almost 180 deg from the leading pad. Fig. 19 shows the BTA multi-edge tool used in this investigation

Due to configuration of the tool the resultant cutting force and its components differ from those of the BTA solid boring tool and the designed tool. The direction of X-axis component of resultant cutting force is towards circle land where that of the other tools is towards trailing pad. For this reason, the pads force ratio is almost 4.0 contrary to

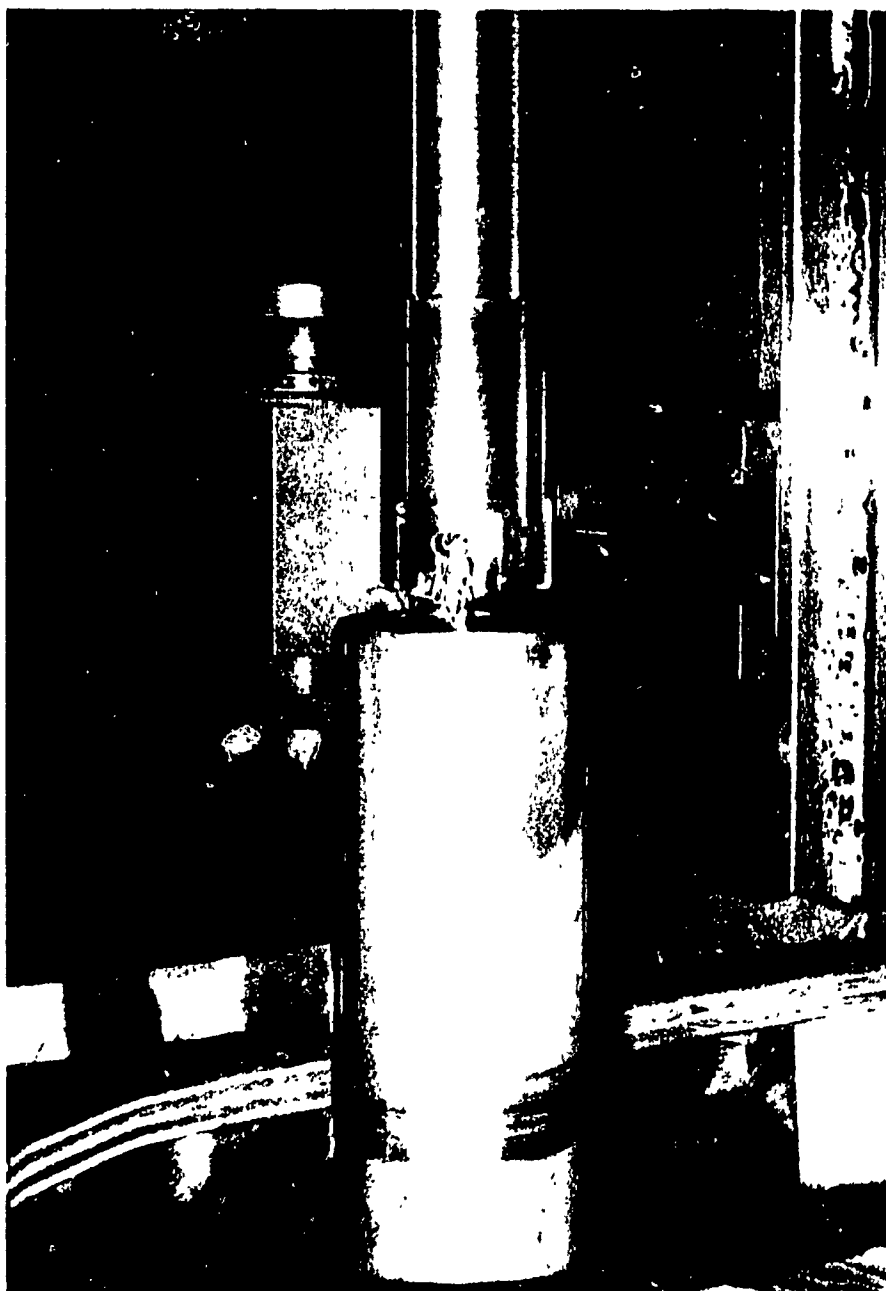


FIG 18 THE BLOCKED CHIP MOUTH

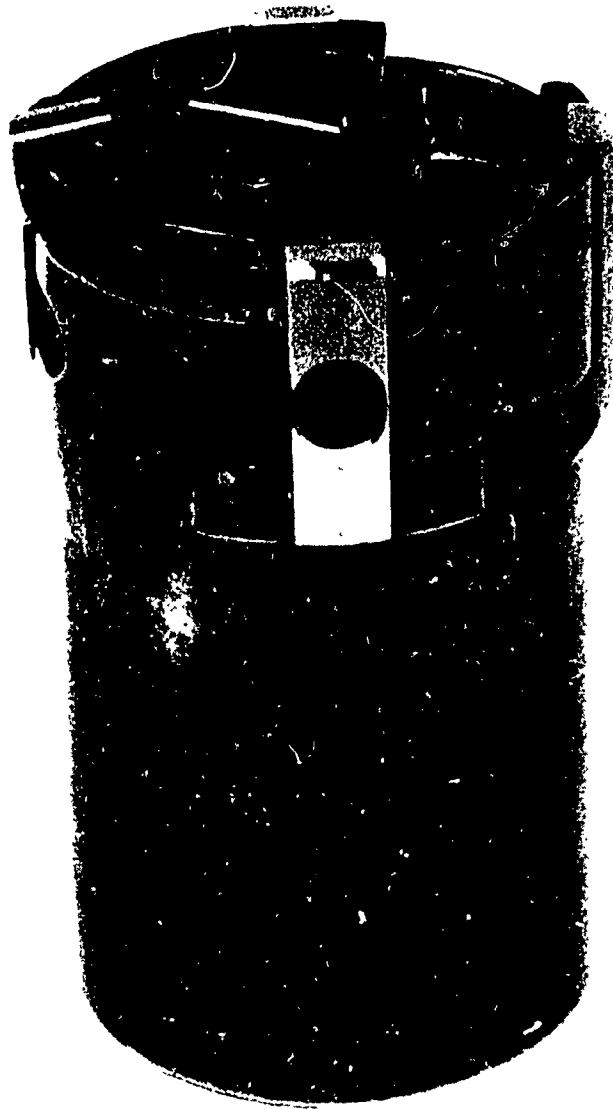


FIG 19 BTA MULTI-EDGE TOOL WITH DISPOSABLE INSERTS

that of BTA solid boring and designed tools which are 2.0 and 1.0 respectively. These properties of BTA multi-edge tool in turn affects the degree of stability and consequently the drilled hole quality.

BTA Solid Boring Tool

The BTA solid boring tool has three major differences as compared to the BTA multi-edge tool and the designed tool which are the cutting edge and the pads configuration and the coolant pressure distribution at the tool head.

It has a single cutting edge which is divided into three steps and extends from tool periphery to the center. The pads which are located 98 deg from each other are larger in size as compared to those used for BTA multi-edge tool and designed tool. The pads bearing surfaces have the same curvature as the hole whereas the pads of the other two tools have smaller curvature. The cutting edge and pads are brazed to the tool thus yielding higher rigidity. The pressure distribution of coolant on tool head is such that better condition for chip removal is created. The pressure distribution on each tool head was measured using plexiglas workpiece and pressure gages. The Fig. 20 shows the coolant pressure distribution on BTA solid boring tool. It was observed that a partial vacuum was created inside the chip mouth which in turn provided less resistance to chip breaking. Similar phenomenon was not observed in the case of the prototype and BTA multi-edge tools.

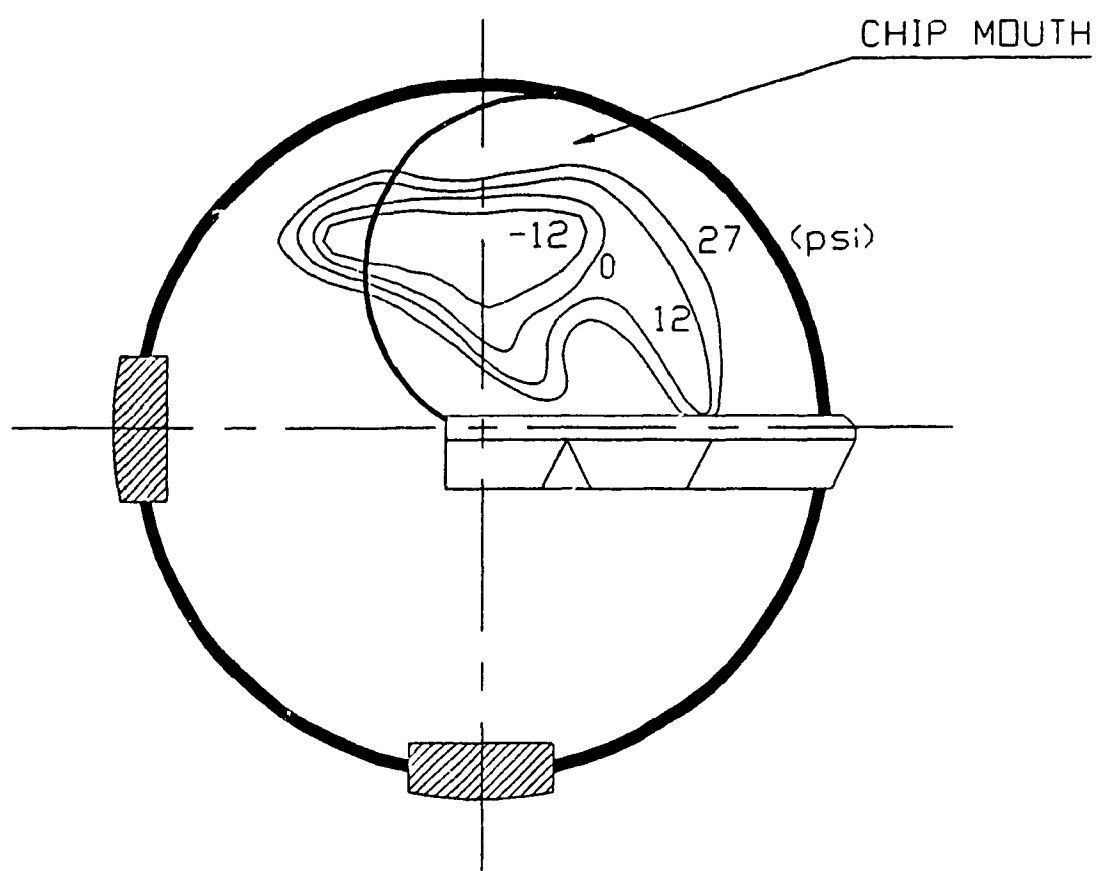


FIG. 20 COOLANT PRESSURE DISTRIBUTION ON BTA
SOLID BORING TOOL CHIP MOUTH

4.2 Machine Tool

The deep hole boring machines are usually a single purpose high production type, designed specifically for the jobs to be performed. Because of generally high forces and cutting speeds associated with this drilling method and the fine finishes and close tolerances produced, these machines have to be manufactured highly rigid to minimize alignment error and vibration. For optimum drilling performance, they should also be equipped with a system of controls to achieve precision work, capable of close-tolerance alignment which is easily set up and maintained and have a infinitely variable feed mechanism. The feed rate should be adjustable in infinitely variable increments to insure the best possible cutting conditions for a particular application. Adjustment in feed and speed should be possible while drilling in progress and while chip formation is being observed [1].

The deep hole drilling machine used for present investigation is essentially a 30HP long bed lathe retrofitted into a deep hole machining system. It is equipped with five major components namely,

- a) The drive unit
- b) The Lanchester damper
- c) The oil pressure head
- d) The cutting oil filtering and cooling system
- e) The boring bar

Fig. 21 shows the machine set up components described in

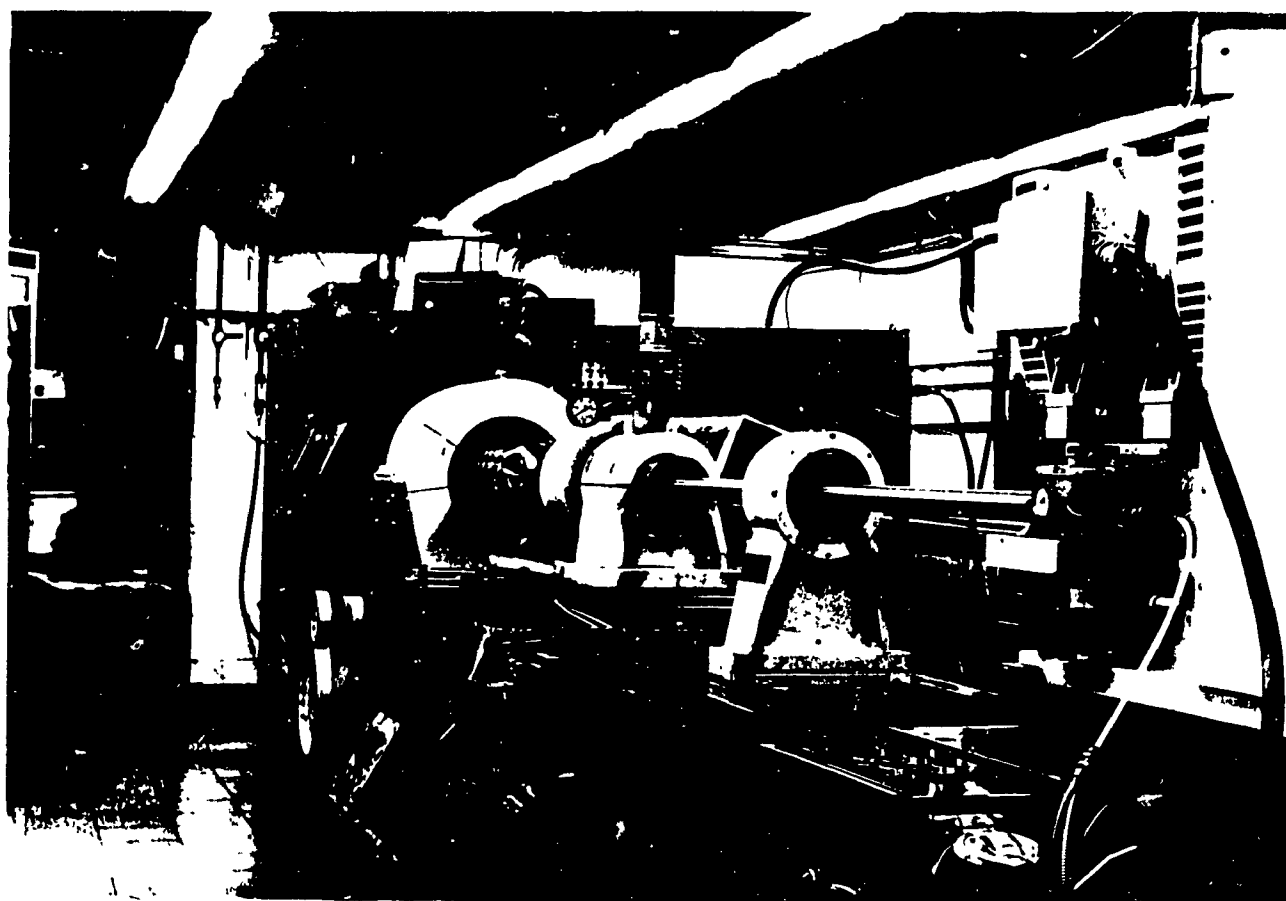


FIG. 21. EXPERIMENTAL SET UP FOR TOOL TESTING

the following paragraphs.

The lathe is a Schaerer HPD631 with a center to center distance of 4 m and the spindle height of 0.45 m. The spindle is supported on two high accuracy roller bearings mounted on a cast iron structure which forms the head stock frame. It is driven by a multi-speed gear box through a set of V belts providing a wide range of speeds. The tail stock has been replaced by the pressure head on the drilling table. The drilling table remains stationary during drilling since the workpiece is clamped between pressure head and spindle chuck.

The drive unit is an accessory to the deep hole machining system. The location of the drive unit on the machine is at the end opposite to that of the head stock assembly and it basically replaces the tail stock of the lathe. It is mounted on a carriage which moves along the bed of the machine by means of the feed screw. It is powered with a 20 HP electromotor and the spindle speed can be varied using a timing belt assembly.

Lanchester damper is a passive type torsional damper. It consists of a cone shaped rotating mass made of a synthetic plastic material and supported by a steady rest by means of roller bearings. It has several longitudinal slots same as a collet by which the friction between the boring bar and damping mass is adjusted. During the drilling process, the steady rest is moved along the machine bed with the speed equal to feed rate, thus

maintaining the boring bar-damping mass coupling point distance constant from drilling tool.

The oil pressure head bolted to drilling table is located between head stock and drive unit. It is one of the most important components of deep hole drilling machine by which a successful boring operation can be achieved. Pressure head has three main functions :

- 1- When starting a bore, the cutting forces are transferred through the guiding bushing and the drilling table.
- 2- The coolant flow is directed through the pressure head around the boring bar to the tool providing fresh oil to the cutters, circle land and guide pads.
- 3- The pressure head provides sealing against boring bar as well as the workpiece using felt seal-rings and a countersunked reception plate respectively.

It has to be precision manufactured and correctly mounted on machine such that the axes of guiding bushing, drive shaft and spindle are aligned and maximum misalignment of axes has to be less than 0.025 mm. The cutting oil used in deep drilling operation has to perform the following functions :

- a) lubrication of the cutting edges and the pads and preventing the formation of built-up edge.
- b) cooling of the cutting edges and the pads.
- c) chips clearance and transportation.
- d) damping the vibration of tool-boring bar assembly

These requirements can only be met using specially

composed low viscosity oils. One of such oil used in this work is Shell Garia H, an extreme pressure oil with sulphur and chlorine additives.

The oil delivery system consists of oil storage tank, pumps and filters. The oil is delivered to the pressure head by several pumps and from pressure head it flows through the annular space between the boring bar and the hole. It passes over the cutting edges and returns through the interior of boring bar carrying away the chips. The oil enters the chip collection basket from where it is drained out through magnetic filters into the storage. The volume of the oil storage has been designed to ensure that there is sufficient time for the oil to cool, settle and defoam before it is recirculated. The pumps can run at different speeds so that by selecting a combination of pumps and speeds it is possible to obtain the required oil flow rate and pressure.

The hollow cylindrical boring bar to which the tool is fixed is made of an alloy steel. It is extremely rigid to resist torsion and bending which helps to provide finer holes. It is clamped to drive unit spindle and passes completely through pressure head while supported in between by the steady rest through Lanchester damper. The boring bar used in this work is 0.043 / 0.031 m in size and 2.25 m in length. Its moment of inertia and torsional rigidity are 1.2248 E-7 m^4 and $9.037 \text{ E+3 N.m/rad}$ respectively.

CHAPTER V

5. Tool Model Tests

The deep hole drilling tools performance is based on the produced hole quality, material removal rate and tool life. For given cutters, pads and workpiece material, workpiece configuration, clamping condition, cutting medium and cutting parameters, the tool performance depends on tool design and its dynamic stability.

Hole quality can be assessed based on run-out, cylindricity error, roundness error, size error and surface finish. Material removal rate is directly related to limit of stability of tool. In this chapter the comparative study of the designed tool, BTA multi-edge tool and BTA solid boring tool is conducted based on the results obtained from experiments. For this purpose two different steels with low and medium strength were drilled with different combination of cutting parameters.

The experiments were mainly conducted for three different purposes which are as follows,

- 1 - Several 400 mm long specimens of low strength material AISI-C12L14 steel were drilled at speed of 67.3 smpm and feed of 0.142 mm/rev. The quality of the holes was assessed and was compared.

- 2 - Specimens of AISI-C12L14 steel were drilled at feed of 0.142 mm/rev and speeds of 57.0, 67.3 and 90.5 smpm and the behavior of tools was compared according to the

hole quality. The same procedure was repeated with specimens drilled at speed of 67.3 smpm and feeds of 0.13, 0.142 and 0.155 mm/rev.

3 - specimens of AISI-C1045 steel were drilled at speed of 67.3 smpm and feed of 0.13 to observe the behavior of tools when material of higher strength is drilled.

The physical properties of AISI-C12L14 steel and AISI-C1045 steel are given in Appendix.

5.1 Hole Run-Out

When drilling shallow holes, the factors which govern bore quality are mostly the size accuracy, roundness and surface finish. On the other hand, the longitudinal accuracy and form may not even be considered or are of secondary importance. In the case of deep drilling operation where the hole length to diameter ratio is large, the longitudinal and form accuracy becomes more pronounced.

The self guidance action in BTA process is a delicate phenomenon which makes possible drilling of perfectly straight holes of large length to diameter ratio. It has been proven that such performance of BTA tools is strongly influenced by machine tool accuracy, drive unit spindle, damper and guiding bushing alignment error, workpiece configuration and workpiece homogeneity, clamping condition and cutting parameters [22,29,30,31]. It has also been shown that the straightness of the hole is affected by tool design. Partially balanced cutting forces on the tool head

were found to contribute less to hole deviation [31]

The hole run-out may take three possible configurations as shown in Fig.22 and are described as follows,

- a) The hole axis is a straight or curved line.
- b) The hole axis spirals about the axis of the workpiece.
- c) The hole axis spirals about a straight line other than the workpiece axis.

It has been found that the most common form of run-out in deep drilling process is of the form (a) [29].

The run-out magnitude and hole axis deviation angle at any section along workpiece can be found by projecting the hole axis exit point on a rectangular plane located at the hole entry Fig.23. The magnitude of run-out and its deviation angle are shown as (r) and (α) . The run-out at any section along the workpiece may also be represented by two components; the first being the distance of the hole axis mean exit point to the current axis exit point and the second from the origin to the hole axis mean exit point. These two components may be called as directional r_{dir} and distributed r_{dis} run-out respectively. The four parameters namely, magnitude of run-out (r) , bore exit angle (α) , directional run-out (r_{dir}) and distributed run-out (r_{dis}) identify the bore axis form as follows,

- 1) The bore axis is of the form (a) when r_{dir} and r_{dis} are of the same order.

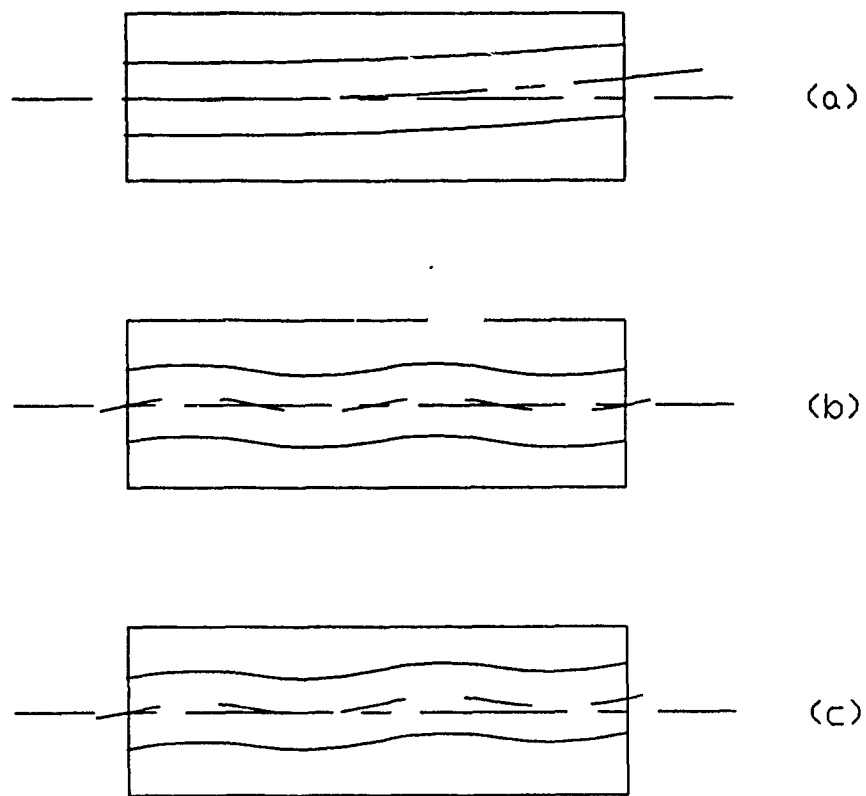


FIG. 22 POSSIBLE CONFIGURATIONS OF HOLE RUN-OUT

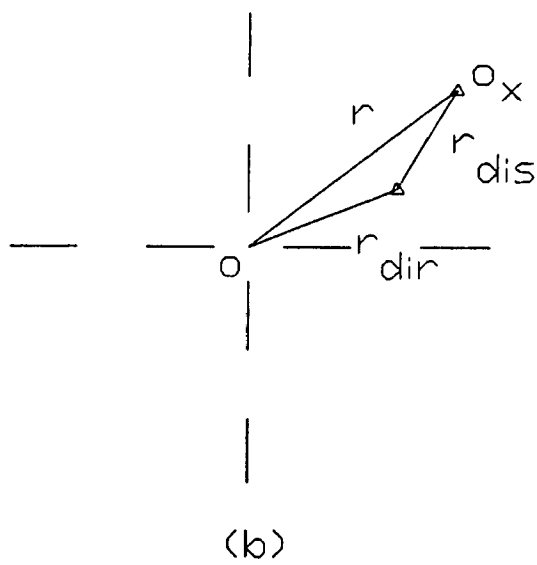
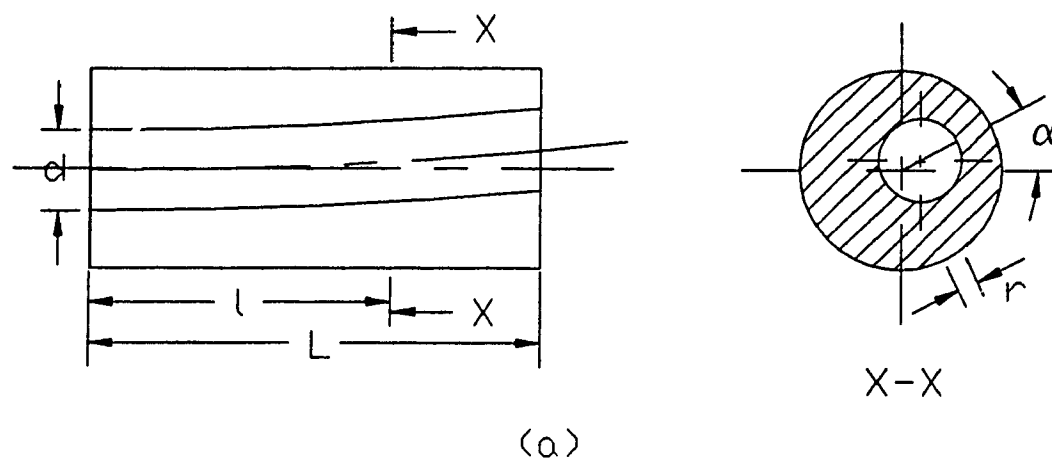


FIG. 23 HOLE RUN-OUT COMPONENTS

2) The deviation of the bore is of the form (b) when r_{dir} curve almost coincide the origin while r_{dis} has approximately a constant non-zero value and α takes any value between 0° and 360° .

3) The deviation of the bore is of the form (c) when α perform a periodic curve with a limited amplitude while r and r_{dir} increase continuously and r_{dis} is approximately constant.

To examine and compare the designed tool, BTA multi-edge tool and BTA solid boring tool several specimens of 400 mm length were drilled using identical feed and cutting speed. The feed and cutting speed were 0.142 mm/rev and 67.3 m/min respectively. The work material was cold rolled AISI-C12114 steel. The run-out was measured at 15 sections of each specimen. The results for r , r_{dir} , r_{dis} and bore axis deviation angle α are plotted and shown from Fig.24 to Fig.29.

By studying the figures and the fact that the directional and distributed components of run-outs were found to be almost of the same order it is concluded that the bore deviation for all three tools are of the form (a). It is also seen that the prototype has the lowest run-out followed by BTA multi-edge tool. The average run-out for prototype after 400 mm drilling is 0.2 mm while that of BTA multi-edge and BTA solid boring tools are 0.23 mm and 0.26 mm respectively. The same trend was found when the distributed and directional run-outs of holes are compared.

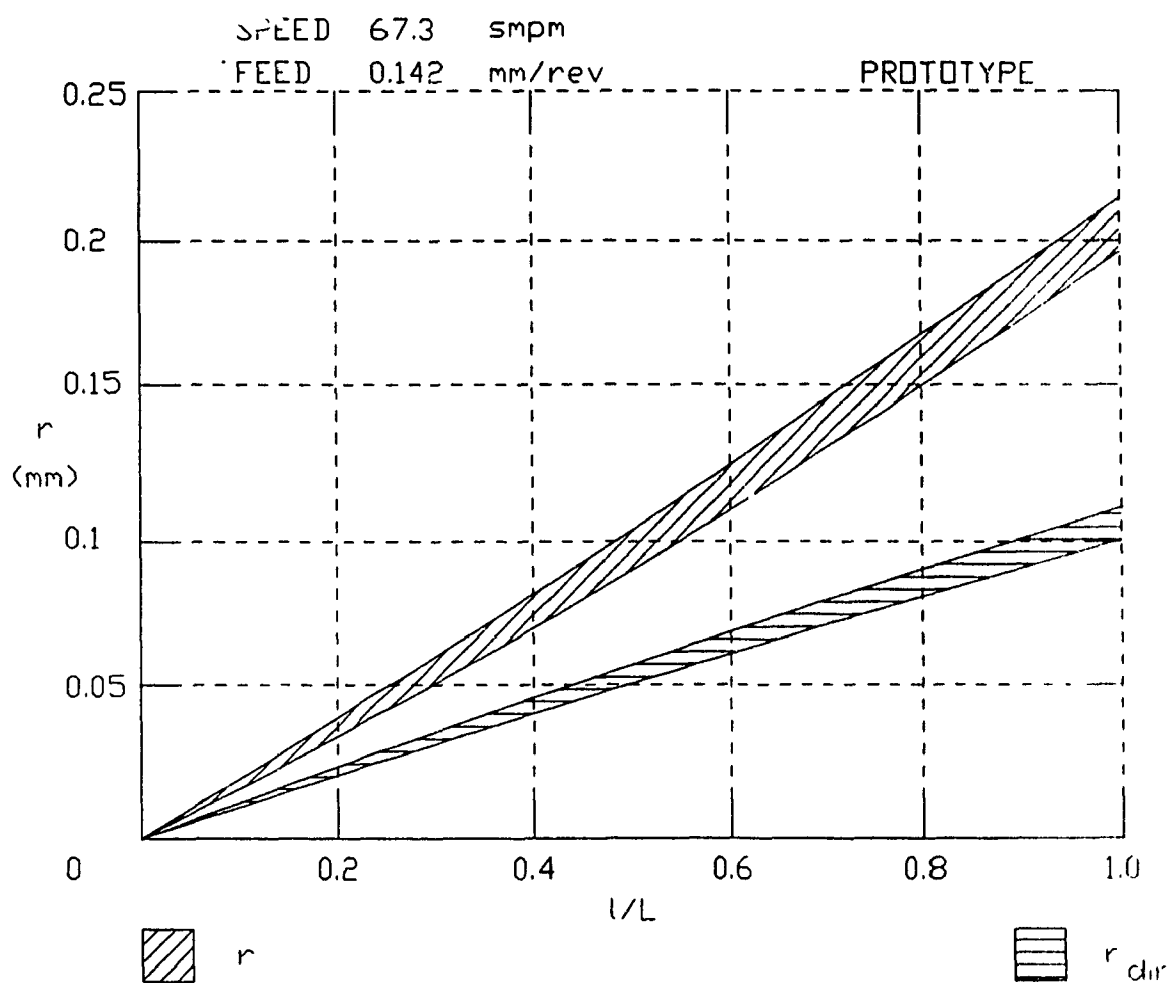


FIG. 24 RUN-OUT OF THE HOLE DRILLED BY THE PROTOTYPE

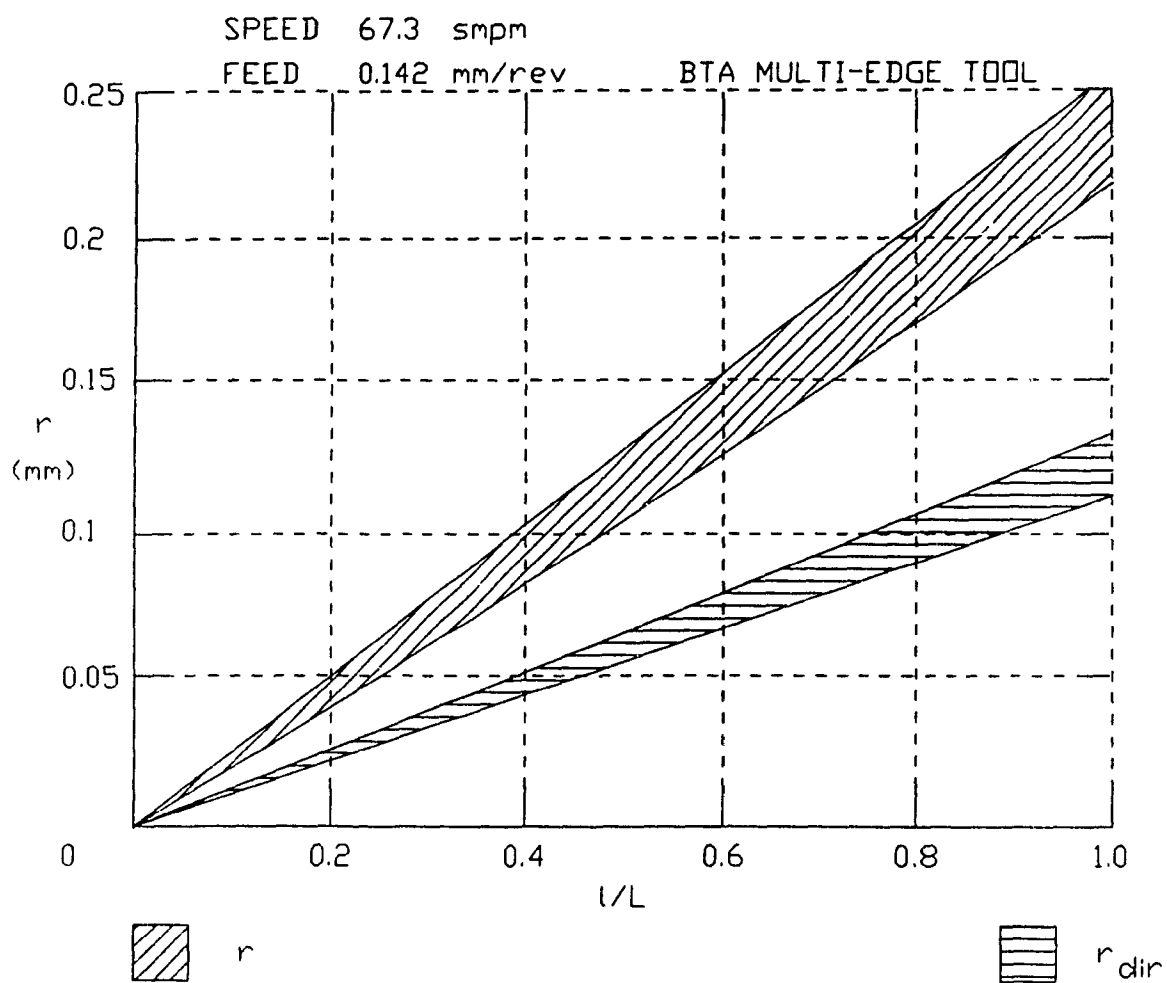


FIG. 25 RUN-OUT OF THE HOLE DRILLED BY
THE BTA MULTI-EDGE TOOL

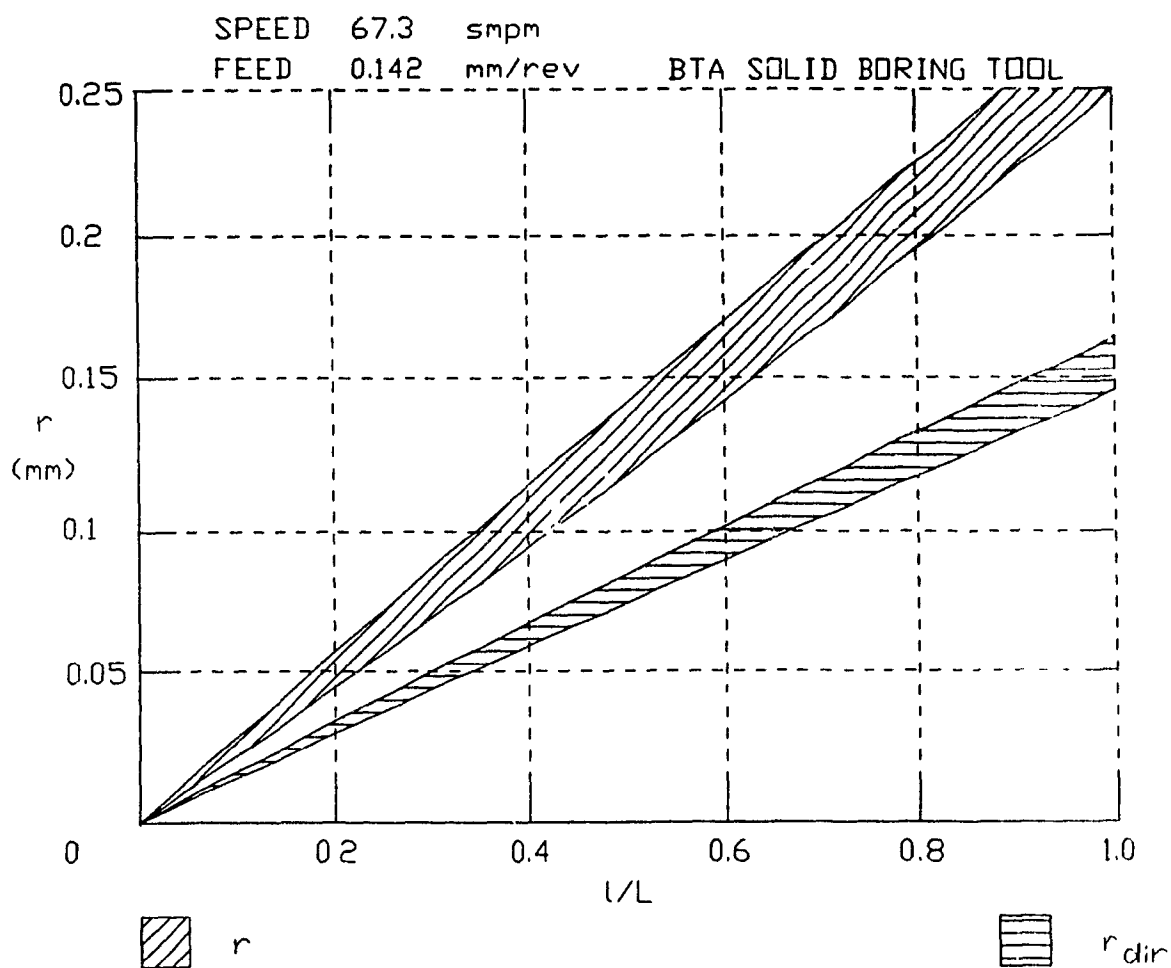


FIG. 26 RUN-OUT OF THE HOLE DRILLED BY
THE BTA SOLID BORING TOOL

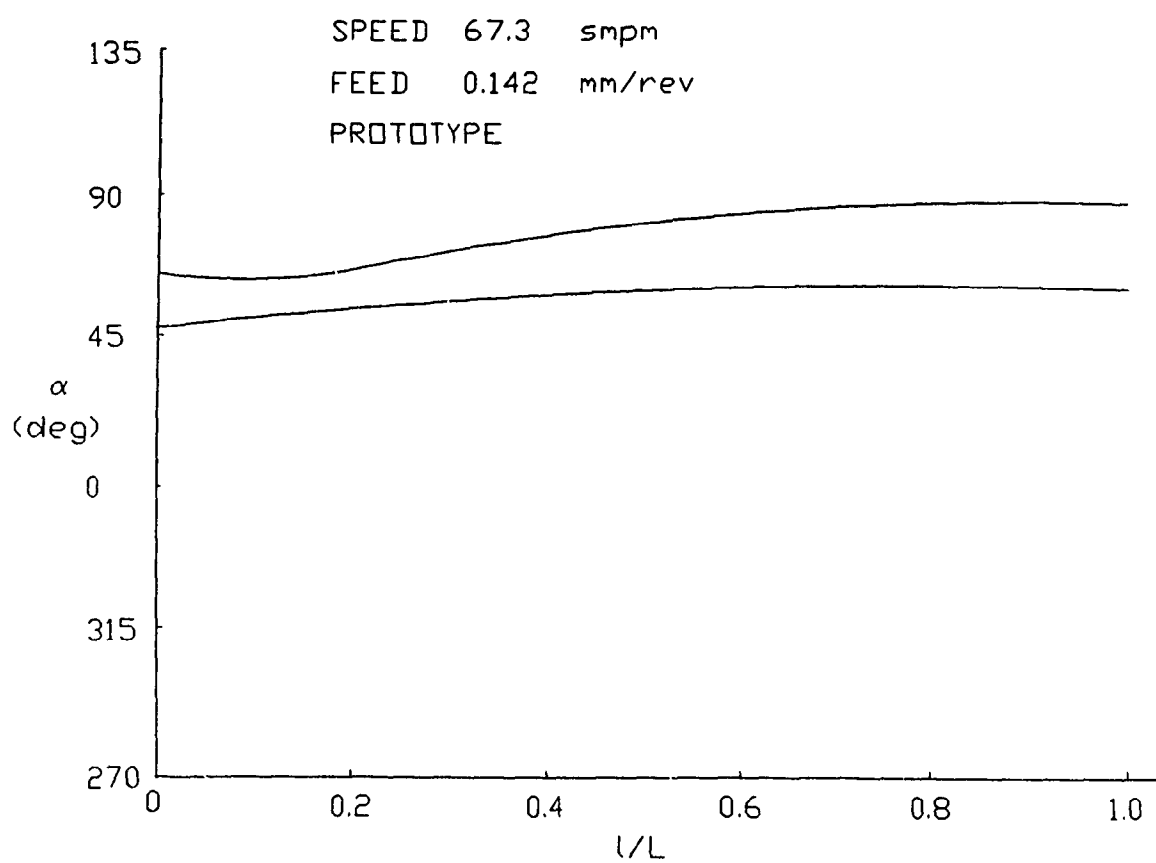


FIG. 27 HOLE AXIS DEVIATION ANGLE

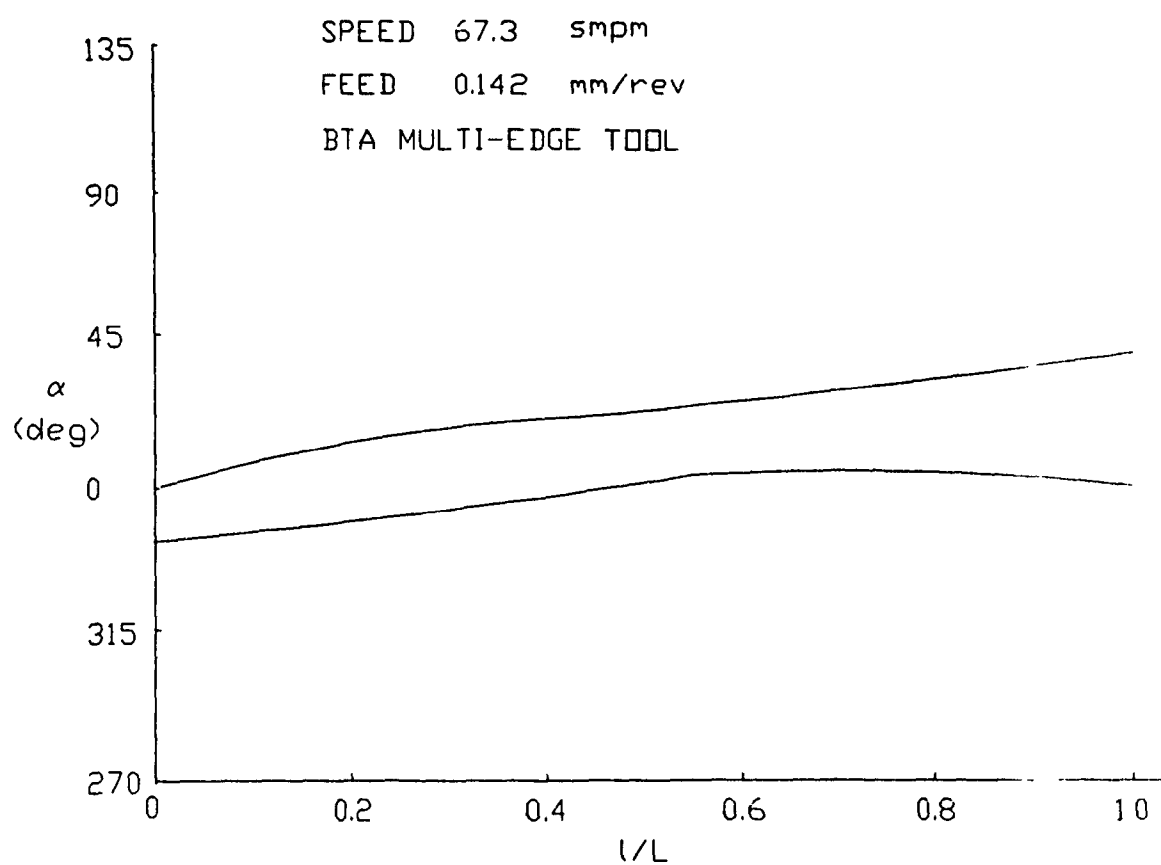


FIG. 28 HOLE AXIS DEVIATION ANGLE

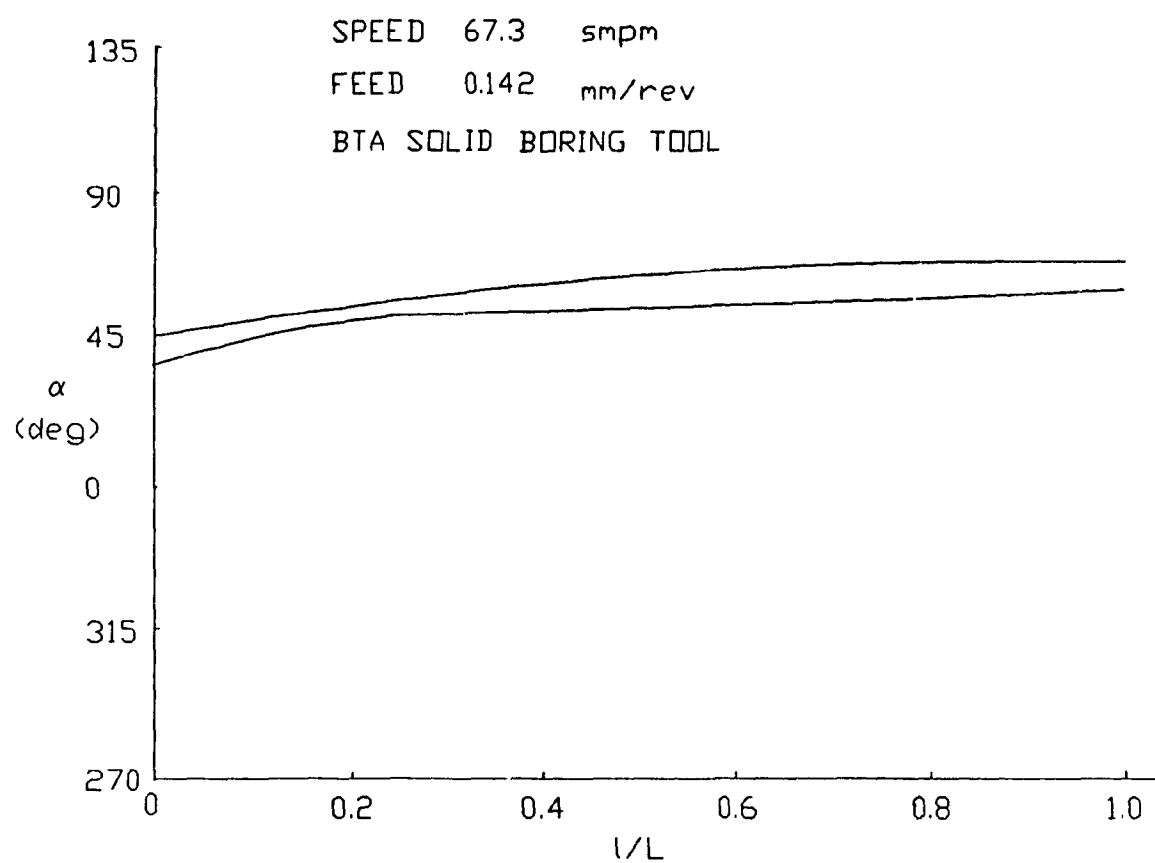


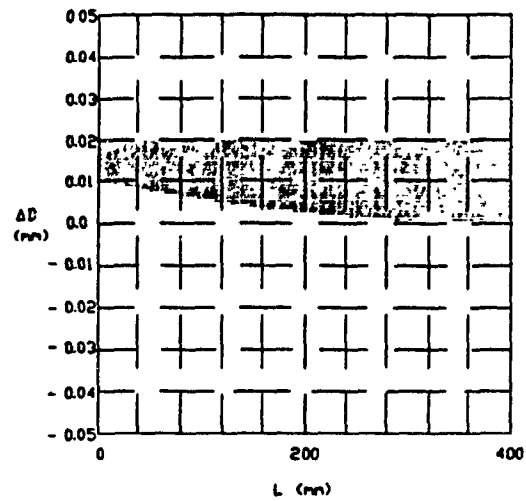
FIG. 29 HOLE AXIS DEVIATION ANGLE

Another criterion by which the straightness of bores produced by tools may be compared is the cylindricity error. Cylindricity error of bores was computed using the analytical method based on least square concept given in Appendix [45,46]. It was found that the holes drilled by the BTA multi-edge and the prototype have almost the same average cylindricity error of 0.06 mm followed by the BTA solid boring tool with 0.071 mm.

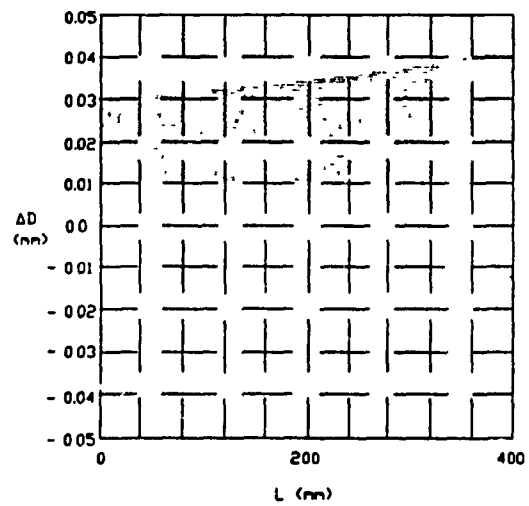
The hole deviation angles for the three tools are shown in Fig.27 to Fig.29. It appears that the holes drilled by the prototype and the BTA solid boring tool are deviated towards upper side of workpiece as hole depth is increased. On the other hand, hole drilled by the BTA multi-edge tool is deviated towards the right side of the workpiece. The difference in behavior of the tools could be due to the tool unbalance.

5.2 Hole Size Error

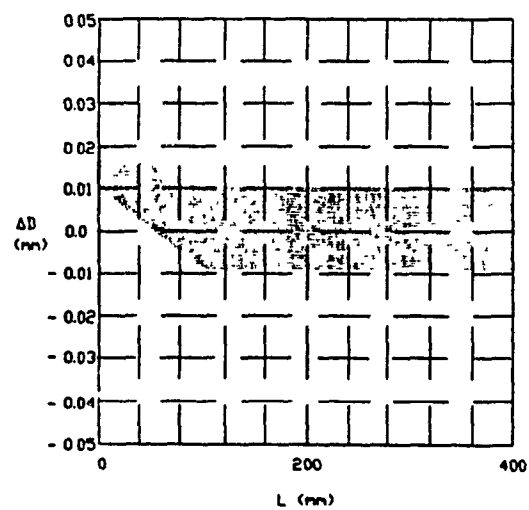
The hole size error may be given as the deviation of both minimum and maximum hole sizes from the nominal size of the tool. The hole size variation for specimens drilled by the three tools at similar conditions are shown in Fig.30. The results are very close to those found by Pfleghar [31] who studied the influence of the degree of stability of gundrill on hole size variation when the pads position angle on tool periphery were changed. It is shown in the figure that all bores are initially oversize due to



(a) PROTOTYPE



(b) BTA MULTI-EDGE TOOL



(c) BTA SOLID BORING TOOL

FIG. 30 HOLE SIZE ERROR

drilling bushing clearance but as the tool drills deeper in workpiece, the bore size variation is direct function of the tool configuration.

There is a significant difference between the three tools in terms of the degree of stability by which the hole size variation may be explained. The degree of stability of each tool with respect to both pads are as follows,

1 - Prototype	$S_1 = 1.7$
	$S_2 = 1.26$
2 - BTA multi-edge tool	$S_1 = 1.16$
	$S_2 = 1.4$
3 - BTA solid boring tool	$S_1 = 1.95$
	$S_2 = 1.6$

It is seen that in the case of BTA multi-edge tool $S_2 > S_1$ contrary to the prototype and the BTA solid boring tool where $S_1 > S_2$. Due to this property of BTA multi-edge tool and small value of S_1 which, by definition is the ratio of holding to lifting moment around the leading pad, the circle-land may forced away from the radial direction creating an oversize hole.

In the case of BTA solid boring tool the hole tends to cut undersize due to higher value of S_1 while in the case of the prototype an intermediate value of S_1 causes the hole follow the nominal size of the tool. Pfleghar showed that a tool having large and close values of S_1 and S_2

produces the hole sizes of narrower scatter around tool nominal size. On the other hand the tools with very low value of S_2 and large value of S_1 produce undersize holes.

The size error of holes drilled in specimen of AISI-C1045 steel by the prototype and the BTA multi-edge tool is shown in Fig. 31. As it could be observed the hole produced by the BTA multi-edge tool is more oversize than the hole produced by the prototype.

In Fig.32 to Fig.37 the span of hole size error for different combinations of cutting parameters are given for holes drilled by each tool in workpiece of AISI-C12L14 steel. In the case of holes drilled by the prototype it could be observed that the hole size error is less sensitive to the feed than to the cutting speed. The holes have minimum size error at the intermediate cutting speed and feed and for the given drilling conditions the hole size error is always smaller for the prototype. It could also be observed that at the intermediate feed the size of the holes drilled by the prototype approaches the nominal size of the tool while in the case of the BTA multi-edge tool the holes are oversize. As shown in Fig 36 and Fig.37 the holes drilled by BTA solid boring tool are always undersize. The size of the holes are practically independent of cutting parameters.

5.3 Hole Roundness Error

The quality of a hole in terms of roundness error may

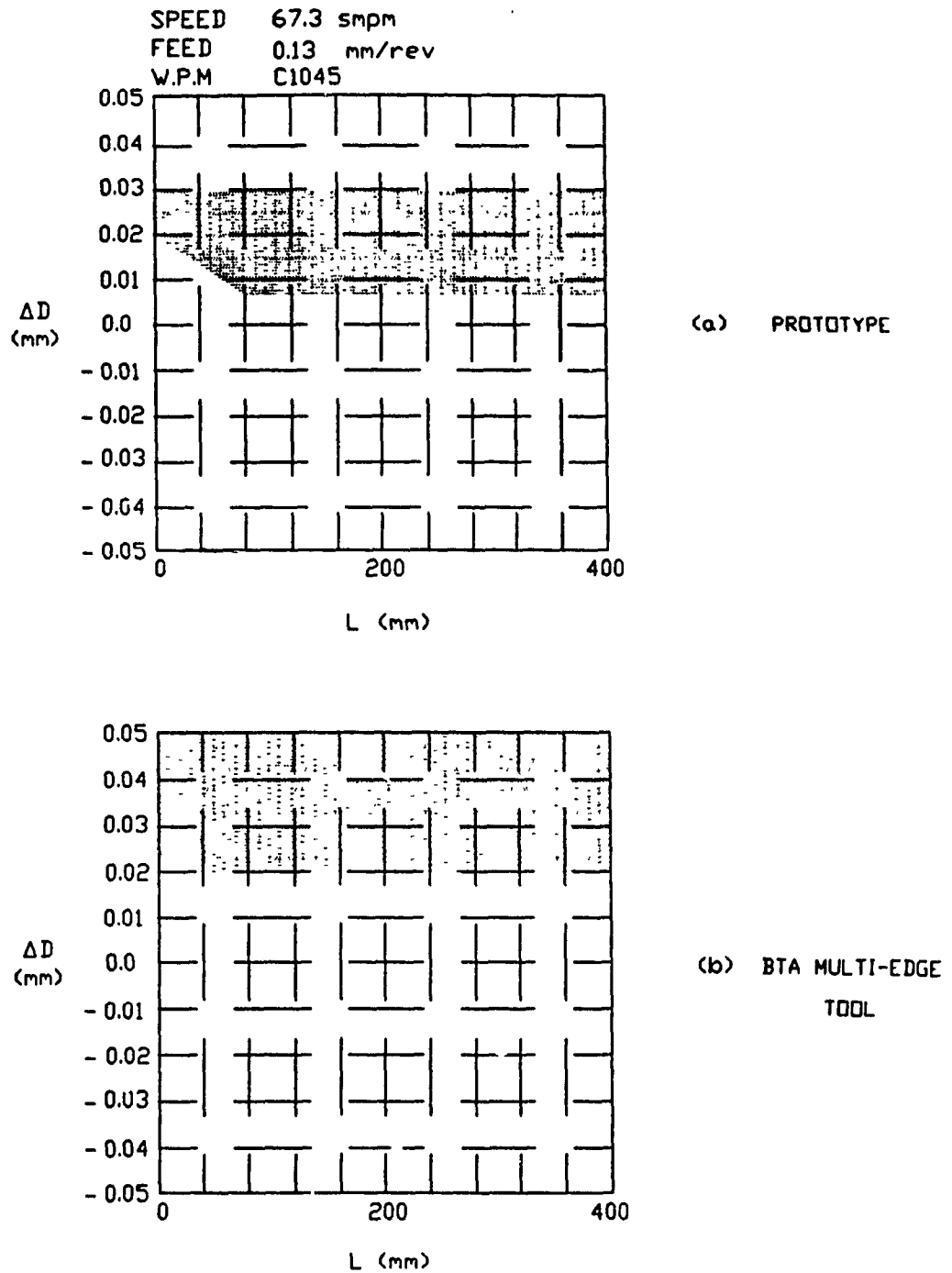


FIG. 31 HOLE SIZE ERROR

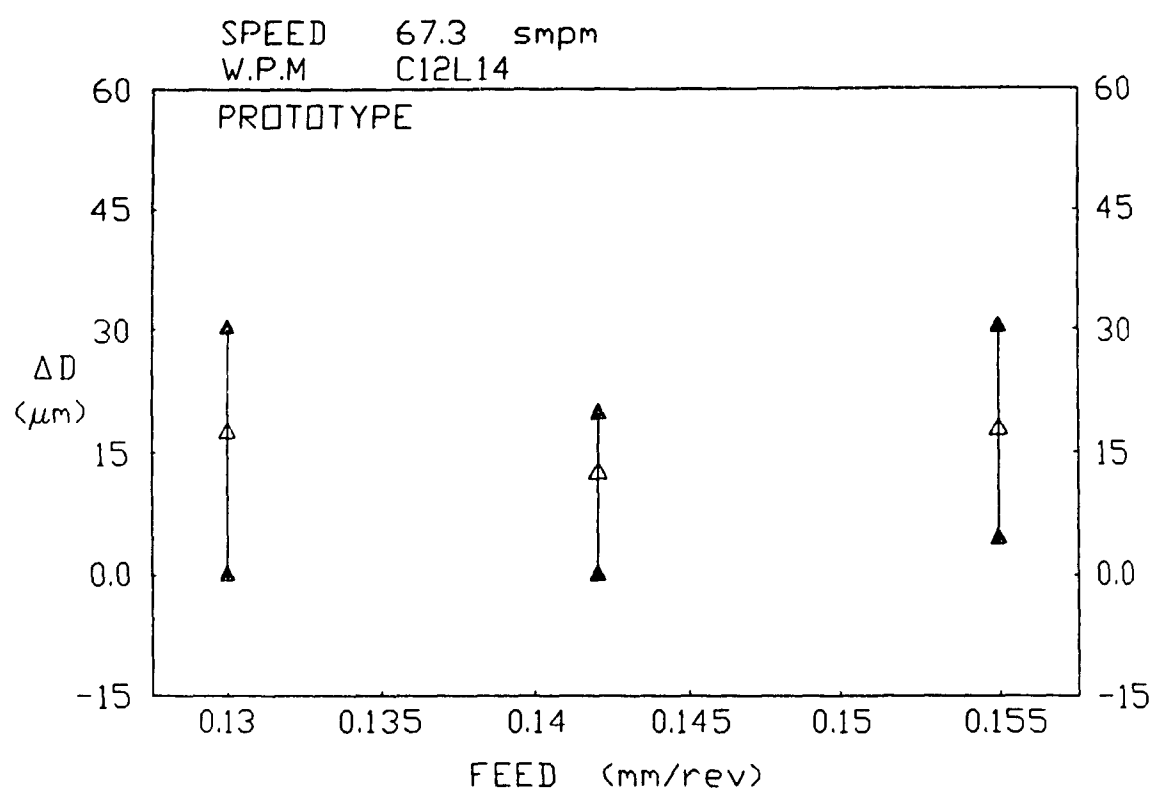


FIG. 32 SIZE ERROR OF THE HOLE DRILLED BY THE PROTOTYPE

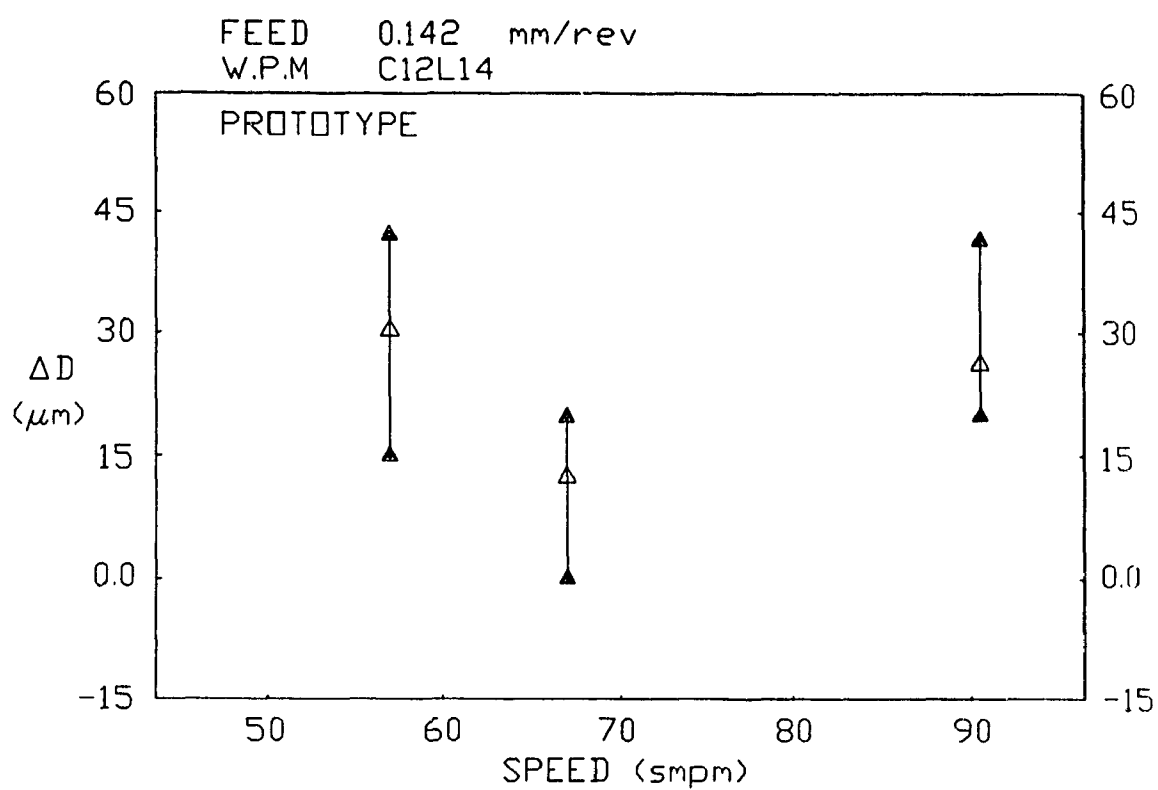


FIG. 33 SIZE ERROR OF THE HOLE DRILLED BY
THE PROTOTYPE

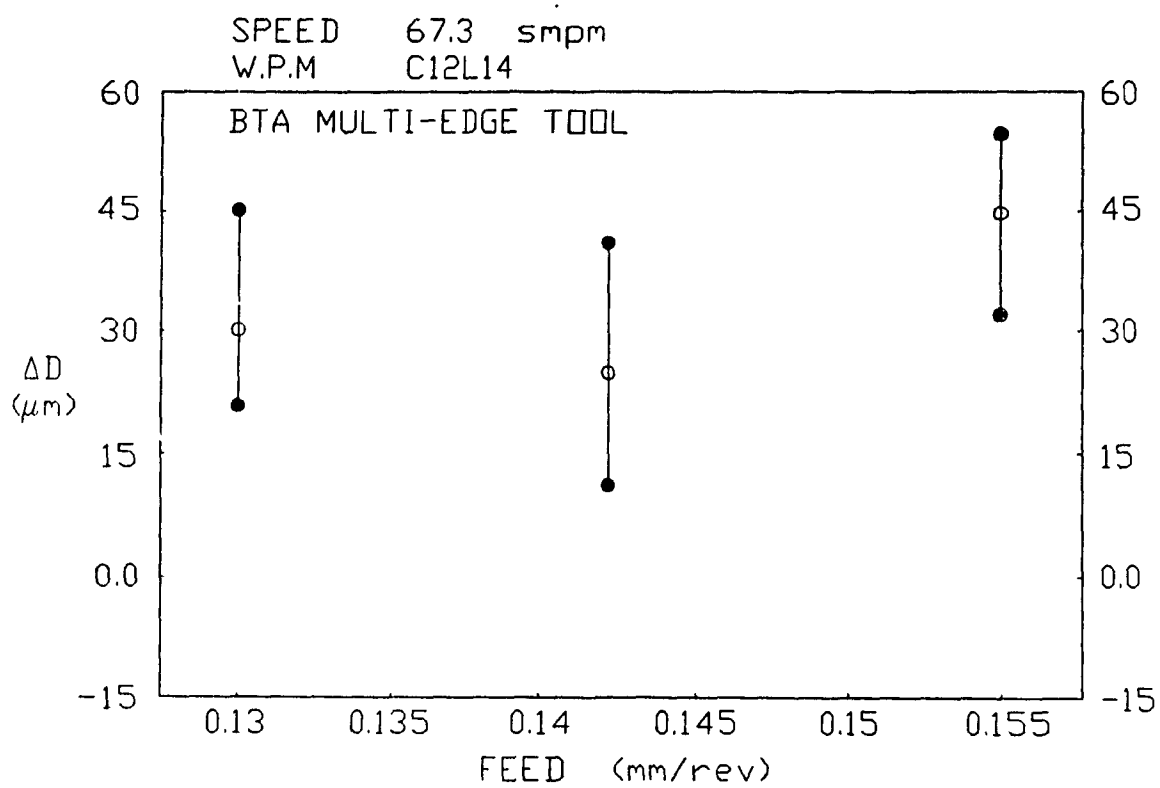


FIG. 34 SIZE ERROR OF THE HOLE DRILLED BY
THE BTA MULTI-EDGE TOOL

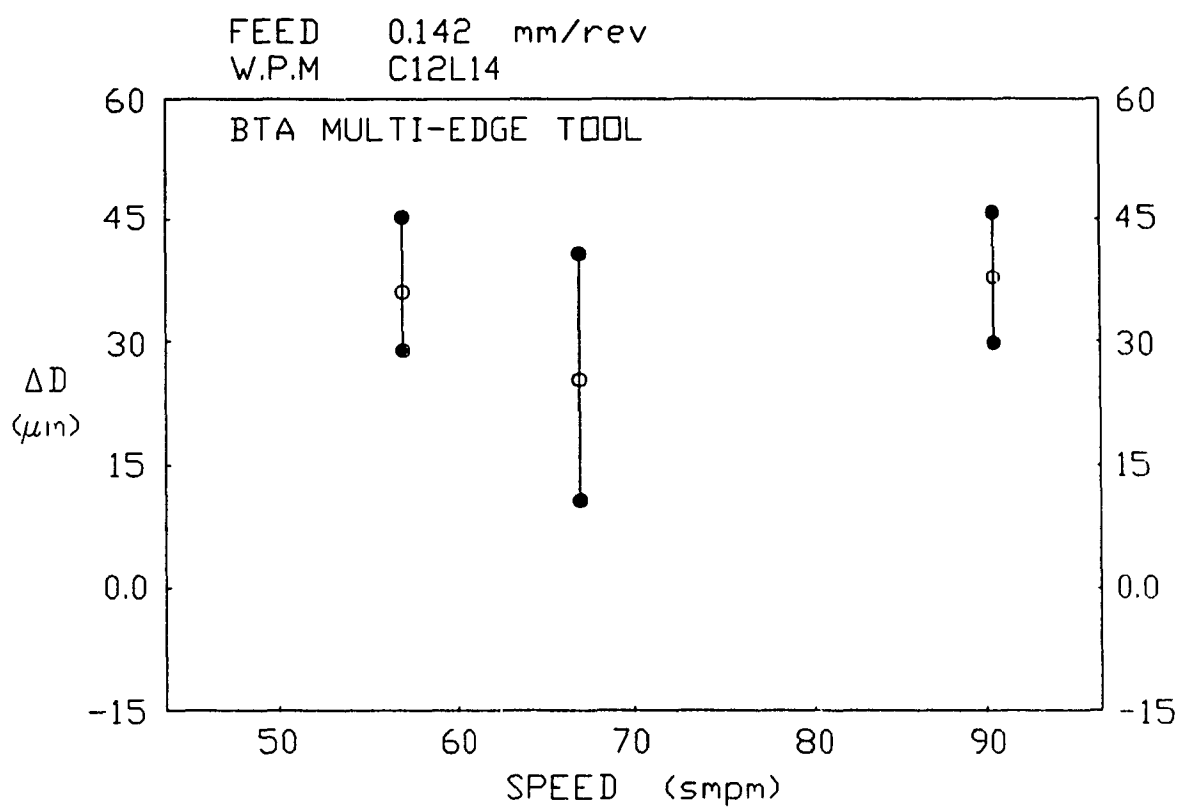


FIG. 35 SIZE ERROR OF THE HOLE DRILLED BY
THE BTA MULTI-EDGE TOOL

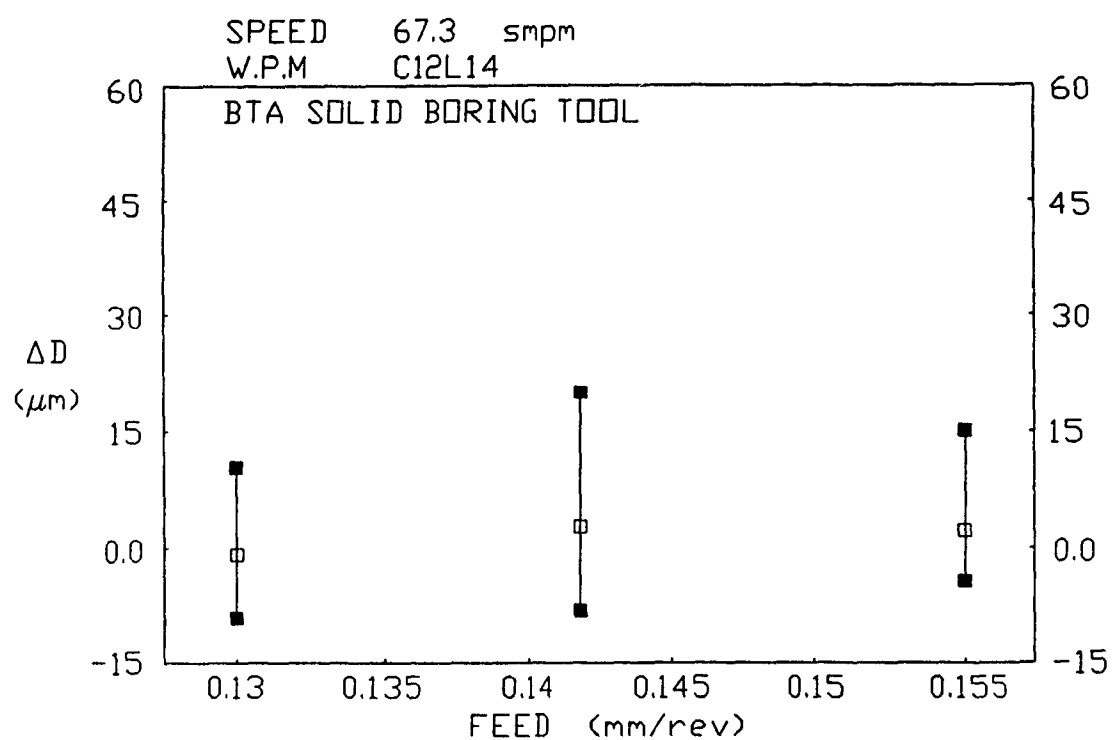


FIG. 36 SIZE ERROR OF THE HOLE DRILLED BY
THE BTA SOLID BORING TOOL

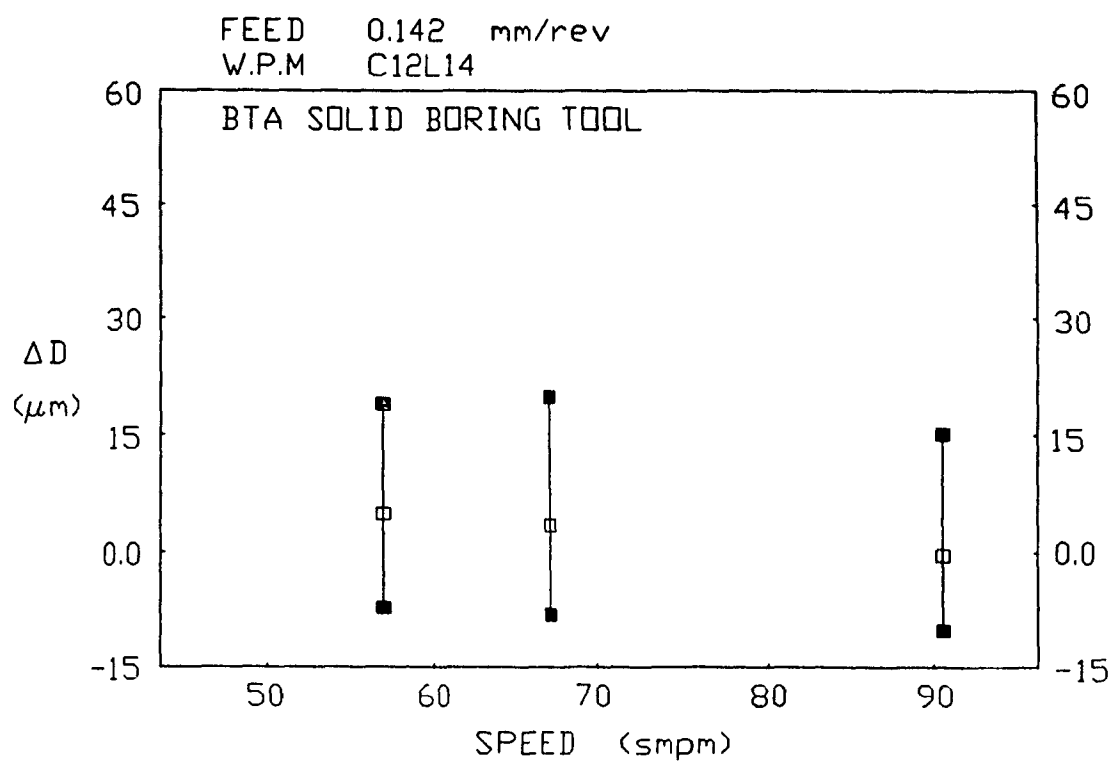


FIG. 37 SIZE ERROR OF THE HOLE DRILLED BY
THE BTA SOLID BORING TOOL

be given by its average along the hole length and along with the maximum and the minimum values. The average value of those found for several specimens will give more reliable information about the tool. The roundness error of holes drilled by tools at intermediate speed and feed is shown in Fig.38. It can be observed that the holes drilled by the BTA solid boring tool has the smallest average roundness error, followed by the BTA multi-edge tool. The prototype is slightly inferior to the two tools with respect to the roundness error.

In Fig.39-a the roundness error of holes drilled by the prototype and the BTA multi-edge tool into the specimens of AISI-C1045 steel are shown. As in the case of holes machined in mild steel, the one drilled by the prototype exhibits a larger roundness error along with its dispersion around the mean value.

The Fig.40 to Fig.45 represent the variation of roundness error for holes drilled by the tools at different combinations of cutting parameters. In the case of the prototype, the hole assumes maximum roundness error at the intermediate feed (Fig.40). On the other hand the hole roundness error continuously decreases by increasing the cutting speed (Fig.41). It is shown in Fig.42 and Fig.43 that the roundness error of holes drilled by BTA multi-edge tool is less sensitive to feed than speed. The roundness error is maximum at intermediate speeds. The hole roundness error for the BTA solid boring tool is maximum at

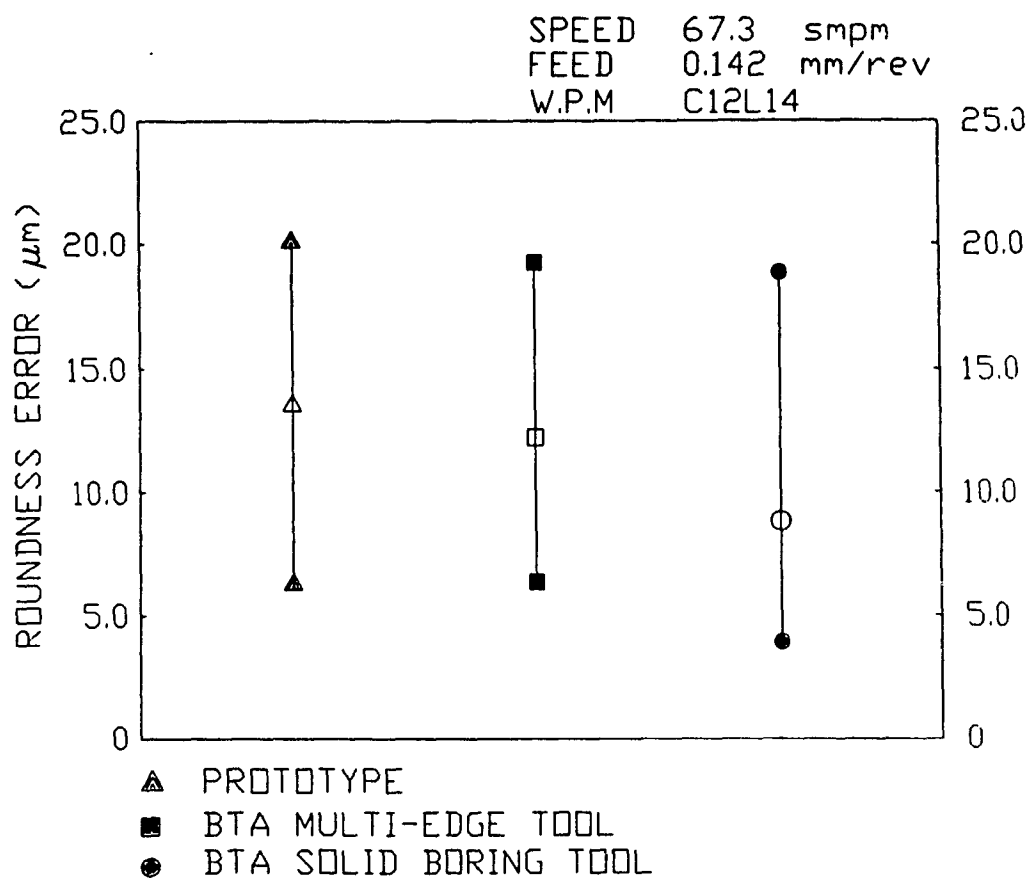


FIG. 38 HOLE ROUNDNESS ERROR

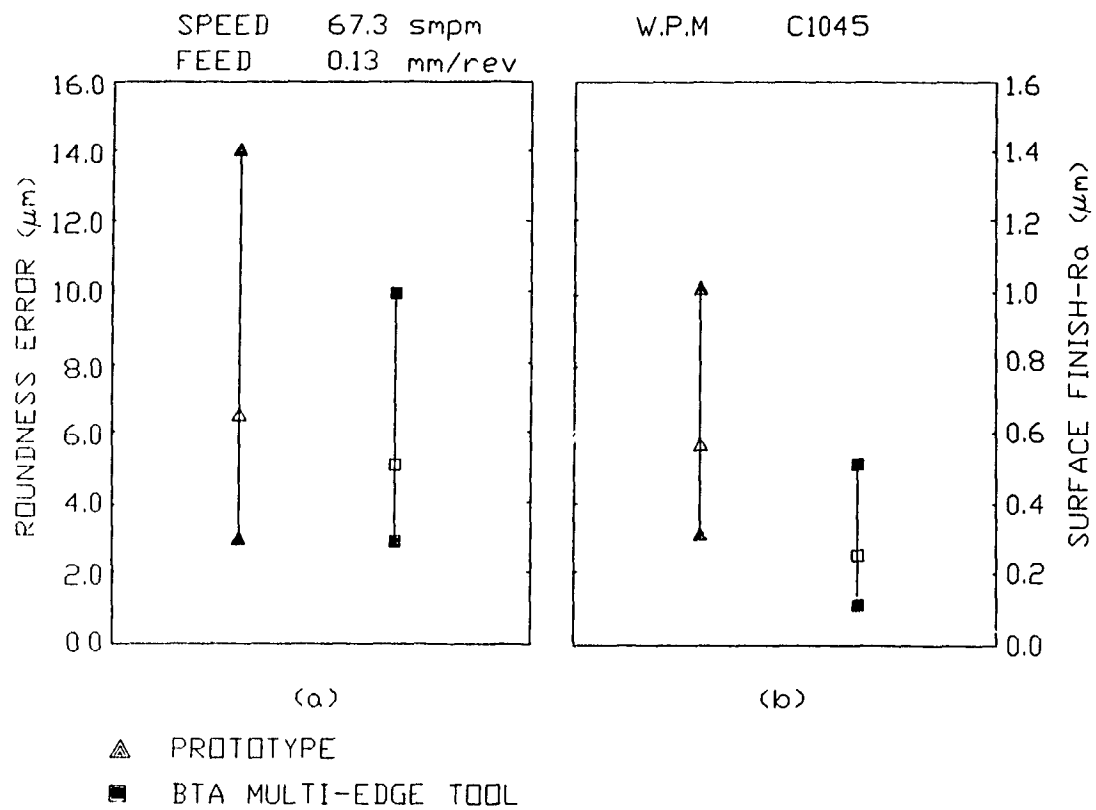


FIG. 39 HOLE ROUNDNESS ERROR AND SURFACE FINISH

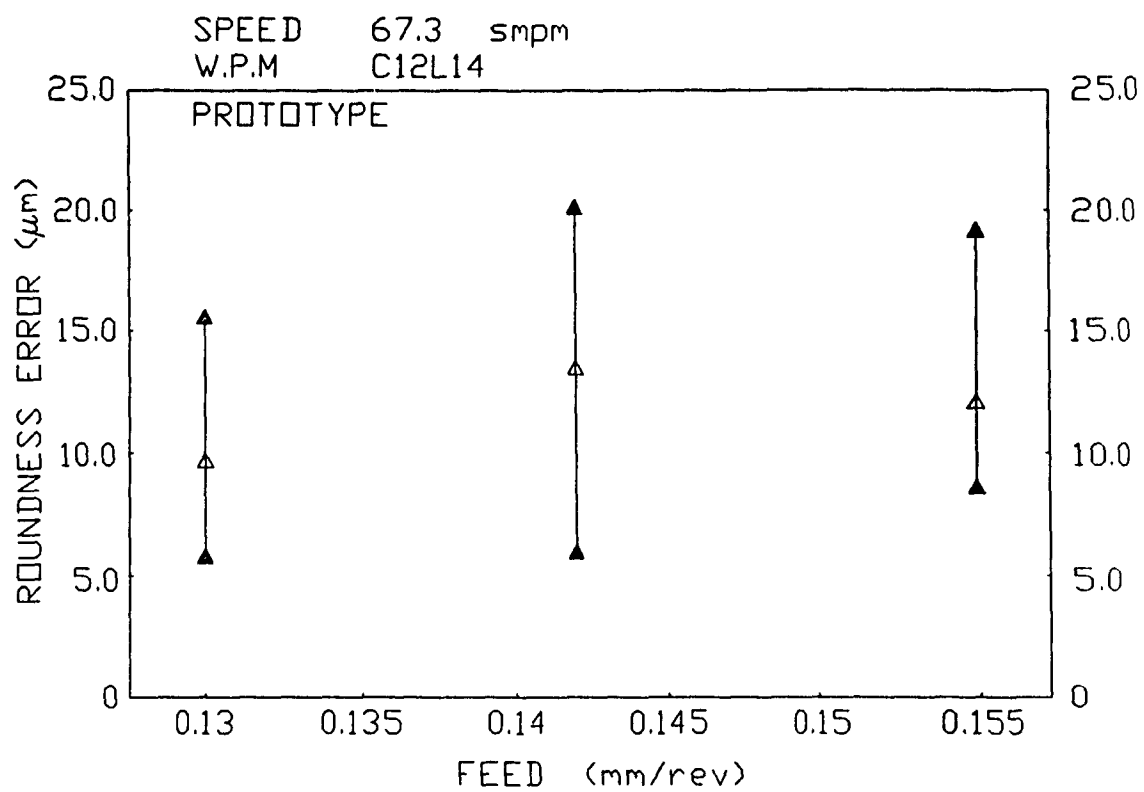


FIG. 40 ROUNDNESS ERROR OF THE HOLE DRILLED BY THE PROTOTYPE

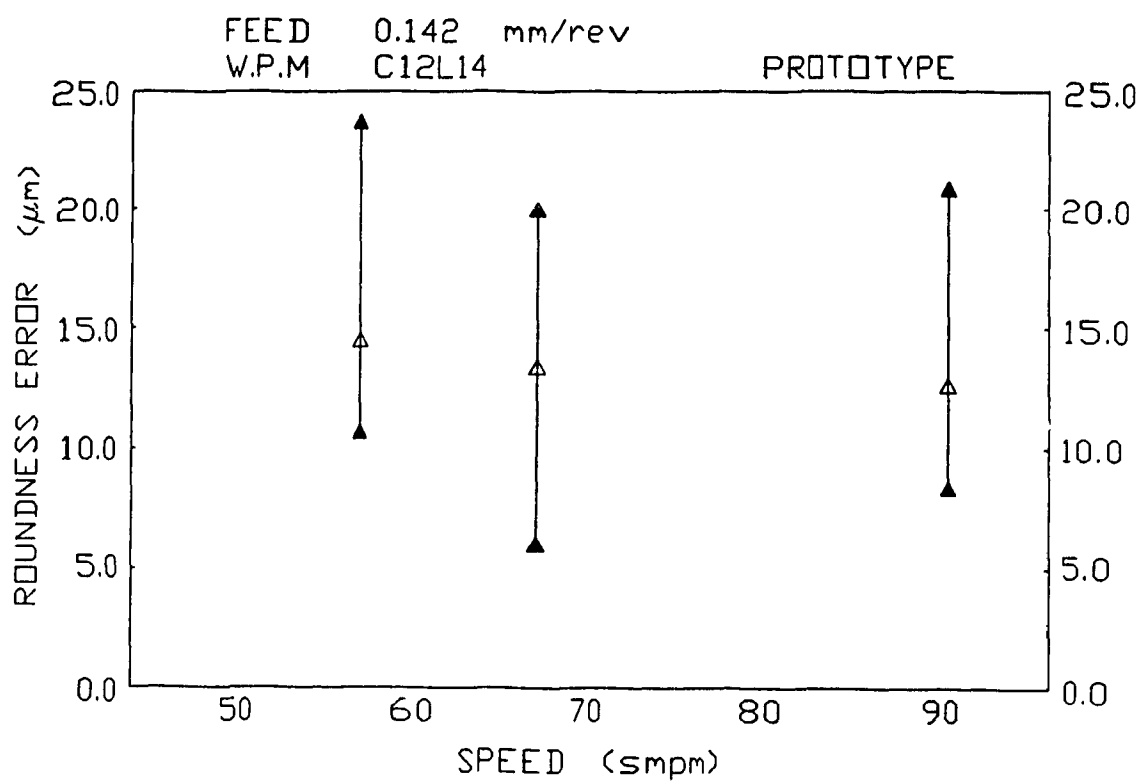


FIG. 41 ROUNDNESS ERROR OF THE HOLE DRILLED BY THE PROTOTYPE

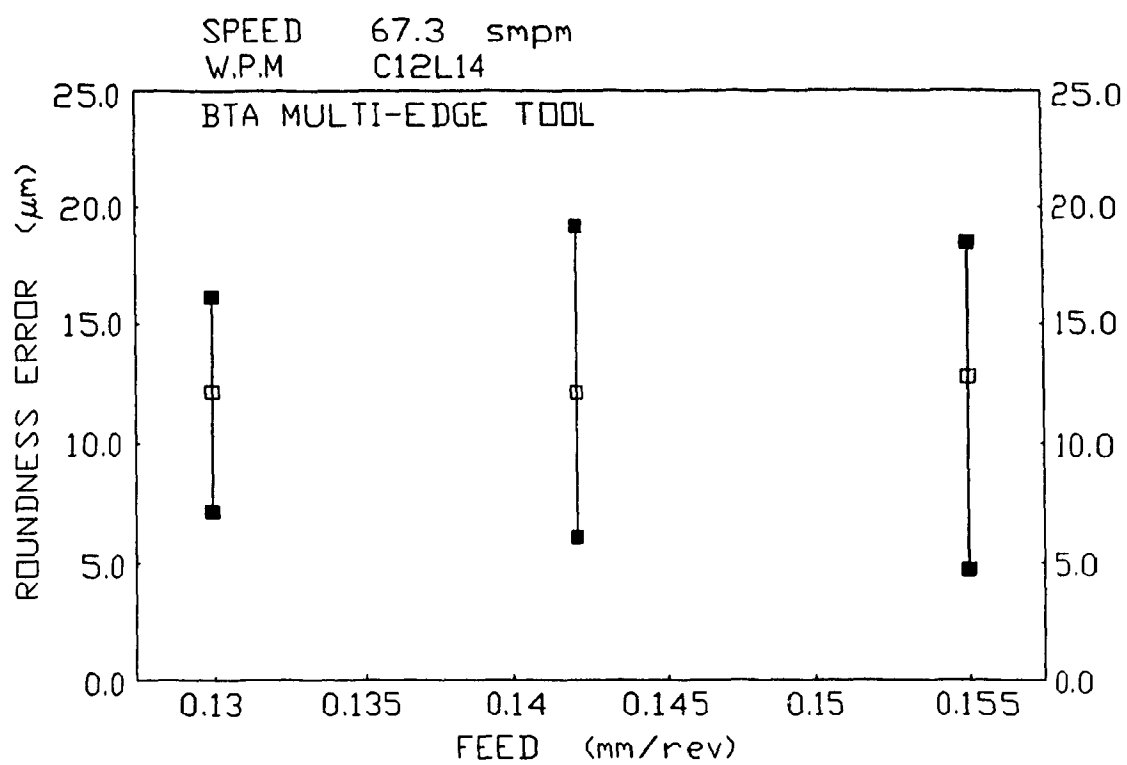


FIG. 42 ROUNDNESS ERROR OF THE HOLE DRILLED BY
THE BTA MULTI-EDGE TOOL

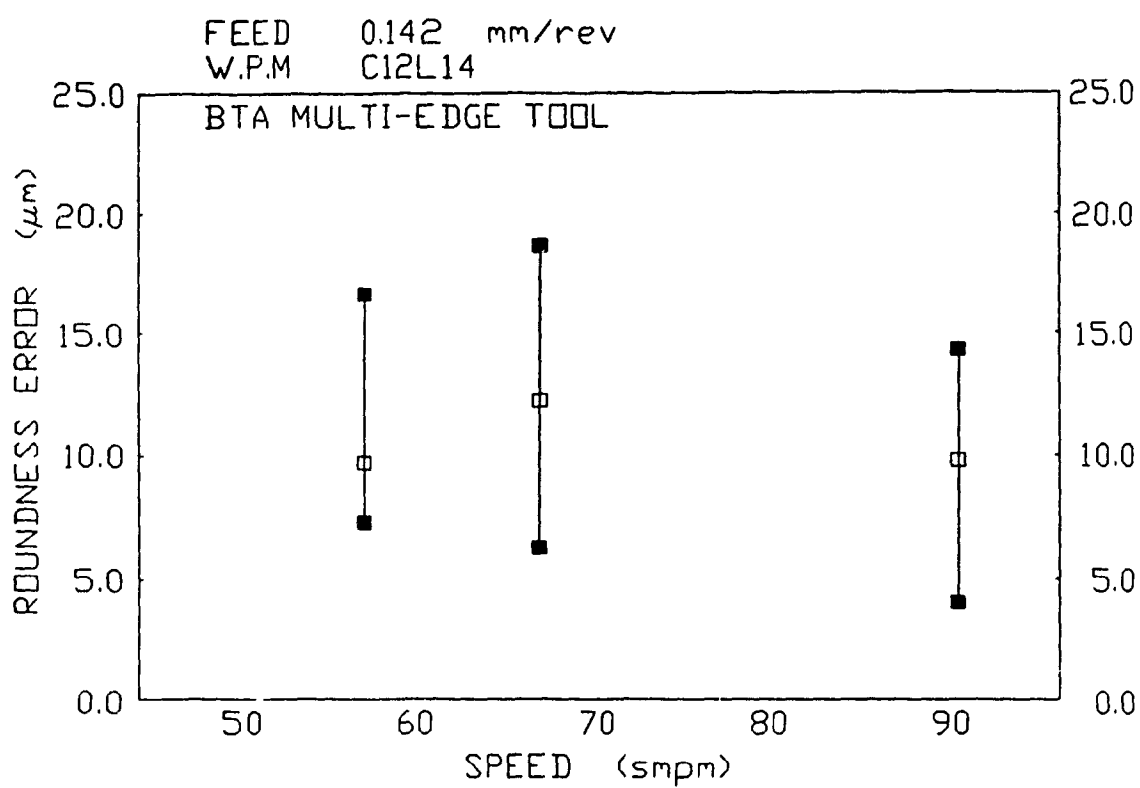


FIG. 43 ROUNDNESS ERROR OF THE HOLE DRILLED BY
THE BTA MULTI-EDGE TOOL

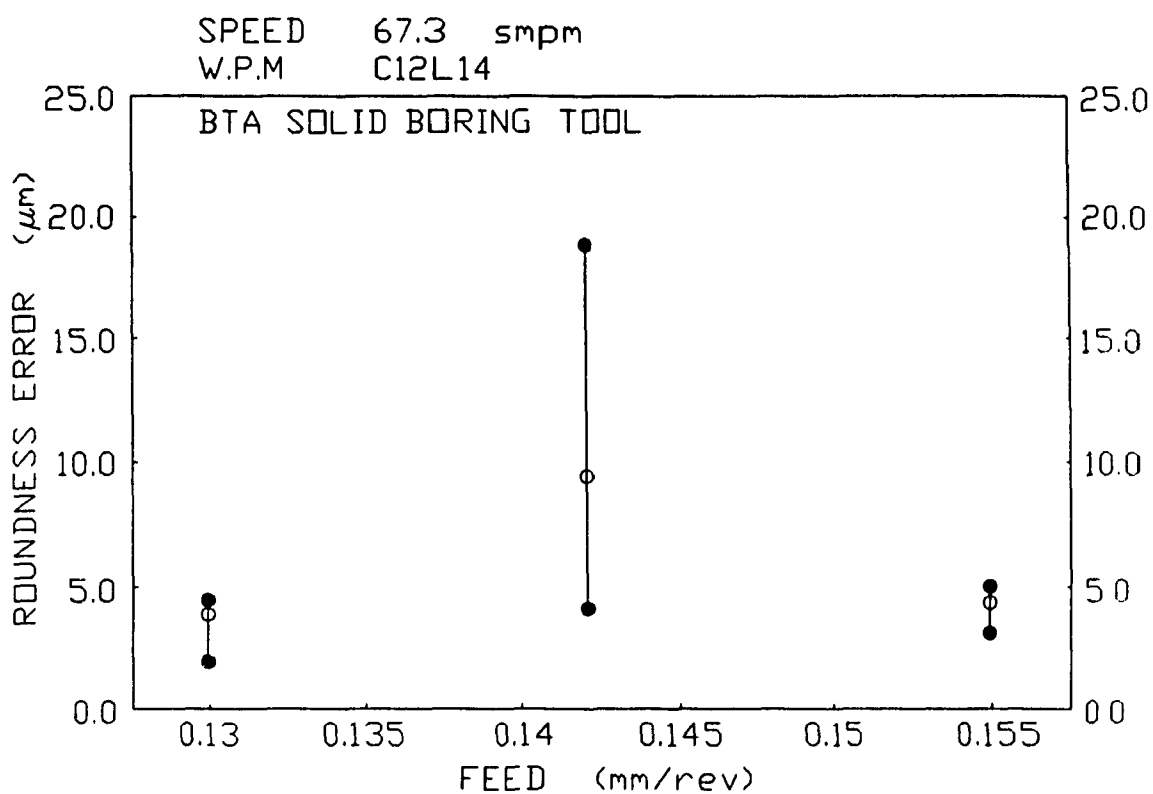


FIG. 44 ROUNDNESS ERROR OF THE HOLE DRILLED BY
THE BTA SOLID BORING TOOL

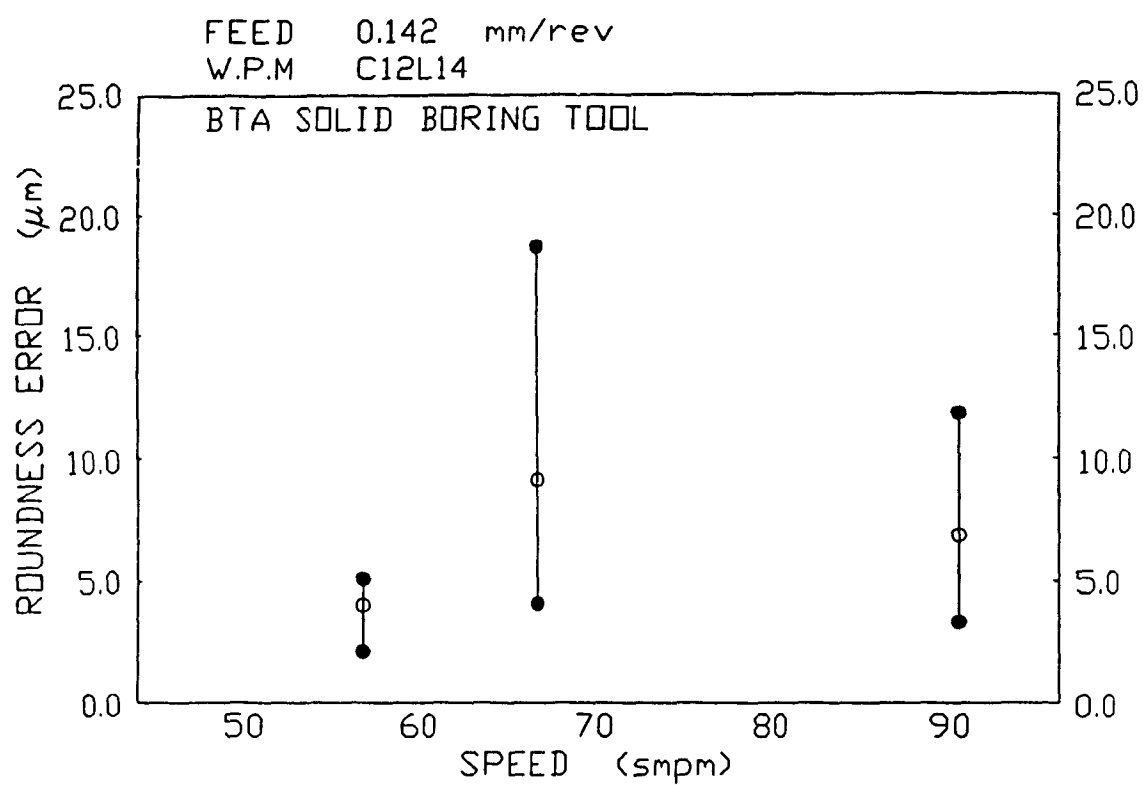


FIG. 45 ROUNDNESS ERROR OF THE HOLE DRILLED BY
THE BTA SOLID BORING TOOL

intermediate feed and speed but it is always smaller than those for the prototype and the BTA multi-edge tool specially at both low and high feeds and speeds (Fig.44, Fig.45).

5.4 Hole Surface Finish

Hole surface finish in deep drilling process is strongly affected by tool configuration through magnitude of the pads burnishing force. For a given drilling condition and workpiece material the BTA solid boring tool imposes the greatest pads burnishing force on bore wall. The BTA multi-edge tool causes less burnishing, while the prototype produces the least burnished surface

The surface finish of holes drilled in workpiece specimens of AISI-C12L14 steel by the tools at an intermediate feed and speed is shown in Fig.46. It is shown that the BTA solid boring tool yields bores with best surface finish. The mean surface finish of holes drilled by the prototype and the BTA multi-edge tool are almost equal with considerably smaller dispersion from mean value for the later. The Fig 39-b shows the surface finish of the holes drilled into the workpieces of AISI-C1045 steel by the prototype and the BTA multi-edge tool at speed of 67.3 smpm and feed of 0.13 mm/rev. It can be observed that the hole drilled by the BTA multi-edge tool has better finish.

In the case of the holes drilled at different combinations of feeds and speeds it can be observed from

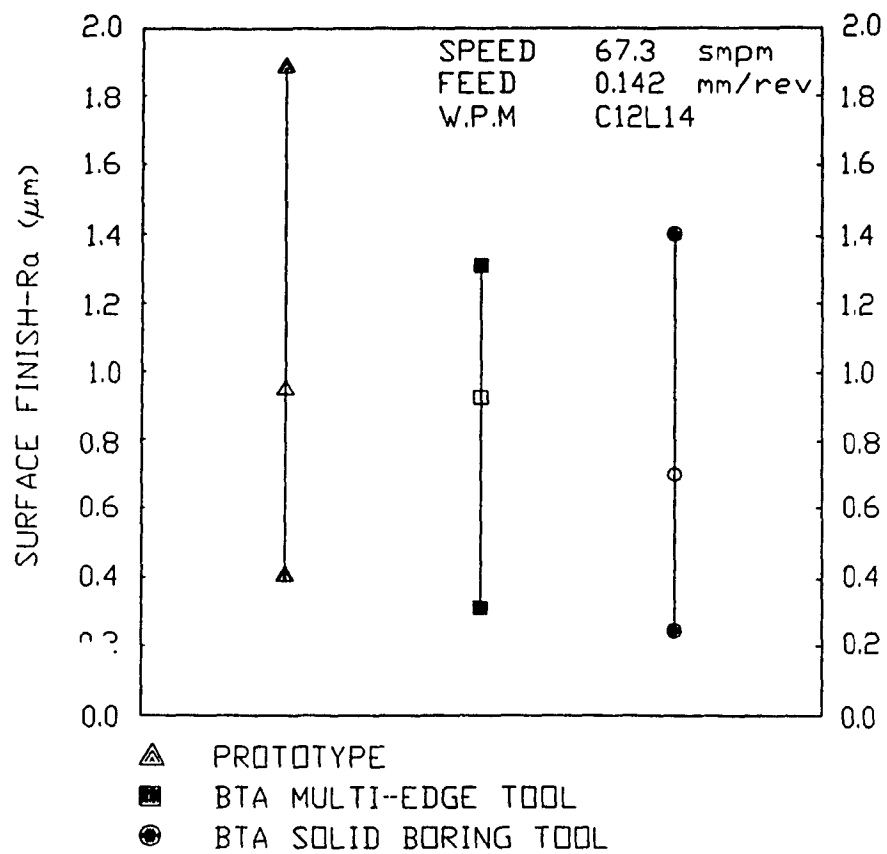


FIG. 46 HOLE SURFACE FINISH

Fig.47 to Fig.52 that all three tools produced better surface finish at low and high feeds. The cutting speed effects the hole surface finish in the same way as the feed when holes are drilled by the prototype and the BTA multi-edge tool but the surface of holes drilled by the BTA solid boring tool continuously deteriorated by increasing cutting speed.

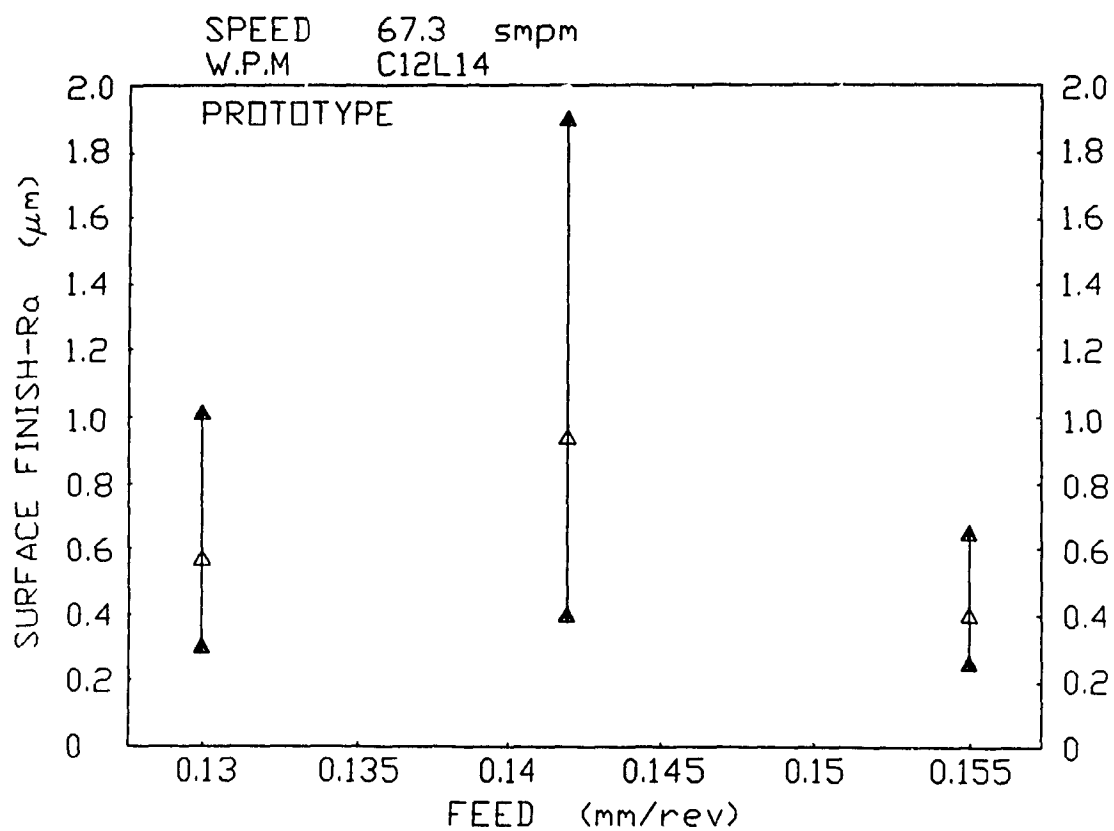


FIG. 47 SURFACE FINISH OF THE HOLE DRILLED BY
THE PROTOTYPE

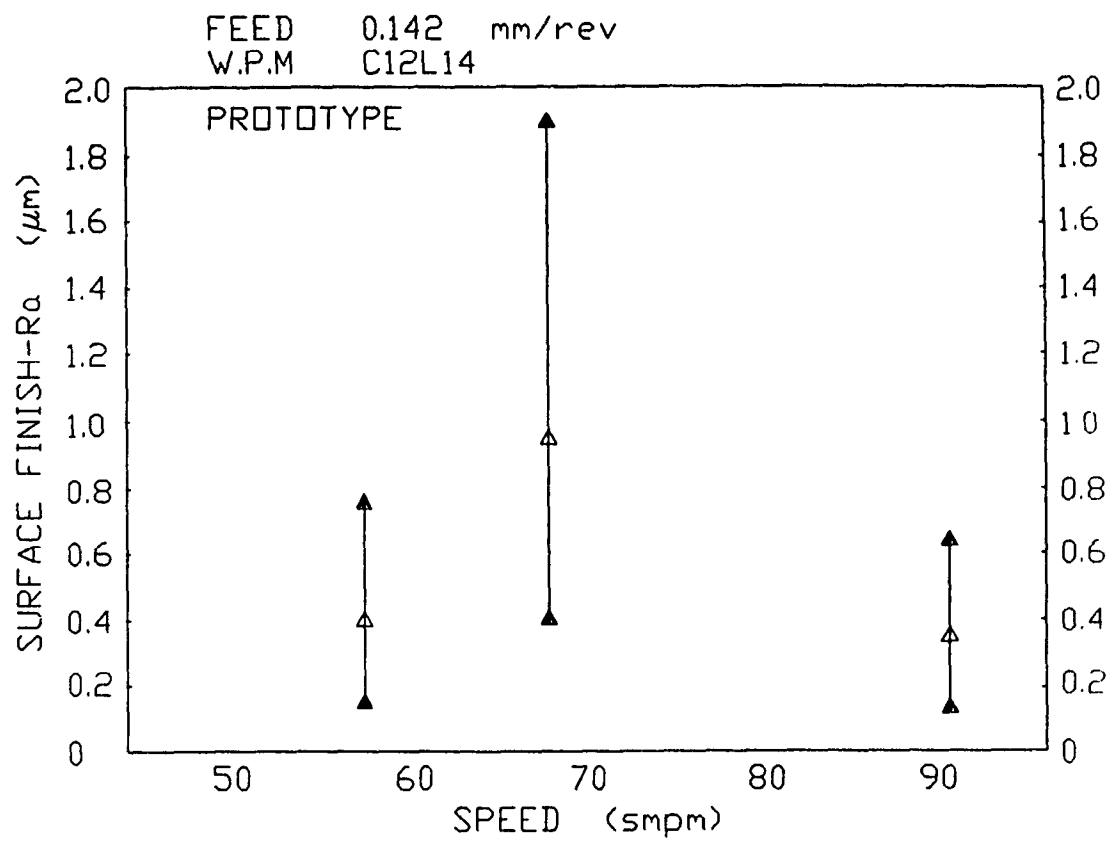


FIG. 48 SURFACE FINISH OF THE HOLE DRILLED BY
THE PROTOTYPE

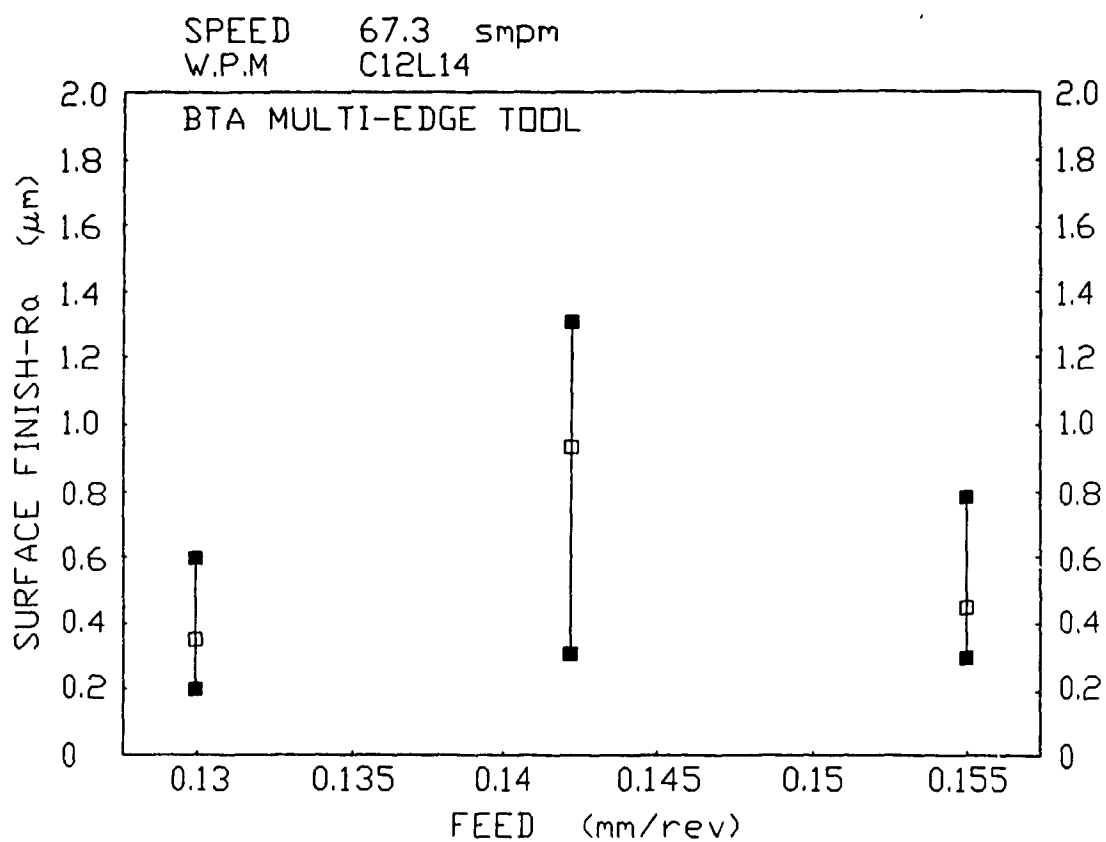


FIG. 49 SURFACE FINISH OF THE HOLE DRILLED BY
THE BTA MULTI-EDGE TOOL

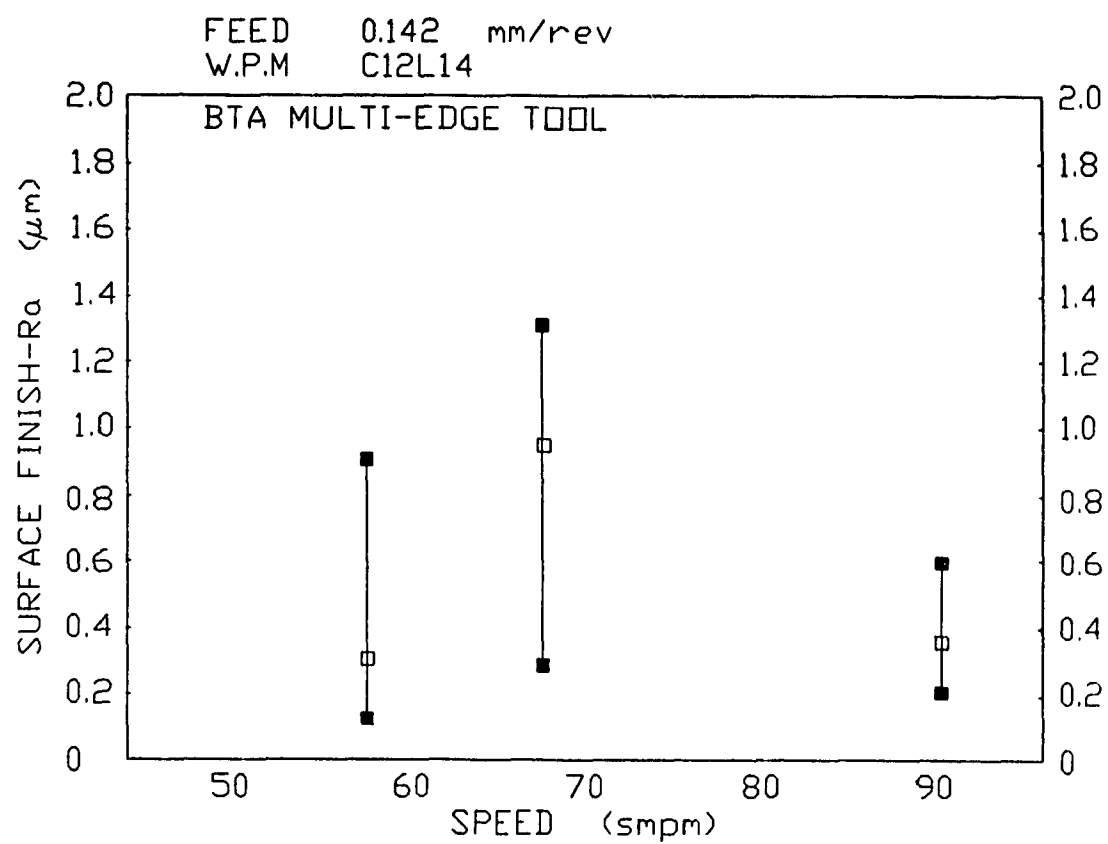


FIG. 50 SURFACE FINISH OF THE HOLE DRILLED BY
THE BTA MULTI-EDGE TOOL

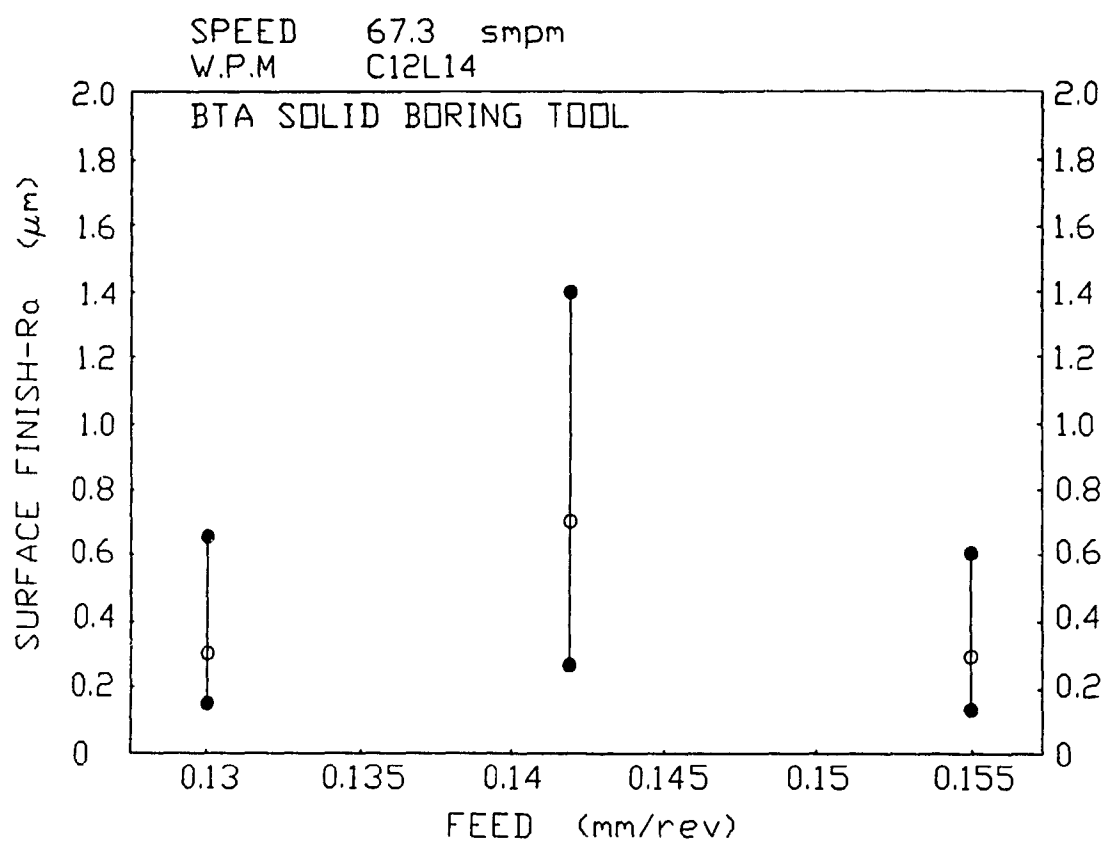


FIG. 51 SURFACE FINISH OF THE HOLE DRILLED BY
THE BTA SOLID BORING TOOL

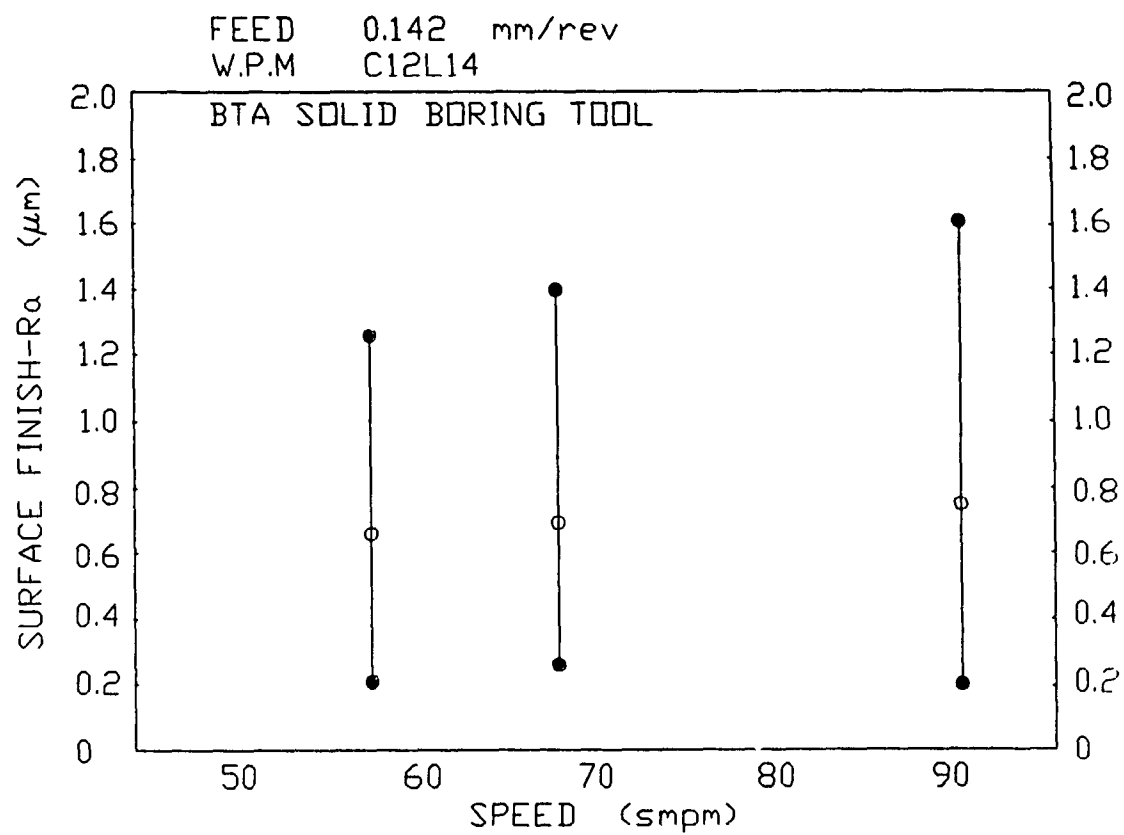


FIG. 52 SURFACE FINISH OF THE HOLE DRILLED BY
THE BTA SOLID BORING TOOL

CHAPTER VI

6.1 Summary

In this work, a comparative study of three deep hole boring and drilling tools is conducted. For this purpose a 2 inches diameter deep hole drilling tool with staggered cutters unsymmetrically located on tool head with respect to the rotational axis is designed and used along with the two commercially available tools. The main criterion in the tool design was to place the cutters with different width on the tool head such that an equal reaction force be generated on both guide pads.

To achieve the objective of the present study the following analytical and experimental work has been carried out.

Formulation and Tool Optimum Design

To design the tool the mathematical model of cutting force system was adopted based on the so called elementary and extended cutting force laws. In this respect, the three cutting force components namely tangential, radial and feed forces are formulated using metal cutting mechanics.

To optimize the tool design base on the given equal pad reaction forces and given size of cutters, the constrained nonlinear penalty function optimization method is used. For this purpose an objective function is developed such that the resultant cutting force and pad

forces balance each other for given equal friction coefficient of guide pads. Several constraints were established in order to achieve a feasible tool design.

Tool Stability Analysis and Experimental Work

The fluctuation of the magnitude of pads resultant force and its position angle are the first criteria for the tool stability analysis. For this purpose the Monte Carlo simulation is used based on assumed fluctuation range for cutting force components and friction coefficient at the pads along with their statistical characteristics. The second method used to assess the stability is called Pflieggar method. In this method the ratio of holding to lifting moment on each pad is found and compared with the values for commercially available two tools. The tool with a higher overall torque ratios on pads is considered to be more stable and expected to perform better. The stability analysis was conducted for designed tool and the two commercially available tools namely BTA multi-edge and BTA solid boring tools and the results were compared.

The tool prototype is manufactured based on the solution of optimization problem and several sets of experiments are conducted using all three tools. For this purpose two different steels are drilled at different combinations of cutting parameters. The results are studied for the hole run-out, size error, roundness error and surface finish.

6.2 Conclusion

1 - The concept of a multi-edge BTA tool with standard disposable carbide inserts arranged in a staggered pattern has been affirmed in this investigation. The mathematical model has been improved to incorporate the requirements for predetermined equal guide pads reaction with friction. This novel feature of the model allowed to define an objective function and necessary constraints in such a way that an optimal tool design is yielded through the optimization on the computer providing tool design parameters such as radial and angular locations of cutters and angular locations of guide pads. Further, the means of stability assessment have been provided by implementing the Monte Carlo simulation and Pfliegner's criteria for stability. An optimal tool layout produced by the procedure was compared to the layouts of two commercially available tools and found superior to the multi-edge BTA tool with disposable inserts presently marketed.

2 - The optimal tool prototype has undergone extensive testing and comparison to the two commercially available tools. The performance was assessed with regard to the hole run-out, size error, surface finish and cylindricity.

- After an initial tun up the prototype has performed well with no major problems to be reported.
- The prototype performed better than the two commercially available tools in terms of hole run-out.
- The prototype produced holes with smaller size error

than the BTA multi-edge tool with disposable inserts presently on the market. The BTA solid boring tool out-performed the prototype in this regard but that was anticipated as a trade-off.

- The prototype showed to be inferior to the two commercially available tools in terms of surface finish and hole roundness. While the surface finish is a trade-off because less burnishing anticipated, the larger hole roundness error may be due to more pronounced relative variation of the pads' reaction forces.
- The prototype has not been assessed with respect to its life. For this purpose much longer time and statistical data would be required. Yet the tool prospect to be superior to the other two with that regard and cutting energy saving is very good.

6.3 Recommendations for Future Work

The designed tool manufactured and tested for its performance by drilling specimens at different conditions but full understanding of tool behavior requires its dynamic analysis by measuring the cutting force system. The comparison of the results acquired from dynamic analysis of three tools can be an essential part of the study.

REFERENCES

1. Osman, M.O.M., "The BTA Technique - Fast Hole Machining", Tooling & Production, No. 2, 1975, pp. 49-51.
2. Latinovic, V., "An Investigation of the Theoretical and Design Aspects of Unsymmetrical Multi-Cutting Action in Deep-Hole Machining", D.Eng. Thesis, Concordia Univ. 1978.
3. Steeds, W., "A History of Machine Tools 1700-1910", Oxford Press, 1969, p. 6.
4. Landis, A.B., "Deep Hole by Continuous Boring", American Machinist, 1886, p. 4.
5. Turner, C.F., "Practical Aspects of Producing Holes", Int. Conf. on Deep Hole Drilling and Boring, Brunel Univ. 1975.
6. Astanin, V.N., "Dynamic of Deep Drilling in Alloy Steel", Russian Machines and Tooling, No. 11, Vol. 34, 1963, pp. 27-29.
7. Greuner, B., "Beitrag zur Frage der Krafte an Schneide und Fuhrungsleisten an Einschneidigen Hartmetallbestuckten Tiefbohrwerkzeugen", Dr.- Ing. Thesis. Technischen Universitat, Hanover, 1970
8. Greuner, B., "New Aspects in the Field of Deep Hole Boring", 2nd. Int. Conf. on Deep Hole Drilling and Boring, Brunel Univ. 1977.

9. Griffiths, B.J., "The Machining Action During Deep Hole Boring and the Resultant Hole Form and Force System", Proc. 2nd. Int. Conf. on Prod. Res, Copenhagen, 1973.
10. Weber, U., "Beitrag zur Messtechnischen Erfassung des Tiefbohrprozesses Dr.-Ing. Thesis, Universitat Dortmund, 1978.
11. Griffiths, B.J., "AN Investigation Into the Role of the Burnishing Pads in the Deep-Hole Drilling Process", Ph.D. Thesis Brunel University, 1982.
12. Candrashekhar, S., "An Analytical and Experimental Stochastic Modeling of the Resultant Force System in BTA Deep-Hole Machining and Its Influence on the Dynamic of the Machine Tool-Workpiece System", Ph.D. Thesis, Concordia Univ. 1982.
13. Latinovic, V., Osman, M.O.M., "Optimal Design of BTA Deep-Hole Cutting Tools With Staggered Cutters", Int. J. of Prod. Res, Vol.27, No.1, 1989, pp. 153-173.
14. Pflegar, F., "Verbesserung der Bohrungsqualitat beim Arbeiten mit Einlippen Tiefbohrwerkzeugen Technischer Verlag Gunter Grossman GmbH. Stuttgart Vaihingen, 1976.
15. Candrashekhar, S., Osman, M.O.M., Sankar, T.S., "An Experimental Investigation for the Stochastic Modeling of the Resultant Force System in BTA Deep-Hole Machining", Int. J. of Prod. Res, Vol. 23, No. 4, 1985, pp. 657-673.

16. Weber, U., "Distribution of Load and Balance of Energy in Deep Hole Boring", 2nd. Int. Conf. on Deep Hole Drilling and Boring, Brunel Univ. 1977.
17. Griffiths, B.J., Greive, R.J., "The Role of the Burnishing Pads in Mechanics of the Deep Drilling Process", Int. J. of Prod. Res, Vol. 23, No. 4, 1985, pp. 647-655
18. Thai, T.P., "Beitrag zur Untersuchung der Selbsterregten Schwingungen von Tiefbohrwerkzeugen", DR.-Ing. Thesis, Universitat Dortmund, 1983.
19. Trent, E.M., "Metal Cutting and the Tribology of Seizure : II - Movement of Work Material Over Tool in Metal Cutting", Wear, Vol. 128, 1988, pp. 47-64
20. Weber, U., "Messen der Zerspankraft Beim Tiefbohren", VDI-Berichte, Nr. 301, 1977, pp. 27-35.
21. Sakuma, K., Taguchi, K., Katsuki, A., "Study on Deep-Hole Drilling With Solid Boring Tool : The Burnishing Action of Guide Pads And Their Influence on Hole Accuracies", Bull. of the JSME, Vol. 23, No. 185, 1980, pp. 1921-1928.
22. Ramakrishna Rao, P.K., Shunmugam, M.S., "Accuracy and Surface Finish in BTA Drilling", Int. J. of Prod. Res, Vol.25, No.1, 1987, pp. 31-44.
23. Sakuma, K., Taguchi, K., Katsuki, A., "Study on Deep-Hole Drilling With Solid Boring Tool : The Effect

of Tool Material on the Cutting Performance", Bull. of the JSME, Vol. 21, No. 153, 1978, pp. 532-539.

24. Bergman, K., Fuß, H., "Untersuchungen zur Führungslieftun Eibung an Tiefbohrwerkzeugen", Tiefbohren, 1986, pp.27-36.
25. Frazao, J., Chandrashekhar, S., Osman, M.O.M., Sankar, T.S., "On the Development of a new BTA Tool to Increase productivity and Workpiece Accuracy in Deep-Hole Machining", The Int. J. of Advanced Manufg. Process, Vol. 1, No. 4, 1986, pp. 3-23.
26. Nicolson, R., "A Comparison of Neat Oils and Water Mixed Fluids for Gun Drilling", 3rd Int. Conf. on Deep Hole Drilling and Boring, Brunel Univ. 1979.
27. Osman, M.O.M., Latinovic, V., Greuner, B., "On the Performance of Cutting Fluids for BTA Deep-Hole Machining", Int. J. of Prod. Res, Vol.19, No.5, 1981, pp. 491-503.
28. Chandrashekhar, S., Ahmad, Z., Sankar, T.S., Osman, M.O.M., "On the Prediction of the Roundness Error in BTA Deep-Hole Machining Based on the Stochastic Description of the Cutting Tool Motion", Int. J. of Prod. Res, Vol. 24, No. 4, 1986, pp. 879-899.
29. Griffiths, B.J., "Axial Hole Run-Out During Deep Drilling (Self Piloting Drilling)", 2nd. Int. Conf. on Deep Hole Drilling and Boring, Brunel Univ. 1977.

30. Sakuma, K., Taguchi, K., Katsuki, A., "Self Guiding Action of Deep-Hole Drilling", C.I.R.P, Vol. 30, No. 1, 1981, pp. 311-316
31. Sakuma, K., Taguchi, K., Katsuki, A., "The Influence of Tool Geometry on Axial Hole Deviation in Deep Drilling : Comparison of Single and Multi-Edge Tools", Int. J. of JSME, Vol. 30, No. 265, 1987, pp. 1167-1174.
32. Pflieger, F., "The Aspect of Stability in Designing Deep-Hole Drilling and Boring Tools", 2nd Int. Conf. on Deep Hole Drilling and Boring, Brunel Univ. 1979.
33. Osman, M.O.M., Latinovic, V., "On the Development of Multi-Edge Cutting Tool for BTA Deep-Hole Machining", Transaction of the ASME, 1976, pp. 474-480.
34. Latinovic, V., Blakely, R., Osman, M.O.M., "Optimal Design of Multi-Edge Cutting Tools for BTA Deep-Hole Machining", Transaction of the ASME, Vol. 101, 1979, pp. 281-290.
35. Stockert, R., "Beitrag zur Optimaten Auslegung Von Tiefbohrwerkzeugen", Dr.-Ing. Thesis. Universitat Dortmund, 1978.
36. Cronjager, L., Stockert, R., Weber, U., "Vibration and Their Effect on Accuracy in Deep-Hole Boring", 3rd Int. Conf. on Deep Hole Drilling and Boring, Brunel Univ. 1979

37. Sakuma, K., Taguchi, K., Katsuki, A., "Study on Deep-Hole Boring by BTA System Solid Boring Tool : Behaviour of Tool and Its Effects on Profile of Machined Hole", Bull. of Japan Soc. of Proc. Engg, Vol. 14, No. 3, 1980, pp. 143-148.
38. Streicher, P., "Tiefbohren der Metalle - Verfahrenstechnische und Konstruktive Problem", Vogel-Verlag Würzburg, Wi-Fachbuchreihe Band 2, 1975.
39. Lundgren, E., "The Role of Cutting Geometry During Deep-Drilling", Int. Conf. on Deep-Hole Drilling and Boring, Brunel Univ. 1975.
40. Corney, J., Griffiths, B., "A Study of the Cutting and Burnishing Operation During Deepo Hole Drilling and Its Relationship to Drill Wear", Int. J. of Prod. Res, Vol.14, No.1, 1976, pp. 1-9.
41. Jurgen, B., "Entwicklung Einer Digitalen AC-Grenzregelung für Tiefbohrmaschinen Unter Betrachtung Geeigneter Prozesskenngrößen", VDI-Berichte No.103, 1986
42. Ramakrishna Rao, P.K., Shunugam, M.S., "Wear Studies in Boring Trepanning Association Drilling", Wear, Vol. 124, 1988, pp. 33-43.
43. Kronenberg, M., "Machining Science and Application", Pergamon Press, 1966.

44. Cronjager, L., "Entwicklungsstand des Tiefbohren Metalischer Werkstoofe", Tiefbohren '77, VDI-Berichte, Nr. 301, 1977, pp. 5-11.
45. Shunmugam, M.S., "On Assessment of Geometric Errors", Int. J. of Prod. Res, Vol. 24, No. 2, 1986, pp. 413-425
46. Ramakrishna Rao, P.K., Shumugam, M.S., "Analysis of Axial and Transvers Profiles of Holes Obtained in BTA Machining", Int. J. of Mach. Tools. Manufact, Vol. 27, No. 4, 1987, PP. 505-515

APPENDIX

Error on form is evaluated with reference to an ideal geometrical feature which must be established from actual measurements so that the deviation between it and the actual feature concerned is the least possible.

To evaluate a one dimensional problem for its accuracy, let such measurements be represented by x_1, x_2, \dots, x_n and the representative value be x_0 . The deviation e_i is then given by,

$$e_i = x_i - x_0$$

According to the principle of least squares,

$$v = \sum_{i=1}^n e_i^2 = \sum_{i=1}^n (x_i - x_0)^2$$

should be minimum and this estimates the representative value x_0 as,

$$x_0 = \sum_{i=1}^n x_i / N$$

Cylindricity is a three-dimensional feature and evaluation of such forms for accuracy is carried out using the same principle. If the results of cylindricity measurements are represented by $(\delta_i, \theta_i, z_i)$ on polar coordinates and if the axis of the cylindrical feature is well aligned with z-axis, then the deviations with reference to the ideal cylinder are given as,

$$e_i = \delta_i - (R_o + x_o \cos \theta_i + y_o \sin \theta_i + l_o z_i \cos \theta_i + m_o z_i \sin \theta_i)$$

The values of x_o , y_o , l_o , m_o , R_o for symmetrical data points (V observations in each section with uniform angular spacing and W horizontal sections equally spaced) are found as,

$$x_o = 2 \sum_{i=1}^n \delta_i \cos \theta_i / V W$$

$$y_o = 2 \sum_{i=1}^n \delta_i \sin \theta_i / V W$$

$$l_o = 24 \sum_{i=1}^n \delta_i z_i \cos \theta_i / V W (W^2 - 1)$$

$$m_o = 24 \sum_{i=1}^n \delta_i z_i \sin \theta_i / V W (W^2 - 1)$$

$$R_o = 24 \sum_{i=1}^n \delta_i / V W$$

The cylindricity error is the sum of the absolute values of the maximum and minimum deviations, e_{\min} and e_{\max} .

TABLE A1 PROPERTIES OF AISI-P20 STEEL

ALLOY CONTENT %	C	Si	Mn	Cr	Ni	Mo
	0.35	0.3	0.7	1.8	0.7	0.3

MECHANICAL PROPERTIES AT 20 °C AND HARDNESS OF 290 HB	TENSIL STRENGTH N/mm ²	YIELD STRESS N/mm ²	REDUCTION OF AREA %	ELONGATION 5 %	IMPACT STRENGTH KJm/Cm ²
	950	750	60	20	10

TABLE A2 PROPERTIES OF AISI-C12L14 AND AISI-C1045 STEELS

ALLOYING ELEMENTS	C %	Mn %	P %	S %	Pb %
C12L14	0.15 max	0.8-1.2	0.04-0.09	0.25-0.35	0.15-0.35
C1045	0.42-0.49	0.7-1.0	0.04	0.04-0.07	-

MECHANICAL PROPERTIES	TENSIL STRENGTH N/mm ²	YIELD STRESS N/mm ²	HARDNESS HB
C1045	106000	79000	223

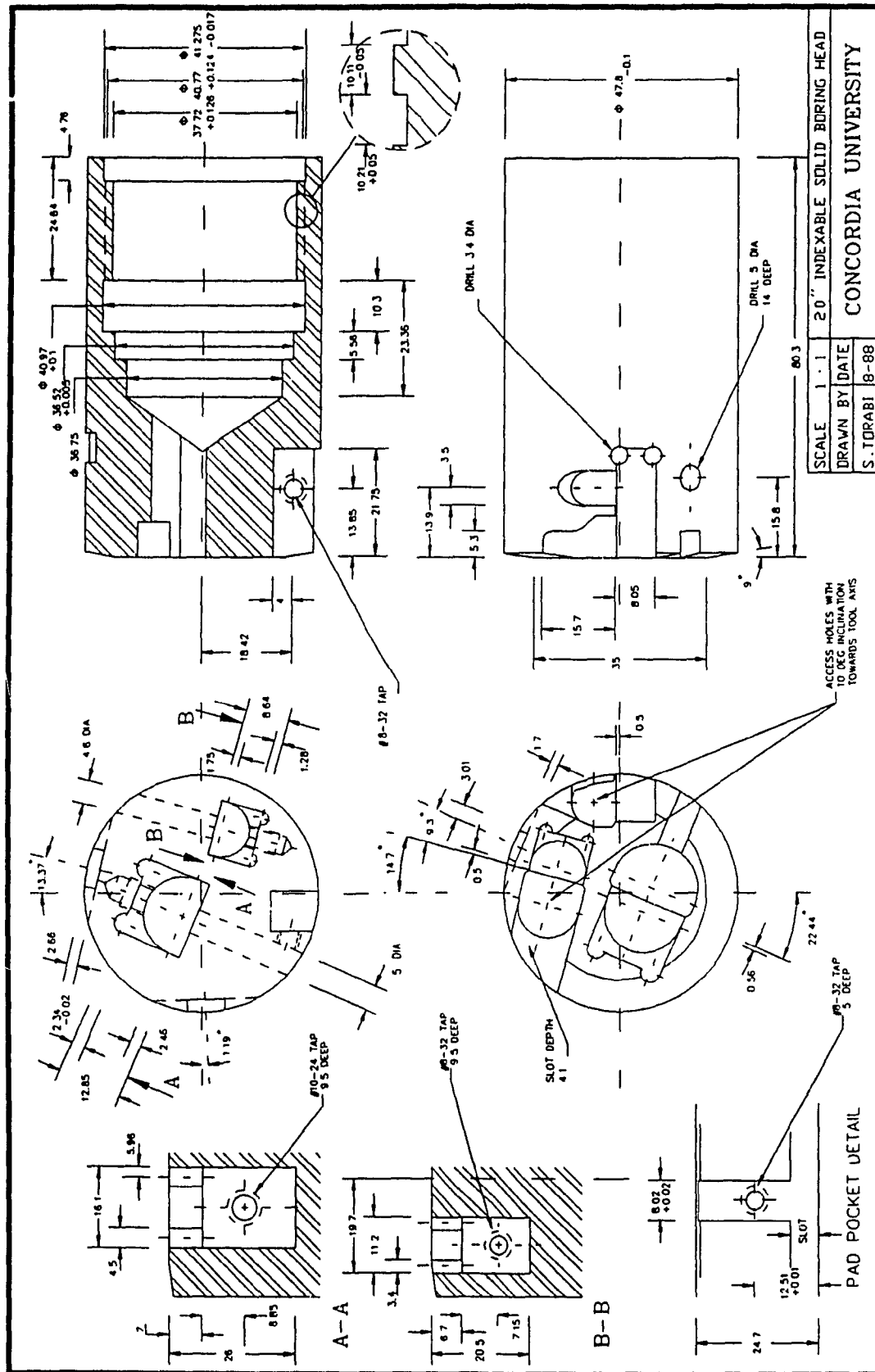


FIG. A1 DETAIL DRAWING OF THE DESIGNED TOOL

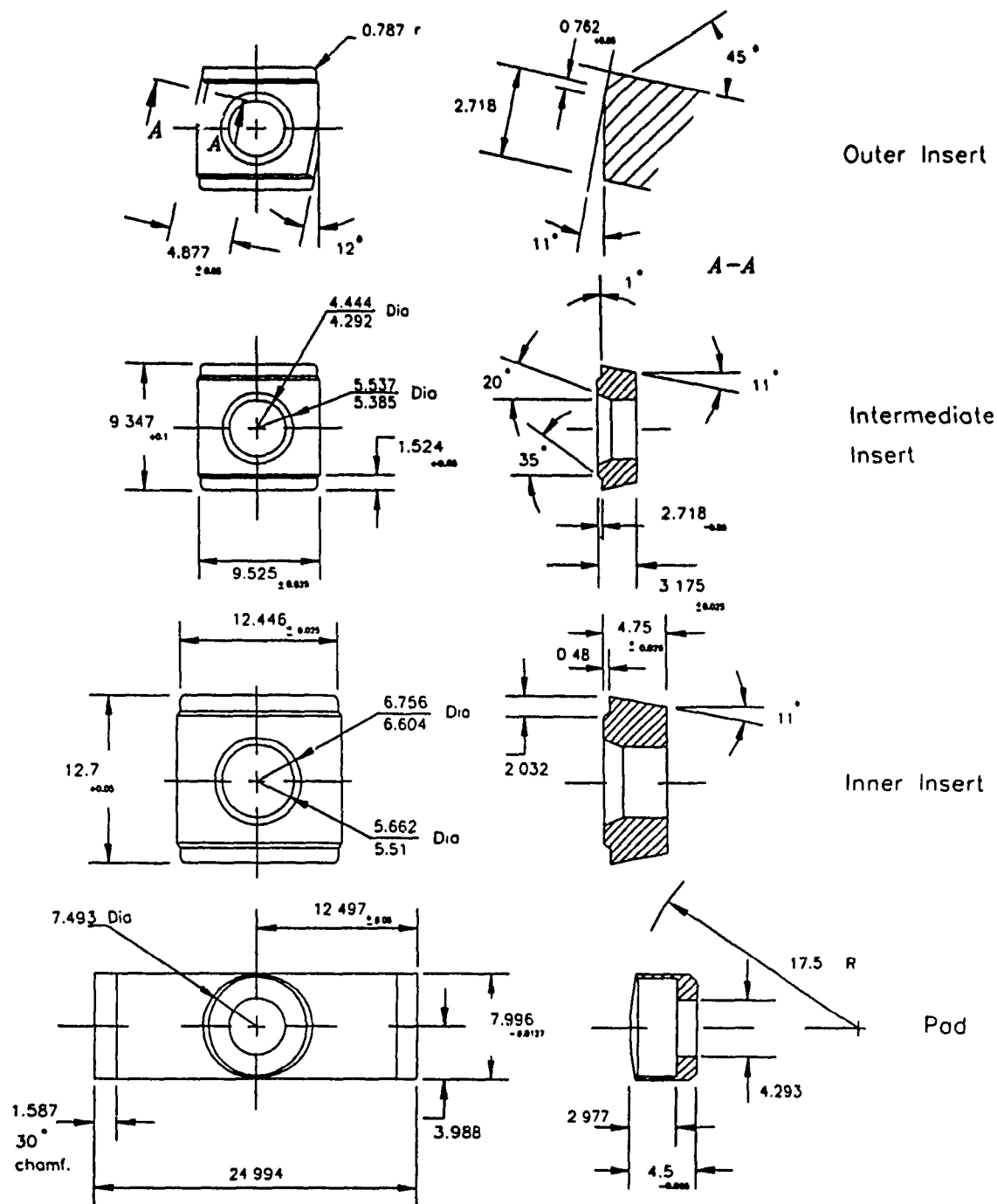


FIG. A2 THE PROTOTYPE'S INSERTS AND PAD